SHEAR STRENGTH OF CONTINUOUS LIGHTLY REINFORCED CONCRETE JOIST SYSTEMS

By

S. Ravikumar

David Darwin

Steven L. McCabe

Gregory P. Pasley

A Report on Research Sponsored by

THE NATIONAL SCIENCE FOUNDATION
Research Grant No. MSM-8816158

Structural Engineering and Engineering Materials
SM Report No. 37

UNIVERSITY OF KANSAS CENTER FOR RESEARCH, INC.
LAWRENCE, KANSAS
March 1994

ABSTRACT

The objective of this research is to study the shear strength of continuous lightly reinforced concrete joist systems. Six two-span joists, with and without web reinforcement, and two multiple web joists without web reinforcement were tested. The main focus of this study was to determine the shear cracking capacity and to investigate load sharing between joists. Shear cracking loads are determined using crack pattern and stirrup strain analyses. Behavior is evaluated in both the positive and the negative moment regions. The primary variables in this research are the longitudinal reinforcement ratio, ρ_w (0.76% and 1.04% for negative moment regions and from 0.79% to 2.43% for positive moment regions), and nominal stirrup strength, $\rho_v f_{vy}$ (0 to 70 psi) for single web joists and placement of the load in multiple web joists. Stirrup effectiveness in joists is analyzed based upon ACI provisions and the number of stirrups intercepted by the critical shear crack. Nominal shear stresses and load sharing between the joists are compared with current ACI design provisions.

The tests indicate that ACI 318-89 overestimates the shear cracking load and shear capacity of lightly reinforced concrete joists in negative moment regions, and under estimates the shear cracking load but not the shear capacity in positive moment regions. In the study, the stirrup contribution in both the negative and positive moment regions equaled or exceeded the value predicted by ACI 318-89. In the positive moment regions of members with stirrups, the concrete contribution to shear capacity was often below the shear cracking load, contrary to the usual assumption. The study indicates that significant load sharing occurs between the joists, but that the load sharing is adequate only to distribute local overloads. The additional 10% in the concrete contribution to shear capacity, as allowed by ACI 318-89, is not available for joist systems as a whole.

ACKNOWLEDGEMENTS

This report is based on research performed by S. Ravikumar in partial fulfillment of the requirements for the MSCE degree. The research was supported by the National Science Foundation under NSF Grant No. MSM-8816158. Reinforcing steel bars were supplied by North Star Steel Company, and wire for stirrups in the test regions was supplied by Ivy Steel and Wire Company. Form release agent, curing compound, and mounting hardware were supplied by Richmond Screw Anchor Company. The vibrating screed used for the multiple web joists was supplied by Allen Engineering. Pan joist forms, along with additional forming materials, were provided by CECO Corpation.

TABLE OF CONTENTS

LIST OF TABLES

LIST OF TABLES (continued)

LIST OF FIGURES

LIST OF FIGURES (continued)

CHAPTER 1

INTRODUCTION

1.1 General

Shear failures are considered undesirable because the failure of a concrete member in shear is usually abrupt and nonductile. Therefore, it is important to accurately predict a concrete member's shear strength. Since the beginning of this century, many investigators have experimentally studied the behavior of reinforced concrete beams in shear. The results are numerous, but not sufficient to develop a universally accepted procedure to predict shear capacity. The absence of a general theory is evidence of the tremendous difficulty experienced in solving the problem. Most of the investigations have been unrelated, and there has been no systematic approach to the test programs. In fact, many times, the test specimens have not been representative of members in real structures. Also, the majority of the available test data are based on simple spans, while continuous members are used in everyday construction practice. Furthermore, previous investigations have concentrated on beams with medium to large amounts of flexural reinforcement. These beams tend to exhibit both concrete and steel shear capacities in excess of those predicted by the empirical design expressions.

In spite of this extensive research and the large volume of experimental research devoted to the prediction of the shear capacity of reinforced concrete beams, there are some areas that have received relatively little attention in the design codes. Of particular concern are lightly reinforced concrete members. The existing research (Rodriguez, Bianchini, Viest and Kesler 1959, Krefeld and Thurston 1962, Kani 1966, Rajagopalan and Ferguson 1968, Attiogbe, Palaskas, and Darwin 1980, Palaskas and Darwin 1980, Batchelor and Kwun 1981, Palaskas, Attiogbe and Darwin 1981, Rodrigues and Darwin 1984, 1987, Phillips and Schultz 1988, Pasley, Gogoi, Darwin

and McCabe 1990) on lightly reinforced concrete members indicates that the contribution of concrete to shear capacity is considerably less in members with low flexural reinforcement ratios, ρ_w, than in members with ρ_w greater than 1%, where $\rho_w = A_s/b_w d$, A_s = cross-sectional area of flexural steel, b_w = web width, and d = effective depth of beam. This is of concern because the present ACI Building Code (ACI 318-89) shear design provisions appear to be unconservative for lightly reinforced flexural members, especially in negative moment regions (Rodrigues and Darwin 1984, 1987, Pasley et al. 1990). However, overall strength in positive moment regions appears to be satisfactory, largely due to conservative code provisions for shear reinforcement.

Concrete joist construction is widely used and is of particular interest since joists are lightly reinforced members. In spite of their widespread use, there has been very little research done regarding the shear capacity of these members, especially continuous members. Also, the current shear provisions for joists in ACI 318-89 (including assumed load sharing between joists) are based on virtually no experimental data. This lack of research is of special concern when the sudden nature of a shear failure is considered. Thus, joists may, in fact, have a lower margin of safety than other components of reinforced concrete structures.

The behavior of normally proportioned reinforced concrete joists with low to moderate percentages of longitudinal reinforcement is the primary interest of this investigation. Hence, the current study is designed to study the shear strength of continuous, lightly reinforced concrete joists and to determine the effects of the flexural reinforcement ratio, the degree of shear reinforcement, and load sharing between joists on shear capacity.

1.2 Background

From the early 1950's to the present, researchers have made numerous shear

tests and found that many variables influence the shear strength of concrete beams (ACI-ASCE Committee 326 1962, ACI-ASCE Committee 426 1973). To give a better picture of the shear strength of concrete, ACI-ASCE Committee 326 on Shear and Diagonal Tension (1962) chose to express the shear capacity of reinforced concrete beams as a function of the square root of the concrete cylinder strength, the shear span-to-depth ratio, and the percentage of longitudinal reinforcement. For beams with web reinforcement, the committee concluded that both the web reinforcement and the concrete contribute to the shear capacity. As noted by ACI-ASCE Committee 326 (1962) and many others (Moretto 1945, Clark 1951, Elstner, Moody, Viest and Hognestad 1954, Fenwick and Pauly 1968, Zsutty 1968, Gergely 1969, Kani 1969, Taylor 1970, ACI-ASCE Committee 426 1973) shear is carried to the supports through the beam by the shear forces in uncracked concrete, tension forces in shear reinforcement, forces due to arch action, dowel forces in flexural reinforcement, and friction forces along the shear cracks. The relative contribution of these mechanisms to shear strength depends on the beam geometry, concrete strength, amount and detailing of reinforcement, stage and location of loading, and the type of supports. The key shortcoming of the ACI-ASCE 326 (1962) provisions is that they do not accurately represent the effects of the various parameters on shear strength and, thus, result in a variable factor of safety in the applicable range of the equation.

Lightly reinforced concrete members are widely used. Investigators (Rodriguez et. al 1959, Krefeld and Thurston 1962, Kani 1966, Rajagopalan and Ferguson 1968, Kani, Huggins, Wuttkop 1979, Attiogbe et al. 1980, Palaskas and Darwin 1980, Batchelor and Kwun 1981, Palaskas et al. 1981, Rodrigues and Darwin 1984, 1987, Phillips and Schultz 1988, Pasley et al. 1990) have studied the effect of the longitudinal reinforcement ratio referenced to the area of the beam web, ρ_w, on the

shear strength of reinforced concrete beams and found that shear strength increases with increasing ρ_w. The longitudinal steel appears to contribute to shear strength both through dowel action and by limiting the extent of cracking: as ρ_w increases, 1) the dowel shear increases, and 2) the flexural cracks become narrower and more inclined, increasing both the shear capacity of the compression zone and the shear transfer between the longitudinal steel and concrete.

Concrete joists are subject to the same concerns as other lightly reinforced members. However, joists are not only lightly reinforced members but are exempt from the ACI design provisions that require shear reinforcement when the factored shear, V_u, is greater than $\phi V_c/2$ but less than ϕV_c, in which ϕ = strength reduction factor. For joists, shear reinforcement must be provided only when V_u exceeds ϕV_c. In addition, the ACI expressions for concrete shear strength, V_c, can be increased by 10% for joists. These criteria are based on the philosophy that, because of their proportions and relatively close spacing, joists can share shear loads and are thus more effective than a single member (ACI-Committee 318 1963, 1989). However, these design provisions have not been vigorously researched and, in fact, there are no published experimental data to support these values.

The 1962 report by ACI-ASCE Committee 326 describing the results of more than 440 tests on beams without web reinforcement indicates that the concrete shear capacity of beams primarily depends on the percentage of flexural reinforcement, ρ_w, the shear span-to-depth ratio, a/d, and the concrete compressive strength, f'_c, with other variables, like aggregate interlock and shear friction, playing minor roles in the contribution of concrete to shear strength. The present ACI Building Code (ACI 318-89) equations for concrete shear capacity, which were first proposed by ACI-ASCE Committee 326 (1962), are based on research done on simply supported beams having flexural reinforcement ratios, ρ_w, above 1%. Previous studies (Rodriguez et al. 1959,

Krefeld and Thurston 1962, Kani 1966, Rajagopalan and Ferguson 1968, Kani, Huggins, Wuttkop 1979, Attiogbe et al. 1980, Palaskas and Darwin 1980, Batchelor and Kwun 1981, Palaskas et al. 1981) have shown that the shear cracking load, V_{cr}, calculated according to ACI 318-89 is conservative for ρ_w greater than 1%, but unconservative for ρ_w less than 1%. These studies were carried out on simply supported beams subjected to positive bending.

Research on the negative moment region shear strength of lightly reinforced T-beams (Rodrigues and Darwin 1984, 1987) has shown a lower concrete shear capacity and stirrup reinforcement effectiveness in negative moment regions than in positive moment regions. The lower negative moment region shear strength is felt to be caused by a smaller effective concrete section resulting from cracking of the flanges and a lower bond strength for negative flexural reinforcement, due to the top-bar effect, which reduces the shear carrying capacity of the concrete.

The ACI provisions for the stirrup contribution to shear strength (ACI Committee 318 1963, 1989) are based on the assumption that the critical diagonal tension crack has a horizontal projection equal to the effective depth of the beam. Previous research (Bresler and Scordelis 1963, Haddadin, Hong, and Mattock 1971, Attiogbe et al. 1980, Palaskas and Darwin 1980, Palaskas et al. 1981, Rodrigues and Darwin 1984, 1987, Pasley et al. 1990) has shown that, in most cases, the critical diagonal tension crack has a greater horizontal projection, and, thus, it intersects more stirrups than predicted by the ACI provisions, producing a higher shear strength. As a result, the ACI shear design equations often underestimate the contribution of web reinforcement to the shear strength of beams (Bresler and Scordelis 1963, Haddadin et al. 1971, Attiogbe et al. 1980, Palaskas and Darwin 1980, Palaskas et al. 1981, Rodrigues and Darwin 1984, 1987, Pasley et al. 1990)

1.3 Previous research

Early studies of shear in concrete beams were performed by Ritter (1899) and Mörsch (1909). Ritter (1899) studied the flow of shear forces in reinforced concrete beams and explained the shear behavior in terms of a truss model. Ritter (1899) modelled the compressive stresses in the concrete as diagonal compression members and the vertical stirrups as tension members of the truss model. This model is often referred to as the "truss analogy". Mörsch (1909) studied the shear cracking angle on two simply supported T-beams subjected to increasing levels of uniformly distributed load. Mörsch (1909) showed that the angle of inclination of shear cracks and the compression diagonals, α, was variable and concluded that it was impossible to mathematically determine the slope of the shear cracks from his experiments. For practical purposes, Mörsch (1909) assumed α to be 45 degrees. Based on the assumption that α equals 45 degrees, an expression for the required amount of transverse reinforcement was developed and became known as the truss equation for shear. In European practice today (CEB-FIP 1978), it is assumed that the transverse reinforcement resists all of the shear, ignoring the concrete contribution of shear strength.

In contrast to European practice, in American practice, it is assumed that concrete shares a portion of the applied total shear, equal to the force at the beginning of diagonal cracking. This force is called the "concrete contribution". The balance of the applied shear is assumed to be carried by stirrups which are proportioned based on the 45 degree truss analogy. The resulting model is referred to as the "modified truss analogy". In the 1950's and 60's, extensive research was conducted to better understand shear mechanisms in concrete. Moody, Viest, Elstner and Hognestad (1954) were some of the first researchers to study shear with the aim of developing strength design equations. Moody et al. (1954) performed over one hundred shear

tests on reinforced concrete beams. The results obtained from their experimental program revealed that the magnitude of the shear failure load is dependent on 1) the cross sectional dimensions, 2) the amount of longitudinal reinforcement, 3) the amount of web reinforcement, 4) the concrete strength, and 5) the length of the shear span, where the shear span is defined as the ratio of the maximum moment to the maximum shear, M_u/V_u. Although these studies added a great amount of knowledge, they did not provide a full understanding of the shear failure mechanism.

The equations for concrete shear capacity given in ACI 318-89, as well as ACI 318-77 and ACI 318-83, were established through experimental and analytical studies of typical flexural members and represent the concrete shear strength in terms of concrete compressive strength, beam size, flexural reinforcement ratio, and the applied loads. For beams without web reinforcement, the concrete shear capacity is given by the following equation:

$$V_c = \left(1.9\sqrt{f'_c} + \frac{2500\rho_w V_u d}{M_u}\right) b_w d \leq 3.5\sqrt{f'_c}\, b_w d \qquad (1.1)$$

in which, f'_c is the compressive strength of concrete in psi; V_c is the factored shear force at the section in lbs; M_u is the factored bending moment at the section in in.-lb; d is the effective depth of the cross-section in in.; and b_w is the the effective width of the web in in.

or in a simplified expression as,

$$V_c = 2\sqrt{f'_c}\, b_w d \qquad (1.2)$$

Eqs. 1.1 and 1.2 correspond to Eqs. 11-3 and 11-6 respectively, in ACI 318-89.

In terms of shear stress, v_c, Eqs. 1.1 and 1.2 can be rewritten, respectively, as

$$v_c = \frac{V_c}{b_w d} = 1.9\sqrt{f'_c} + \frac{2500\rho_w V_u d}{M_u} \leq 3.5\sqrt{f'_c} \qquad (1.3)$$

or

$$v_c = 2\sqrt{f'_c} \qquad (1.4)$$

Eqs. 1.1 and 1.2 were originally derived using test results from 194 rectangular beams without web reinforcement (ACI-ASCE Committee 326 1962). Most of these beams were simply supported.

The nominal shear strength provided by stirrups is

$$V_s = \frac{A_v f_{vy} d}{s} \qquad (1.5)$$

in which A_v is the shear reinforcement area within a length, s, of the beam; s is the shear reinforcement spacing; and f_{vy} is the steel yield stress. Eq. 1.5 corresponds to Eq. 11-17 in the ACI Building Code (ACI 318-89) and is based on the assumption that the critical diagonal shear crack is inclined at an angle of about 45 degrees and intersects stirrups over a length equal to the effective depth of the beam. In cases

where the critical diagonal shear crack is flatter than 45 degrees, Eq. 1.5 underestimates the stirrup contribution.

Rodriguez et al. 1959, Krefeld and Thurston (1962), Kani (1966), Rajagopalan and Ferguson (1968), Attiogbe et al. 1980, Palaskas and Darwin 1980 and Batchelor and Kwun (1981), and Pasley et al. 1990 have shown that the ACI shear design procedures are unconservative for reinforced concrete beams without stirrups and with ρ_w less than 1%. Gergely (1977) suggested that, for lightlty reinforced concrete members, minimum web reinforcement may be understrength in shear, especially in regions away from points of maximum moment, where some of the longitudinal reinforcement has been terminated. Rangan (1974) suggested that Eqs. 1.1 and 1.2 be multiplied by the factor $(1 + 100\rho_w)/2$ for ρ_w less than or equal to 1% in order to make the expression more conservative.

Mathey and Watstein (1958) used strain gages on the compressive face of the test beams to verify the accuracy of the cracking load, obtained from visual studies of the cracks. They studied beams without web reinforcement with a/d ratios ranging from 1.51 to 3.78 and values of ρ_w ranging from 0.47% to 3.05%. For test specimens with shear span-to-depth ratios greater than 1.51, they noted an abrupt increase in the steel stress near the support and a marked reduction in the rate of the development of strain on the compressive face of the beams near concentrated loads following the formation of a well-defined diagonal crack. Mathey and Watstein (1958) concluded that, for a/d ratios greater than 1.5 and values of ρ_w lower than 1%, the ACI expressions for concrete shear strength (Eqs. 1.1 and 1.2) were unconservative, in some cases by as much as 47%.

Mathey and Watstein (1958) suggested an expression for the nominal concrete shear stress, v_c:

$$v_c = \frac{3.1\sqrt{f'_c}\,Vd}{M} + 4000\rho_w \qquad (1.6)$$

in which V/M is the ratio of shear to maximum bending moment in the shear span in which the diagonal tension crack forms.

Zsutty (1968), after carrying out dimensional and regression analyses on shear test data obtained from various investigators, proposed the following equation for the shear cracking stress:

$$v_c = 59(f'_c\rho_w d/a)^{1/3} \qquad (1.7)$$

in which "a" is the shear span from the beam reaction to the first concentrated load point. Eq. 1.7 was derived using the test results from 151 beams without web reinforcement, having ρ_w greater than 1% and a shear span-to-depth ratio, a/d, greater than 2.5. Eq. 1.7 accurately predicts the effects of concrete strength, flexural reinforcement ratio, and shear span-to-depth ratio for beams with depth, d, approximately equal to 12 in. However, it is unconservative for beams with greater depth. This lower average shear cracking stress with increasing depth is often referred to as the shear "size effect" (Bazant and Kim 1984).

Rajagopalan and Ferguson (1968) tested 13 rectangular beams (10 without stirrups and 3 with stirrups) with ρ_w ranging from 0.25% to 1.73%. 27 other beams with ρ_w less than 1.2% and without web reinforcement tested by other investigators were also considered in their analysis. All beams were simply supported and had a/d ratios greater than 2.75. Combining their test results with data from other studies, they verified that Eqs. 1.1 and 1.3 did not accurately reflect the shear strength of

concrete members as a function of reinforcement ratio. To account for the effect of low ρ_w, Rajagopalan and Ferguson (1968) proposed the following equation for the shear cracking stress:

$$v_c = \frac{V_c}{b_w d} = (0.8 + 100\rho_w)\sqrt{f'_c} \leq 2\sqrt{f'_c} \qquad (1.8)$$

Placas and Regan (1971) tested 63 simply supported beams with T, I and rectangular sections. The a/d ratios were greater than 3.4, and ρ_w varied from 0.98 to 4.1%. They proposed the following equation for the shear cracking stress:

$$v_c = 8(f'_c\ 100\rho_w)^{1/3} \qquad (1.9)$$

Placas and Regan (1971) imposed an upper bound on v_c in Eq. 1.9 of $12(f'_c)^{1/3}$ to limit the effect of large values of ρ_w "in T - beams in which the main steel has only a limited effect on stress conditions in the web." Eq. 1.9 provides results similar to those of Eq. 1.7 for a/d approximately equal to 4.

After evaluating research on the shear strength of lightly reinforced concrete beams (Rodriguez et al. 1959, Krefeld and Thurston 1962, Kani 1966, Rajagopalan and Ferguson 1968, Placas and Regan 1971) and in recognition of the lack of conservatism in Eqs. 1.1-1.4 for low values of ρ_w, ACI-ASCE Committee 426 (1977) proposed an equation similar to Eq. 1.8 to account for the effect of low ρ_w:

$$\sqrt{f'_c} \leq v_b = (0.8 + 120\rho_w)\sqrt{f'_c} \leq 2.3\sqrt{f'_c} \qquad (1.10)$$

in which v_b = basic shear stress.

Batchelor and Kwun (1981) conducted tests on 10 continuous and 4 simply supported rectangular reinforced concrete beams without web reinforcement, with values of ρ_w as low as 0.17%. They also considered test results of 262 additional beams with rectangular and T-sections without shear reinforcement in their analysis. The 276 beams had a/d ratios greater than 2.0. Based on their analysis, they proposed the following equation for the shear cracking stress:

$$v_c = 1.10\sqrt{f'_c} \le (0.60 + 110\rho_w)\sqrt{f'_c} \le 2.25\sqrt{f'_c} \qquad (1.11)$$

Batchelor and Kwun (1981) felt that Eq. 1.10 proposed by ACI-ASCE Committee 426 (1977) was feasible to use as a design expression; however, they pointed out that, when compared to the data, Eq. 1.10 has a higher coefficient of variation and is not as conservative as Eq. 1.11. For their continuous beams, they found the shear cracking stress, v_c, to be greater in the negative moment regions than in the positive moment regions.

In 1984, Bazant and Kim (1984) introduced an expression for the cracking shear stress, v_c, based on fracture mechanics concepts:

$$v_c = \frac{10^3\sqrt{\rho_w}}{\sqrt{1 + 0.04\,\frac{d}{d_a}}}\left(\sqrt{f'_c} + 3000\sqrt{\frac{\rho_w}{\left(\frac{a}{d}\right)^5}}\right) \qquad (1.12)$$

in which d_a is the maximum size aggregate. With some sacrifice of simplicity, Eq. 1.12 improves on the accuracy of Eq. 1.7 and appears to accurately capture the "size effect". Bazant and Kim (1984) proposed a design expression equal to 80% of Eq. 1.12.

Palaskas et al. (Attiogbe et al. 1980, Palaskas and Darwin 1980, Palaskas et al. 1981) tested 15 simply supported T-beams with low values of flexural and shear reinforcement. The tests included 11 beams with stirrups and 4 beams without stirrups. The shear span-to-depth ratio, a/d was 4 and the flexural reinforcement ratio, ρ_w, ranged from 0.5 to 1%. Palaskas et al. (1981) used nonprestressed prestressing strands as flexural reinforcement. Palaskas et al. (1981) found that the ACI Building Code shear design provisions for v_c are unconservative for members with ρ_w less than 1%. The ratio of their test shear cracking stress to the calculated shear cracking stress using Eq. 1.1 was equal to 0.82, with a coefficent of variation of 10%. Palaskas et al. (1981) observed that, for their beams, the shear contribution of the stirrups was about 50% greater than predicted by the ACI Building Code design provisions (Eq. 1.5). The added strength was due to the fact that the critical shear cracks had a horizontal projection greater than the effective depth of the beam, thereby intercepting more stirrups than predicted by ACI 318. Based on their experiments, Palaskas et al. (1981) came to the conclusion that, despite the low test values of v_c, the shear provisions of the ACI Building Code were safe for lightly reinforced beams, mainly because of 1) the shear contribution of the stirrups, and 2) the minimum shear reinforcement requirements for beams with $V_u > \phi V_c/2$. Largely because of this research, ACI Committee 318 did not adopt Eq. 1.10.

Rodrigues and Darwin (1984, 1987) extended the research of Palaskas et al. (1980, 1981) to lightly reinforced T-beams subjected to negative bending. Like Palaskas et al. (1980, 1981), Rodrigues and Darwin (1984, 1987) used nonprestessed

prestressing strands as flexural reinforcement. Test data from nine T-beams with ρ_w equal to 0.47 or 0.70% and with a/d equal to 4 provided further evidence that the ACI equations for V_c and V_s were inaccurate for lightly reinforced beams. Rodrigues and Darwin (1984) inferred that the smaller effective concrete section at the negative moment region, caused by cracking of the flanges, and the lower bond strength for negative flexural reinforcement, due to the "top-bar effect," were the causes of the lower shear cracking loads in the negative moment regions. In positive moment regions, the shear cracking load was 13% lower and the stirrup contribution was 50% higher than predicted by the ACI equations, while in the negative moment regions, the shear cracking load was 29% lower and the stirrup contribution was 20% higher than, predicted by the ACI equations. The lower shear reinforcement effectiveness was due to the fact that critical shear cracks were steeper in the negative moment regions and, thus, intercepted fewer stirrups than in positive moment regions. In all, they concluded that the ACI Building Code overestimates the shear cracking load in the positive and negative moment regions and underestimates the stirrup contribution in the positive and negative moment regions.

In studies by Haddadin et al. (1971), the contribution of shear reinforcement to the shear strength of T-beams was 75% higher than the strength calculated using the ACI provisions. Beams in their studies had flexural reinforcement ratios in excess of 1.8%. Haddadin et al. (1971) found that the shear cracking load was higher in the positive moment regions than in the negative moment regions.

Al-Nahlawi and Wight (1989) tested 25 short rectangular beams with low longitudinal reinforcement ratios. Concrete compressive strength ranged from 5600 psi to 10600 psi. Stirrup spacings of d, 0.75d, 0.5d, and 0.33d were used. Test results indicated that the conservativeness of the ACI Code equations for concrete beams with nominal stirrup strength $v_s = \rho_v f_{vy} = 50$ psi decreased as the concrete

strength increased. The reduced conservativeness was mainly attributed to diminished aggregate interlock due to smooth failure planes for high strength concrete. Based on their analysis, they recommended a minimum value of stirrup reinforcement

$$\rho_v f_{vy} = \frac{A_v f_{vy}}{b_w s} \geq \frac{f'_c}{100} \geq 50 \text{ psi} \qquad (1.13)$$

to counter the effect of diminished aggregate interlock in high strength concrete, and an increase in the maximum stirrup spacing to $0.75d_v$, where d_v was the distance between top and bottom longitudinal steel.

In 1990, Pasley et al. (1990) studied the shear strength of six two-span T-beams with and without web reinforcement. The primary variables in their investigation were the longitudinal flexural reinforcement ratio, ρ_w (0.75% and 1.0%) and nominal stirrup strength, $\rho_v f_{vy}$ (0 to 82 psi). Their tests indicated that the ACI Building Code overpredicts the concrete shear capacity of lightly reinforced beams without shear reinforcement. They observed little difference between shear cracking stresses in the negative and positive moment regions for beams. Also, for both the negative and positive moment regions, the stirrup contribution to shear strength exceeded the value predicted by ACI 318-89 and increased with increasing flexural reinforcement ratio.

Similar to other lightly reinforced concrete members, joists are open to concerns regarding shear strength and stirrup effectiveness. Though studies on joists are very limited, some of the concerns for other lightly reinforced concrete members became apparent in studies by Hanson (1969) and Somes and Corley (1974) of joists with web openings. The studies involved simple span joists tested in a inverted

position to simulate adjacent negative moment regions at a girder. Six of the specimens in the two studies (five with lightweight concrete and one with normal weight concrete) did not contain web openings. A short transverse girder was included in the specimen, and the webs were tapered. The joists had no web reinforcement. These specimens had values of ρ_w = 1.01 or 1.38% and a/d between 4.4 and 4.8. The one normal weight concrete joist failed at a load equal to 94% of the value predicted by ACI 318-89 and the other five lightweight concrete joists failed at an average load equal to 85% of that predicted by ACI Building Code (ACI 318-89). The predicted strengths were thought to be high because the average web width was used to calculate the shear force V_c. Using the minimum width resulted in conservative predictions. These results prompted ACI Committee 318 to consider the use of the minimum web width for b_w in negative moment regions, but, ACI Committee 318 made no changes in design provisions. The tests conducted by Rodrigues and Darwin (1987) suggest that the problem has little to do with the reduction in shear strength due to tapered web. Rather, the joists tested by Hanson (1969) and Somes and Corely (1974) had a reduced shear strength due to cracking of the flange and a reduction in flexural bond strength due to the top-bar effect - problems that occur in negative moment regions.

CECO Corporation (1985) commissioned three tests at the New Jersey Institute of Technology to study the effect of using the average width in the negative moment regions. The specimens were short simple span double web joists tested in negative moment regions. The results showed that using an average value of b_w, rather than the minimum web width, was satisfactory. These tests used a high value of ρ_w, 1.6%, to obtain a flexural failure, which is considerably higher than normally used. Hence, the tests should have been expected to produce unrealistically high values of concrete shear strength.

Phillips and Schultz (1988) suggested that the low shear strengths obtained by Rodrigues and Darwin (1984, 1987) may have been due to the use of nonprestressed prestressing strand as flexural reinforcement. They felt that the prestressing steel may have been subjected to larger strains and deformations than would occur with typical Grade 60 reinforcing bars. The larger deformations would produce larger and wider flexural cracks in the concrete, thereby reducing the effective cross-sectional area in shear. Phillips and Schultz (1988) used deformed reinforcing bars to study the effect of web taper on the shear strength of lightly reinforced concrete joists, with $\rho_w = 0.6$ and $a/d < 2.5$, and observed that the average web width is the best choice for calculating the shear capacity of joists. The shear strength of the members averaged less than 80% of the predicted cracking shear strength of ACI 318-83 (without regard for the 10% increase in capacity allowed for joists). Unlike Rodrigues and Darwin (1987), Phillips and Schultz (1988) found the positive moment regions to have lower strength than the negative moment regions. Phillips and Schultz (1988) concluded that this lower shear strength was due to the low a/d used to preclude a flexural failure. The low a/d values qualified the joists tested by Phillips and Schultz (1988) as "deep beams" for shear evaluation and resulted in significant arching in the negative moment regions. They concluded that results similar to those obtained by Rodrigues and Darwin (1984, 1987) would be expected with longer spans.

1.4 Current design provisions

The current design provisions for concrete shear capacity in ACI 318-89 are based on the load required to cause diagonal tension cracking in the member. The design philosophy for shear recommended by ACI 318-89 is to calculate the factored shear force, V_u, and to insure that this force is less than the total contribution of the concrete and the shear reinforcement. The concept can be expressed as:

$$V_u \leq \phi(V_c + V_s) \qquad (1.14)$$

in which V_u is the factored shear force at the section considered; ϕ is the strength reduction factor = 0.85; V_c is the normal shear strength of the concrete; and V_s is the nominal shear strength provided by shear reinforcement.

The design provisions in ACI 318-89 require the use of a minimum amount of shear reinforcement when the factored shear, V_u, exceeds $\phi V_c/2$. The minimum shear reinforcement provision does not apply to joist construction, where shear reinforcement is required only for the portion of the factored load that exceeds the full concrete design strength, ϕV_c. ACI 318-89 requires that shear reinforcement be provided when the factored shear, V_c, exceeds $\phi V_c/2$ for beams or ϕV_c for joists.

The ACI Building Code (1989) specifies that the stirrup spacing, s, must not exceed one-half of the effective depth, or 24 inches, and that the shear reinforcement, A_v, must be at least:

$$A_v = 50\frac{b_w s}{f_{vy}} \qquad (1.15)$$

which corresponds to a nominal shear of stress, $\rho_v f_{vy} = A_v f_{vy}/b_w s = V_s/b_w d = 50$ psi. The ACI 318-89 requirement for minimum shear reinforcement, Eq. 1.15, closely matches the recommendation given by Al-Nahlawi and Wight (1989) in Eq. 1.13. A_v in Eq 1.15 must be multiplied by $f'_c/5000 \leq 3$ for $f'_c \geq 10000$ psi to allow $\sqrt{f'_c}$ to exceed 100 psi in Eq 1.1 and 1.2. Otherwise, $\sqrt{f'_c}$ in Eq 1.1 and 1.2 is limited to a maximum of 100 psi. The requirements for $\sqrt{f'_c}$ > 100 psi were added in 1989 (ACI 318-89).

For concrete joists, section 8.11.8 of ACI 318-89 permits the concrete contribution to shear strength, V_c, in Eqs. 1.1 and 1.2, to be increased by 10%. This increase in shear strength is justified by ACI 318-89 on the basis of: 1) "satisfactory performance of joist construction with shear strengths, designed under previous ACI Building Codes, which allowed comparable shear stresses," and 2) "redistribution of local overloads to adjacent joists." To insure that joist floors possess an adequate local overload redistribution capability, Chapter 8 of ACI 318-89 places restrictions on the geometry and spacing of joists.

1.5 Object and Scope

The purpose of this research is to study the behavior and measure the shear capacity of continuous lightly reinforced concrete joists. The focus is two fold. First, the behavior of single web members is observed to determine how well the ACI Building Code provisions reflect their shear capacity. Second, multiple web joists are tested to determine if the additional 10% shear capacity, as permitted for joist design by ACI rules, is justified. The investigation includes tests of six continuous two-span single web joists and two continuous two-span triple web joists, with joist-girder connections. The flexural reinforcement ratio, ρ_w, in the negative moment region ranges from 0.76% to 1.04% for all tests and the amount of shear reinforcement, $\rho_v f_{vy}$, ranges from 0 psi to 70 psi.

Chapter 2 presents the properties of the materials used, the test procedures, and the experimental observations for the current investigation. Chapter 3 presents the techniques used to determine the shear cracking load and the analysis of the current test results. In addition, in Chapter 3, the measured cracking and ultimate shears are compared with current ACI Building Code (1989) shear provisions, and, also, with previous investigators' predictive equations. Chapter 4 summarizes the research effort,

presents the conclusions, and suggests additional avenues of research.

CHAPTER 2

EXPERIMENTAL INVESTIGATION

2.1 General

The experimental investigation was designed to study the shear behavior of lightly reinforced concrete joists, with emphasis on the negative moment region of the joists. The primary variables were flexural reinforcement ratio referenced to the average width of the web, ρ_w, in the negative moment test region (one percent or less for all tests), the amount of shear reinforcement (between 0 to 70 psi), and the number of joists sharing the load (one or three). A description of the materials, the procedure used during the experimental work, and the experimental observations are presented in this chapter.

2.2 TEST SPECIMENS

Six single web and two triple web continuous joists of standard size (Figs. 2.1and 2.2) were constructed and tested. The joists consisted of two 17.5 ft spans. The flange width for the single web joists was 25 in., and the total flange width for the multiple web joists was 75 in. A flange thickness of 3 in. was used for both the single and multiple joist specimens, except for the negative moment regions of multiple web joist M1 where the depth was increased to 3.5 in. due to difficulty in fabrication caused by low slump concrete. The joists were 15 in. deep with a tapered web that ranged in width from 7 in. at the flange to 5 in. at the soffit.

The single web joists were supported by rollers at the free ends and by a transverse girder at the middle support. The multiple web joists were supported by transverse girders at both the free ends and at the middle support. The transverse girders had a depth of 15 in., a width of 12 in., and spans of 61 or 117 in. for single

web and multiple web joists, respectively. The transverse girder (for both the single and multiple web joists) at the middle support rested on pins at each end, that were in turn supported by load cells, as shown in Fig. 2.3. The transverse girders at the ends of the multiple web joists rested on rollers. The rollers and the load cells were supported on concrete pedestals. Two 1/32 in. thick teflon sheets were used between the bearing surfaces of pin supports to reduce friction. The pins and rollers were oriented to allow rotation in the longitudinal direction, performing as pin supports for the test joists and partially restrained supports for the girders. The test regions in the joists extended from the faces of the center transverse girder to the points of maximum positive moment in each span. The longitudinal reinforcement in the joists was placed on top of the corresponding longitudinal reinforcement in the girder at the joist-girder junction. Concrete cover and reinforcement details followed the provisions of the ACI 318-89. Joist dimensions and properties are shown in Figs. 2.1 and 2.2 and Tables 2.1 and 2.2.

The two series of single web joists, designated K and L, had nominal negative moment region flexural reinforcement ratios, ρ_w, of 0.8 and 1.0 percent, respectively. The multiple web specimens had a nominal negative moment region flexural reinforcement ratio of 1.0 percent. For the multiple web specimens, the individual joists were identified as center-east, center-west, north-east, north-west, south-east, and south-west joists. The joists were designed to fail in shear in the negative moment regions and, in some cases, to yield in negative bending. To prevent the formation of a mechanism prior to shear failure, the bottom steel was designed to insure that the joists did not fail in positive bending. Stirrups provided within the test regions consisted of smooth low carbon steel wires, with diameters of 0.125, 0.167, or 0.210 in., at a spacing of 6 in. To prevent a shear failure outside of the test regions, No. 3 bar stirrups were provided at a spacing of 6 in. The flanges of both single and

multiple web joists were reinforced transversely with No. 3 bars spaced at 6 in.

The longitudinal flexural reinforcement provided for the single and multiple web joists is summarized next and in Fig. 2.4:

Joist K1: Both the top and the bottom reinforcement consisted of two No. 5 bars, providing ρ_w of 0.79 percent for both the positive and negative moment regions.

Joist K2: Two No. 5 bars and two No. 6 bars were used as bottom reinforcement and two No. 5 bars were used as top reinforcement, providing ρ_w of 2.05 percent in the positive moment regions and ρ_w of 0.77 in the negative moment regions.

Joist K3: Four No. 5 bars were used as bottom reinforcement and two No. 5 bars were used as top reinforcement, providing ρ_w of 1.63 percent in the positive moment regions and ρ_w of 0.77 percent in the negative moment regions.

Joist L1: Two No. 6 bars and four No. 4 bars were used as bottom and top reinforcement, respectively, providing ρ_w of 1.13 percent for the positive moment regions and ρ_w of 1.04 percent in the negative moment regions.

Joist L2: Four No. 6 bars were used for the positive regions and four No. 4 bars were used for the negative moment regions, providing ρ_w of 2.43 percent in the positive moment regions and ρ_w of 1.04 percent in the negative moment regions.

Joist L3: Two No. 6 bars and four No. 4 bars were used as bottom and top reinforcement, respectively, providing ρ_w of 1.12 percent in the positive moment regions and ρ_w of 1.0 percent in the negative moment regions.

Specimens M1 and M2: For the multiple web joists, M1 and M2, the flexural reinforcement and reinforcing ratio were the same as provided for joist L3.

If more than two bars were used as flexural reinforcement in either the positive or the negative moment regions, the steel was placed in two layers (Fig. 2.4).

2.3 Materials

2.3.1 Concrete

Air-entrained concrete was supplied by a local ready mix plant. Type I Portland cement, 3/4 in. nominal maximum size crushed limestone, and Kansas River sand were used to make the concrete. The specific gravity of the coarse and fine aggregate was 2.62 and 2.59, respectively. During casting, air content and slump were measured both at the ready mix plant and at the structural testing laboratory. Air content ranged from 3.1 to 4.8 percent. Slump ranged from 3 in. to 5 1/4 in., except for joist M1, which had a 2 in. slump. The compressive strength of the concrete, f'_c, ranged from 4200 psi to 4910 psi. Standard 6 x 12 inch compressive test cylinders were cast and tested for each joist. Concrete mixture proportions and properties are presented in Table 2.3.

2.3.2 Steel

The longitudinal reinforcement consisted of ASTM A 615 Grade 60 No. 4, No. 5, and No. 6 bars. Shear reinforcement in the test regions (single web joists only) was provided by smooth low carbon wires with diameters of 0.125, 0.167, and 0.210 in. To prepare the wire stirrups, the steel wire was cut into the required lengths from a main coil and heat treated in a heat furnace at 700° F for 20 minutes. This annealing process provided a sharp yield plateau. Shear reinforcement in the nontest region was provided by No. 3 bars. Steel properties are presented in Table 2.4.

2.4 Specimen Preparation

Standard pan joist forms and BB plyform were used to construct the forms, which were supported on tables made out of 2 x 4 in. wood studs. The wood forms were lacquered before casting each specimen to limit water damage. Polyvinyl

Chloride (PVC) pipe insets were placed in the multiple web specimen forms to provide holes to pass load rods through the joist slab. After the reinforcing cage was fabricated in place using commercially available ties and steel chairs, strain gages were installed on test stirrups. The forms were oiled with form release agent and bolted in place. Care was taken to prevent oil from coming in contact with the reinforcement.

The No. 3 bar stirrups in the non-test regions were fabricated with 90 degree angle hooks in a reinforcing bar bender. The wire stirrups in the test region were fabricated in a jig and welded at the top over a lap length equal to the width of the stirrup to provide adequate anchorage. Typical reinforcement cages used for joists with and without test stirrups are shown in Figs. 2.4 and 2.5.

Micro-Measurements Type EA-06-060LZ-120 strain gages were used to measure strains in the stirrups and flexural steel. The strain gages were installed following the procedures used by Palaskas and Darwin (1980) and polysulfide encapsulated with Micro-Measurements Type M-Coat J for protection against water. The gages were located at the mid-height on the test stirrups and at points of maximum bending on the flexure steel. Typical strain gage locations are shown in Fig. 2.6. The lead wires from the strain gages were bound together with plastic ties and passed out through holes in the sides of the forms.

A systematic approach was used while placing concrete. The initial and final discharge of the concrete from the concrete truck was used to pour the end regions of the joist. The test region was poured from the middle portion of the discharge. A one cubic yard steel bucket was used to cast the joists in two stages: First the web and then the flanges. Each layer was consolidated using internal vibrators. The concrete samples were made in accordance with ASTM C 31. The joists were screeded in longitudinal direction and magnesium bull floated in the transverse

direction. For the multiple web joists, screeding was performed using a vibrating screed.

Care was taken not to over-finish the surface of the joists so that minimum bleed water was present after screeding. After the bleed water evaporated, curing compound was applied to the test specimen and the concrete samples, and the specimens were covered with polyethylene sheets to limit moisture escape. The forms were stripped when the concrete attained a compressive strength of 3000 psi. The joists and the test cylinders were kept moist until a compressive strength of 4000 psi was attained. The concrete was then allowed to air dry until the time of test, at a strength of about 4500 psi. Tests were conducted 7 to 16 days after casting. The test cylinders were cured at the same manner as the joists.

After the forms were stripped, the joists were prepared for testing. Diluted white latex paint was applied within the test regions on the south face of the single web joists and on all faces of the multiple web joists. Diluting the latex paint allowed cracks to be seen without creating a thick film that could bridge over a developing crack. Stirrup and longitudinal reinforcement locations were marked on the south face of joist. Marking of the reinforcement locations helped to serve as a coordinate system for the cracks that formed during the test.

Following the procedures used by Palaskas and Darwin (1980) to measure concrete strains, Precision Type W240-120 paper backed strain gages were installed on the top and bottom surfaces of the joists. Concrete gages were installed in both the maximum positive and maximum negative moment regions. Concrete strain gage locations are shown in Fig. 2.6.

2.5 Loading System

For the single web joists, loads were applied midway between the face of the

transverse girder and the center of the outside roller in each of the two spans (hereafter referred to as "midspan"), as shown in Figs. 2.5 and 2.7. For multiple web joists, load was applied to study the effect of load sharing between the joists. For specimen M1, loading was applied at the midspan of the center-east and center-west joists. For specimen M2, loading was applied at the midspan of the south-east and south-west (edge) joists.

Two cylindrical compression load cells were positioned below the supports of the center transverse girder to measure the joist reactions at mid-support (Figs. 2.3 and 2.7). The load cells were strain-gaged with a full bridge. Four steel load rods were used to transfer the load from hydraulic jacks to the joists (Fig. 2.7). The load rods were strain gaged as load cells. The hydraulic jacks, located below the structural floor and powered by an Amsler hydraulic testing machine, were used to pull down on the four load rods. A longitudinal steel beam was used at each loading point to transfer the load from two load rods to the joist. The applied load was transmitted from the loading steel beam to the test joist by a bolster. The total weight of the loading system, (i.e., steel beams, bolster and rollers) on one span was 300 lbs.

2.6 Instrumentation

The load cells and the load rods were calibrated for every three single web joist tests and before each of the multiple web joist tests. Midspan deflections were monitored using linear variable differential transformers (LVDT's) placed at the bottom of the joists (Fig. 2.6). Load rod strain gage, concrete strain gage, and stirrup strain gage readings, and midspan deflections were recorded by a Hewlett-Packard data acquisition system which was remotely controlled by a microcomputer. A Hewlett-Packard plotter was used to plot the load versus average midspan deflection throughout the test. During the test, applied loads and the corresponding reaction at

the center support were printed out at every load step, and all data were recorded on a floppy disk. After the test, the recorded voltage readings from the strain gages and LVDT's were reduced and converted to strain values using a computer spread sheet.

2.7 Test Procedure

At the initiation of each test, the joist was loaded within the elastic range and then unloaded to ensure that all equipment and gages were in working order. The initial load was 30 percent of the calculated cracking load (approximately 6 kips). Initial readings were again taken for all strain gages, load rods, load cells, and LVDT's at zero load. A 2 kip load step was used. At each load step, load, strain, and deflection readings were taken while maintaining the load constant. Cracks were marked after the application of each load step using felt-tipped markers. The total applied load was inscribed next to the end of the crack at each load step. The entire operation of marking cracks was done as quickly as possible in order to limit the effects of creep.

After a joist had undergone failure, it was unloaded and external stirrups were used to clamp the failed region, as shown in Fig. 2.8. Clamping with the external stirrups helped to increase the shear capacity of the failed region and allow the test to continue to determine the shear capacity of other test regions. The external stirrups were tightened sufficiently to avoid slippage during reloading. After installation of the external stirrups, the joist was reloaded to the point at which the first section failed. Load was then increased in steps of 2 kips until the next region failed. After the second failure, additional external stirrups were added in the new failure region. The entire process was repeated until the joist failed in all test regions or had reached its maximum load carrying capacity. An entire test took three to four hours to complete. Concrete cylinders and wire samples were tested immediately after the test.

Photographs of the cracked surfaces of joist were taken during and after the test. During the test, experimental observations were entered in a time log.

2.8 Experimental observations

The experimental observations are summarized in this section. The crack patterns are shown in Figs. 2.9a through 2.9d. Plots of total load versus average midspan deflection for all joists are shown in Figs. 2.10a through 2.10f. A detailed analysis of the results is presented in Chapter 3.

2.8.1 Single web joists

In general, for single web joists, flexural cracks formed first at the bottom of the webs in the maximum positive moment regions. In the negative moment regions, the flexural cracks appeared at the top of the flange near the face of the transverse girder and travelled vertically downwards. As the load increased, cracks appeared further away from the face of the transverse girder, extended vertically downwards until they met the web, and then propagated toward the support until they met the face of the transverse girder near the level of the bottom flexural steel. The angle of inclination of the cracks changed gradually, becoming flatter as the cracks approached the transverse girder. At shear failure, wide cracks propagated along the bottom of the flange from the negative moment region to the middle of the positive moment region, intersecting two or three stirrups before passing diagonally upward through the flange. In the positive moment region, cracks formed near the bottom of the web and propagated upward towards the point of maximum positive moment. These diagonal cracks occurred after the formation of flexural cracks in the negative moment regions. As the load increased, more cracks formed away from the loading points in the positive moment regions. Fewer cracks were observed in the negative moment

regions than in the positive moment regions. The lower number of cracks may be due to lower bond strength of the top-cast flexural reinforcement compared to that of the bottom-cast flexural reinforcement. Few flexure cracks formed in the non-test regions. For the six single web joists tested there were a total of sixteen failures, of which nine occurred in negative moment regions.

The six single web joists were fabricated and tested in the following order: K1, K2, L1, L2, K3, L3. The loads and the middle support reaction at failure are given in Table. 2.5. The force values account for the weight of the loading system but do not account for the self weight of the joist. The crack patterns for the single web joists are shown in Figs. 2.9a and 2.9b. The peak shear forces, V_n(test) and peak shear stresses, v_n(test) are given in Table 2.6. Summaries of the loading and failure sequences are given below:

Joist K1: The west test region had shear reinforcement, $\rho_v f_{vy}$, of 24.8 psi (0.17 MPa). No shear reinforcement was provided in the east test region. Shear cracks appeared in the west negative moment region at 14.1 kips (62.74 kN). Shear failure occurred first in the east negative moment region at a total applied load of 24.48 kips (108.93 kN). After clamping the east span negative moment region with external stirrups, the test was continued, and during reloading, concrete on the bottom of the transverse girder spalled off at 15.5 kips (68.97 kN). Upon further loading, sudden failure occurred in the west negative moment region at 26 kips (115.70 kN). This failure occurred simultaneously with yielding of the flexural steel in the positive moment regions (the steel in the negative moment region was already yielding). Hence, the west negative moment region failure cannot be considered a true shear failure. The test was terminated at this point.

Joist K2: Both the east and west test regions had shear reinforcement, $\rho_v f_{vy}$, of 25.5 psi (0.17 MPa). Shear failure occurred first in the east positive moment

region at 44.08 kips (196.15 kN). After the failure, the joist was unloaded, external stirrups were installed, and the joist was reloaded. The second shear failure occurred in the east negative moment region at 48.37 kips (215.24 kN). External stirrups were again installed, and the joist was reloaded. The third shear failure occurred in the west negative moment region at 50.25 kips (223.61 kN). Once again external stirrups were installed, and the joist was reloaded. The fourth shear failure occurred in the west positive moment region at 57.18 kips (254.45 kN). This specimen was the only single web joist that failed in all four of the test regions. At failure, the shear cracks intercepted 5 and 4 stirrups in east and west negative moment regions, respectively, and 4 and 3 stirrups in the east and west positive moment regions, respectively.

Joist K3: The west test region had shear reinforcement, $\rho_v f_{vy}$, of 23.8 psi (0.16 MPa). The east test region had no shear reinforcement. Shear failure occurred first in the east negative moment region at 34.0 kips (151.30 kN). After installing the external stirrups and reloading, wide cracks formed in the west negative moment region. Failure occurred simultaneously in east positive and west negative moment regions at 38.29 kips (170.39 kN). At failure, the shear crack intercepted 3 stirrups in the west negative moment region.

Joist L1: The west test region had shear reinforcement, $\rho_v f_{vy}$, of 25.1 psi (0.17 MPa). The east test region had no shear reinforcement. Shear failure occurred first in the east negative moment region at 28.39 kips (126.33 kN). After installing the external stirrups and reloading, the second shear failure occurred in the west negative moment region at 28.83 kips (128.29 kN). After clamping with external stirrups and reloading again, the third shear failure occurred in the east positive moment region at 37.59 kips (167.27 kN). Upon further loading, concrete spalled off at the bottom of the negative moment region of the joist. At this point wide cracks in the negative moment regions prevented the joist from picking up any additional load, and the test

was terminated. At failure, the shear crack intercepted 4 stirrups in the west negative moment region.

Joist L2: The west test region had shear reinforcement, $\rho_v f_{vy}$, of 69.7 psi (0.48 MPa) and the east test region had shear reinforcement, $\rho_v f_{vy}$, 44.6 psi (0.31 MPa). Shear failure occurred first in the east negative moment region at 51.98 kips (231.31 kN). The cracks propagated diagonally between the flange and the bottom of the web. After installing external stirrups and reloading, the second shear failure occurred in the west positive moment region at 62.81 kips (279.50 kN). At this point, wide cracks in the negative moment regions prevented the joist from picking up any additional load and the test was terminated. At failure, the shear cracks intercepted 4 stirrups in both the east negative moment region and west positive moment region.

Joist L3: Similar to joist L1, this joist had shear reinforcement in the west test region, $\rho_v f_{vy}$, of 23.8 psi (0.16 MPa). No test stirrups were provided in east test region. Shear failure first occurred in east negative moment region at 35.40 kips (157.53 kN). Upon clamping external stirrups and reloading, the west positive moment region failed in shear at 37.0 kips (164.65 kN). Wide cracks in the positive moment regions prevented the joist from picking up any additional load. At failure, the shear crack intercepted 3 stirrups in the west positive moment region.

2.8.2 Multiple web joists

Experimental observations for the multiple web joists are presented in this section. Two multiple web joists, M1 and M2, were fabricated and tested. Peak loads and middle support reactions at failure are given in Table 2.7. The force values account for the weight of the loading system but not for the self weight of the joist. For specimen M1, loading was applied at the midspan of the center-east and center-west joists. For specimen M2, loading was applied at the midspan of the south-east

and south-west (edge) joists. Crack patterns for the multiple web joists are shown in Fig. 2.9c and 2.9d.

As the test progressed, the applied load was initially carried by the joist on which it was applied. As the load increased, however, the applied load was transferred to and shared by the adjacent joists. In general, cracks began as a flexure cracks and, as the loading increased, the cracks traveled toward the load points and supports. Shear cracks that formed in the positive moment regions propagated to the level of the bottom longitudinal reinforcement of the loaded joist. The cracks then propagated along the reinforcement toward the negative moment regions as bond cracks. Summaries of the loading and failure sequences are given below:

Specimen M1: Load was applied to the center-east and center-west joists at midspan. Initial cracks started at 14 kips (62.30 kN) at the bottom of flange in the negative moment region of center-west joist. As the load increased, cracks formed at the top of the flange of the center-west joist's negative moment region and propagated across the width of the specimen. At 42 kips (186.90 kN), shear cracks appeared in the positive moment regions of center-east and center-west joists. Upon loading further, shear cracks in the positive moment regions of center-east and center-west joists propagated to the top of the flange and to the bottom longitudinal reinforcement, thereby causing splitting of the bottom concrete cover. Shear cracks appeared in the negative moment regions of the north-west joist at 45.96 (204.52 kN) and south-west joist at 52.00 kips (231.40 kN), respectively. Further increase in the load caused all of the bottom concrete cover of center-east and center-west joist's test regions (east positive to west positive) to split and separate from the longitudinal reinforcement. Failure occurred first in the center-east and center-west joist's positive moment region at 59.48 kips (264.68 kN) (Fig. 2.9c). After installing external stirrups in the positive moment regions of center-east and center-west joists, only a small

additional load could be applied before failure occurred simultaneously in the negative moment regions of center-east and center-west joists (bond failure of bottom bars) and in the negative moment regions of the north-west and south-west joists (shear failure) at 62.27 kips (277.10 kN). At failure, no shear failure cracks were observed in the negative moment regions of the center-east and center-west joists. A key observation from the test was that, although the load was applied to the center-east and center-west joists, the negative moment region shear was carried primarily by the adjacent joists at failure. This was likely due to the fact that the adjacent joists were stiffer near the middle support due to their proximity to the ends of the transverse girder.

Specimen M2: Load was applied on the south-east and south-west joists at midspan. Flexural cracking through the slab in the negative moment regions of the south-east and south-west joists occurred at 34 kips (151.30 kN). Shear cracks appeared in the webs of south-west and center-west joist's negative moment regions at 40.10 kips (178.44 kN). Simultaneously, at 40.10 kips (178.44 kN), wide flexural cracks appeared in the south-east joist's positive moment region. Upon further loading, shear cracks appeared in south-east joist's negative moment region at 44.06 kips (196.07 kN). Flexural cracks appeared in the adjacent center-east and center-west joist's positive moment regions at 48 kips (213.60 kN). At 50.06 kips (222.76 KN), shear cracks in the positive moment region of south-west joist propagated to the bottom of the flange and to the bottom longitudinal reinforcement, traveling towards the south-west joist's negative moment region. A further increase in the load caused all of the bottom cover of south-west joist's test region to split and separate from the longitudinal reinforcement. A shear crack appeared in the negative moment region of the center-east joist at 52.06 kips (231.66 kN) and failure occurred simultaneously in the south-east (shear failure) and south-west (bond failure of bottom bars) joist's negative moment regions. After installing external stirrups in both failure regions, the

loading could be increased only by a small amount before shear failure occurred in the south-east and south-west joist's positive moment regions at 52.32 kips (232.81 kN). Few flexure cracks appeared on the north-east and north-west joists (Fig. 2.9d).

Chapter 3

ANALYSIS AND DISCUSSION OF TEST RESULTS

3.1 General

In this chapter, the test results are analyzed and presented separately, first for single web joists and then for multiple web joists. The analyses include three procedures for determining the shear cracking load. Shear cracking stresses are compared with the values obtained using empirical expressions from ACI 318-89, Zsutty (1968), Rajagopalan and Ferguson (1968), ACI-ASCE Committee 426 (1973), Batchelor and Kwun (1981), and Bazant and Kim (1984). The effectiveness of stirrups in carrying shear is estimated and the degree of load sharing between adjacent joists is investigated. Nominal shear stresses are compared with the design provisions in ACI 318-89.

3.2 Procedures for Determining the Shear Cracking Load

Three techniques, based on the crack pattern, stirrup strain, and concrete strain, are used to establish the shear cracking load. These methods are explained briefly in the following sections prior to their application. Generally, the shear cracking load is defined as the load at which significant changes in a load carrying mechanisms occur, resulting in the redistribution of stresses within a beam. The objective is to determine the load at which the change in load carrying mechanism occurs.

3.2.1 Crack pattern analysis

Determination of the shear cracking load using crack pattern analysis is based on the identification of a diagonal tension crack. There are a number of definitions for shear cracking load. Haddadin et. al (1971) defined the shear cracking load as the

load at which a diagonal tension crack makes an angle of 45 degrees with the transformed neutral axis of the beam. Batchelor and Kwun (1981) described the shear cracking load as the load at which an inclined crack extends from the longitudinal tension reinforcement into the compression zone, making a 45 degree angle with the flexural reinforcement. Mathey and Watstein (1958) studied rectangular beams and defined the shear cracking load as the load at which a diagonal tension crack, intersecting the level of longitudinal reinforcement at about 45 degrees, first crosses the neutral axis of the beam. Palaskas et. al (1981) observed that only critical diagonal tension cracks (i.e. those that cause failure) make angles of 45 degrees or less with the longitudinal reinforcement, and noted that the use of Mathey and Watstein's (1958) definition of shear crack, clearly overestimates the shear cracking load. Hence, they defined the shear cracking load as the load at which a shear crack makes an angle of 45 degrees or flatter at, or above, the transformed neutral axis of a beam. Rodrigues and Darwin (1984, 1987) extended this definition to continuous beams and defined the shear cracking load as the load at which a diagonal tension crack first makes an angle of 45 degree or less, at or above the neutral axis in the positive moment region, or at or below the neutral axis in the negative moment region. The current research uses the definition of shear cracking load presented by Rodrigues and Darwin (1984, 1987). The crack patterns for the test specimens are shown in Figs. 2.9a through 2.9d. Cracks, along with the corresponding total applied load, were marked on the exterior face of the joist after each load step. Photographs were taken of the joists after failure and used to determine the load at which the shear cracking occurred. The values of shear cracking load and shear cracking stress based on crack pattern are presented in Tables 3.1a and 3.1b for the negative and positive moment regions, respectively.

3.2.2 Stirrup Strain Analysis

The second method used to determine the shear cracking load is based on the stirrup strain. Since, the formation of shear cracks requires stirrups to carry load, the shear cracking load is defined as the load at which a sharp increase in stirrup strain is observed. Before joist cracking, strain gages on stirrups record little strain. Measurable strain gage readings are obtained when either a flexural crack or a shear crack crosses a stirrup. A gradual increase in stirrup strain indicates that a flexural crack has intercepted the stirrup, while a sharp increase in stirrup strain indicates that a shear crack has intercepted the stirrup. A sharp increase is seen for the shear crack because it transfers more force to the stirrup than a flexural crack due to the flatter angle of inclination of the shear crack. Therefore, the load at which a sharp increase in stirrup strain occurs is taken to be the shear cracking load.

The load versus stirrup strain curves were plotted for all of the stirrup strain gages. Although, the strain gages were checked for functionality before concrete placement, a few gages were found to be defective after the casting or during the test. Therefore, not all of the plots could used to determine the shear cracking load.

The lowest load at which any of the total load - stirrup strain plots in a shear span exhibited a sharp increase in stirrup strain was selected as the shear cracking load. The specific plots used for the single web joists are shown in Figs. 3.1a through 3.1p. The stirrup for which each plot was selected is identified in the title of the plot by a number representing the position of the stirrup with respect to the center support (closest stirrup is 1, etc.). The values of shear cracking load and shear cracking stress based on stirrup strain are presented in Tables 3.1a and 3.1b for the negative and positive moment regions, respectively, along with those based on crack pattern.

3.2.3 Concrete Strain Analysis

The third method used to determine the shear cracking load is based on concrete strain. This method was successfully used by Palaskas et al. (1981), Rodrigues and Darwin (1984), and Pasley et al. (1990).

As the joist is loaded, the concrete strain on the compressive face of the joist increases until shear cracking occurs. Then a change in the load carrying mechanism occurs within the joist, the stresses are redistributed within the concrete, and the strain along the compressive face of the member decreases sharply, sometimes even changing from compression to tension. The shear cracking load is taken as the load at which a reduction in the concrete compressive strain occurs. For the current study, concrete gages were placed in maximum negative and positive moment regions. Unfortunately, the load versus concrete strain curves obtained from these gages did not consistently reveal the expected trends, and hence, concrete strain analysis is not used to determine the shear cracking load for the joists in this study.

3.3 Single web joists

This section presents and discusses the shear cracking stresses, stirrup effectiveness, horizontal crack projections, and nominal strength of the single web joists. Measured shear strengths are compared with empirical predictions.

3.3.1 Comparison of shear cracking stresses based on analysis method and moment region

In this section, the shear cracking stresses for the single web joists based upon crack pattern and stirrup strain analysis are compared. Shear cracking forces and stresses for negative and positive moment regions based upon the two techniques are given in Tables 3.1a and 3.1b.

Rodrigues and Darwin (1984, 1987) found that the shear cracking stresses based on crack pattern were lower in most cases than those determined using stirrup strain analysis. Pasley et al. (1990) found in most cases that the shear cracking stresses based on crack pattern were higher than those determined using stirrup strain analysis. The trends observed in the current study match those obtained by Pasley et al. (1990).

For the negative moment regions (Table 3.1a), the shear cracking stress based on crack pattern is higher than the shear cracking stress based on stirrup strain in 6 out of 8 cases.

For the positive moment regions (Table 3.1b), the shear cracking stress based on crack pattern is higher than the shear cracking stress based on steel stirrup analysis in 6 out of 7 cases, and equal in the seventh case (Joist L2-positive moment region-west span). In one other case (Joist K1-positive moment region-west span), shear cracking was measured based on stirrup strain although no shear crack was observed.

Comparing the stresses between the negative and the positive moment regions, Rodrigues and Darwin (1984, 1987) found that the shear cracking stresses determined by the crack pattern method were lower in the negative moment regions than in the positive moment regions. Pasley et al. (1990) found that the shear cracking stresses determined by the crack pattern method were higher in the negative moment regions than in the positive moment regions, as did Phillips and Schultz (1988) for their lightly reinforced joists with low shear span-to-depth ratio. In the current study, the shear cracking stress based upon crack pattern was lower in the negative moment region than in the positive moment region in 8 out of 12 cases, and essentially equal in the other 4 cases, agreeing with the observations of Rodrigues and Darwin (1984, 1987).

3.3.2 Comparison of measured strengths and empirical predictions

In this section, the shear cracking stresses obtained in Section 3.3.1 are compared with the values predicted by empirical equations. The predicted shear cracking stresses for the joists in the current study based upon ACI 318-89 (Eq. 1.2), Zsutty (1968) (Eq. 1.7), Rajagopalan and Ferguson (1968) (Eq. 1.8), ACI-ASCE Committee 426 (1977) (Eq. 1.10), Batchelor and Kwun (1981) (Eq. 1.11), and Bazant and Kim (1984) (Eq. 1.12) are presented in Tables 3.2a and 3.2b for the negative and positive moment regions, respectively. The equations from Zsutty (1968) and Bazant and Kim (1984) require a value for the shear span-to-depth ratio, a/d or M/(Vd), to calculate the shear strength (shear span, a, is set equal to the ratio of the moment to the shear, M/V). The moment and shear used in the shear span-to-depth ratio are taken at the face of the joist for the negative moment region shear stresses and at the loading point for the positive moment region shear stresses, respectively. M and V for use in the predictive equations are established using the loads based on crack patterns. It should be noted that the Zsutty (1968) and Bazant and Kim (1984) equations are not valid when the ratio M/(Vd) is less than 2.5. The values of M, V and M/(Vd) at each section are summarized in Tables 3.3a and 3.3b. For negative moment regions, the values of (M/Vd) based upon crack pattern analysis range from 2.13 to 3.85. For positive moment regions, the values of M/(Vd) range from 5.33 to 6.60.

Shear cracking stresses obtained based upon crack pattern analysis and stirrup strain analysis are compared with the values obtained from the empirical equations in Tables 3.4 and 3.5, respectively. The coefficients of variation for the ratios of test to predicted strength for the two techniques show that comparison with v_c based on crack pattern (Tables 3.4a and 3.4b) produce significantly lower coefficients of variation than comparisons with v_c based on stirrup strain (Tables 3.5a and 3.5b). For that

reason, the discussions that follows addresses only comparisons with the shear cracking stresses based on crack pattern.

For negative moment regions, the average ratio of the shear cracking stress to the value predicted by ACI 318-89 is 83%, with a coefficient of variation of 11.83%, as shown in Table. 3.4a. The low test/prediction ratio agrees with the findings of previous researchers (Rodriguez et. al 1959, Krefeld and Thurston 1962, Kani 1966, Rajagopalan and Ferguson 1968, Kani et. al 1979, Attiogbe et. al 1980, Palaskas and Darwin 1980, Batchelor and Kwun 1981, Palaskas et. al 1981, Rodrigues and Darwin 1984, 1987, Pasley et. al 1990) who found that the ACI design provisions overestimate the shear cracking stress of lightly reinforced concrete beams, especially for negative moment regions. The average test/prediction ratios for shear cracking stress are 79% and 104% for the expressions developed by Zsutty (1968) and Bazant and Kim (1984), respectively, with coefficients of variation 8.24% and 11.39%. The test/prediction ratios are 106%, 89%, and 105% for the expressions developed by Rajagopalan and Ferguson (1968), ACI-ASCE Committee 426 (1977), and Batchelor and Kwun (1981), respectively, with coefficients of variation 11.58%, 11.82%, and 12.11%.

For positive moment regions, the average ratio of the shear cracking stress to the value predicted by ACI 318-89 is 103%, with a coefficient of variation of 19.52% (Table 3.4b). The ratio is 101% and 102%, respectively, for comparisons based on expressions developed by Zsutty (1968) and Bazant and Kim (1984), with coefficients of variation 11.90% and 10.38%; the ratio is 83%, 74%, and 85% for the comparisons based on expressions developed by Rajagopalan and Ferguson (1968), ACI-ASCE Committee 426 (1977), and Batchelor and Kwun (1981), respectively, with coefficients of variation 8.66%, 9.25%, and 9.98%.

Comparing the coefficients of variation obtained using the empirical equations

in crack pattern analysis, it is observed, that the positive moment regions have lower coefficients of variation than the negative moment regions (Tables 3.4a and 3.4b). Higher coefficients of variation in the negative moment regions mean more scatter with respect to the predictive equations. The greater coefficients of variation are likely due to the widely varying shear span-to-depth ratios in the negative moment regions, which are not accounted by the equations given by ACI 318-89, Rajagopalan and Ferguson (1968), ACI-ASCE Committee 426 (1977), and Bachelor and Kim (1984).

The equation by Bazant and Kim (1984) produces mean values closest to 1.0 both for the negative and positive moment regions, 1.04 and 1.02, respectively (Tables 3.4a and 3.4b). The Bazant - Kim (1984) expression also produces the lowest overall coefficient of variation, 10.58%, compared to 19.13% for ACI 318-89, 15.98% for Zsutty (1954), 13.23% for Rajagopalan and Ferguson (1968), 14.30% for ASCE-Committee 426 (1977), and 15.49% for Bachlor and Kwun (1981).

Overall, Eq. 1.2 (ACI 318-89) overestimates the shear cracking stress for concrete joists in the negative moment regions. In the positive moment regions, Eq. 1.2 predicts the shear strength of lightly reinforced concrete joists with an acceptable degree of accuracy. Overall, the coefficient of variation for ACI 318-89 is higher than the coefficients of variation for the other predictive equations (Table 3.4b).

3.3.3 Stirrup effectiveness

As load is increased above the shear cracking load, any additional capacity must be provided by stirrups. Thus, the increase in total shear stress above the shear cracking stress, v_n-v_c, can be used as a measure of the effectiveness of the shear reinforcement. v_n-v_c includes the shear carried by stirrups as well as by dowel action and aggregate interlock. Values of v_n-v_c for the single web joists based on crack

pattern and the nominal stirrup strength, $\rho_v f_{vy}$, in psi, are presented in Table 3.6.

Rodrigues and Darwin (1984, 1987) performed a regression analysis on the negative moment region data from their research and found the following relationship:

$$v_n - v_c = 1.19\rho_v f_{vy} + 4.70 \qquad (3.1)$$

with a correlation coefficient, r, of 0.96. Pasley et al. (1990) evaluated stirrup effectiveness for their beams in the negative moment region and obtained the following the expression:

$$v_n - v_c = 1.35\rho_v f_{vy} + 12.26 \qquad (3.2)$$

with a correlation coefficient, r, 0.87. In both cases, the total stirrup effectiveness was greater than would be expected based on a horizontal crack projection equal to the effective depth of the member (which would give v_n-v_c = $\rho_v f_{vy}$). Pasley et al. (1990) deduced that the difference between their results (Eq. 3.2) and the results of Rodrigues and Darwin (1984, 1987) (Eq. 3.1) was due to the use of lower reinforcement ratios and the use of prestressing strands as flexural reinforcement by Rodrigues and Darwin (1984, 1987), which caused the section to experience more flexural tensile strain than if a higher reinforcement ratio and deformed bars had been used. The higher flexural strain results in steeper cracks. Thus, the steeper cracks intercept fewer stirrups, and the stirrup contribution to shear strength is decreased. In the current study, there were nine failures in negative moment regions of which five involved members with stirrups. v_n - v_c is compared to $\rho_v f_{vy}$ for the five joists in Fig. 3.2a. For these

members a linear regression analysis produces the following relationship:

$$v_n - v_c = 2.02\rho_v f_{vy} + 6.45 \qquad (3.3)$$

with a correlation coefficient, r = 0.79. The low correlation coefficient indicates relatively high scatter in the data. This relatively high scatter is not unexpected because of the small amount of data produced in this study.

In general, it can be seen in the current study, as well as in other studies, that the shear reinforcement contribution in the negative moment region of lightly reinforced concrete members is greater than that predicted by the Eq. 1.5 from ACI 318-89.

Rodrigues and Darwin (1984, 1987) noted that the stirrup effectiveness in negative moment regions was lower than in positive moment regions. They suggested that this difference could be caused by the top-bar effect. Pasley et al. (1990) obtained no failures in positive moment regions of beams with stirrups. They studied the stirrup contribution in positive moment regions by combining the data from Rodrigues and Darwin (1984, 1987) and Palaskas et al. (1981). For the combined data, Pasley et al. (1990) found that the stirrups to be 59% more effective than predicted in ACI 318-89.

In the current study, four failures occurred in positive moment regions of members with stirrups. The values v_n - v_c are compared to $\rho_v f_{vy}$ in Table 3.6 and Fig. 3.2b. For these four members, a linear regression analysis produces the following relationship:

$$v_n - v_c = 1.05\rho_v f_{vy} - 4.26 \qquad (3.4)$$

with a correlation coefficient, r, of 0.88. The value of v_n - v_c in Eq. 3.4 is in close agreement with the expected value based on ACI 318-89, but is much less than expected (Pasley et al. 1990). This result is discussed in more detail in the next section.

3.3.4 Horizontal Crack Projection

Another perspective on stirrup effectiveness can be obtained by studying the horizontal crack projections and the number of stirrups intercepted by the critical shear cracks at failure. The increase in shear stress above the shear cracking stress, v_n - v_c, provides a measure of the amount shear carried by stirrups, as well as dowel action and aggregate interlock. The nominal shear stress carried by the stirrups alone can be expressed as:

$$v_{si} = \frac{V_{si}}{b_w d} = \frac{nA_v f_{vy}}{b_w d} \qquad (3.5)$$

in which V_{si} = shear force carried by the stirrups and n = number of stirrups intercepted by the critical shear crack at failure. v_{si} can be determined using the crack maps shown in Figs. 2.9a and 2.9b.

Rodrigues and Darwin (1984, 1987) noted that, in their tests, the positive moment region had longer horizontal crack projections than the negative moment region due to shallower crack angles and because the cracks propagated along the intersection of the web and the flange before they entered the flange. Due to the longer horizontal crack projections in the positive moment region, more stirrups were intercepted by the critical crack, thereby increasing the stirrup effectiveness. Pasley et al. (1990) did not experience any positive moment region failures in beams that

contained test stirrups.

Studies by Rodrigues and Darwin (1984, 1987) found that the number of stirrups intercepted by the critical shear crack in negative moment regions where approximately equal to the number of predicted by ACI 318-89. Studies by Pasley et al. (1990) found more stirrups intercepted than predicted by ACI 318-89. Pasley et al. (1990) concluded that the differences in the amount and type of flexural reinforcement used by Rodrigues and Darwin (1984, 1987), as well as differing shear span-to-depth ratios, likely caused the differences in the horizontal crack projections.

ACI 318-89 predicts the stirrup contribution to shear strength based on the assumption that a horizontal crack projection at failure is equal to the effective depth of the member, d. In the current study, the horizontal crack projection of the critical shear cracks was greater than that predicted by ACI 318-89 in all cases. The number of stirrups intercepted by the critical shear crack at failure and shear carried by the stirrups alone are presented in Table 3.7.

Based on the number of stirrups intercepted by the critical shear crack at failure, a linear regression analysis is performed for the negative moment region results, producing the following relationship between the shear carried by stirrups alone, v_{si}, and nominal stirrup capacity, $\rho_v f_{vy}$ (Fig. 3.3a):

$$v_{si} = 2.02\rho_v f_{vy} - 6.13 \qquad (3.6)$$

with a correlation coefficient, r, of 0.95, representing a reasonably good correlation. Eq. 3.6 shows that, on the average, twice as many stirrups were intercepted in the negative moment region than predicted by ACI 318-89. Eq. 3.6 is nearly identical to Eq. 3.3; the two expressions represent parallel lines with a difference of 12.58 psi.

For the positive moment regions the relationship between the shear carried by the stirrups alone, v_{si}, and nominal stirrup capacity, $\rho_v f_{vy}$ (Fig. 3.3b) is:

$$v_{si} = 2.17\rho_v f_{vy} - 17.55 \qquad (3.7)$$

with a correlation of coefficient 0.97. Eq. 3.7 is quite similar to Eq. 3.6 for the negative moment region. However, Eq. 3.7 does not match Eq. 3.4 for $v_n - v_c$, which suggests a much lower stirrup contribution - one that closely matches the assumptions in ACI 318-89. Since the stirrups in the positive moment regions were, in fact, yielding, the value of v_{si} in Eq. 3.7 should provide a close match to the real stirrup contribution. As a result, it must be concluded that the concrete contribution in the positive moment regions at failure was considerably below the value of corresponding to initial shear cracking. The fact that such a reduction in the concrete contribution has not been observed before may be due to the relatively low number of continuous members that have been used in shear studies.

3.3.5 Nominal Shear Stress

For the negative moment region, Rodrigues and Darwin (1984, 1987) obtained an average ratio of $v_n(\text{test})/v_n(\text{ACI})$ equal to 0.91, with a coefficient of variation of 8.4%. Pasley et al. (1990), obtained on average of $v_n(\text{test})/v_n(\text{ACI})$ in the negative moment region of 1.04, with a coefficient of variation of 9.5%. Rodrigues and Darwin (1984, 1987) tested statically determinate beams with a constant shear span-to-depth ratio. The reason for the lower strength obtained by Rodrigues and Darwin (1984, 1987) was attributed by Pasley et al. (1990) to Rodrigues and Darwin's (1984, 1987) use of prestressing strands rather than deformed reinforcement and the fact that

Rodrigues and Darwin (1984, 1987) had a constant (and higher) shear span-to-depth ratio than Pasley et al. (1990). For the positive moment regions, Rodrigues and Darwin (1984, 1987) obtained an average of v_n(test)/v_n(ACI) of 1.04, with a coefficient of variation of 9.3%. Pasley et al. (1990) did not obtain positive moment region failure in members that contained test stirrups.

The nominal shear stresses at failure, v_n(test), from the current study are compared to the calculated nominal shear capacities based on ACI 318-89, v_n (ACI) in Table 3.8 and in Figs. 3.4a and 3.4b. v_n(ACI) does not include the additional 10% in shear capacity allowed by section 8.11.8 of ACI 318-89.

The average value of the ratio v_n(test)/v_n(ACI) in the negative moment region for all joists, with or without stirrups in the test region, is 1.06, with a range of 0.87 to 1.17, and a coefficient of variation of 9.48%. The average value of v_n(test)/v_n(ACI) in the positive moment region for all joists, with or without stirrups is 1.13, with a range of 0.90 to 1.22, and coefficient of variation of 10.19%. The average value of v_n(test)/v_n(ACI) for joists with stirrups for both the negative and positive moment regions is 1.07, with a range from 0.87 to 1.22, and a coefficient of variation of 11.94%. The average value of v_n(test)/v_n(ACI) for joists without stirrups for both the negative and positive moment regions is 1.10 with a range from 0.94 to 1.17 and a coefficient of variation of 8.06%.

Overall, the current research results for negative moment regions with $\rho_w \leq$ 1.0%, with or without stirrups, show that the shear cracking stress (discussed in sections 3.3.1 and 3.3.2), the traditional measure of shear strength, is less than that predicted by ACI 318-89. For positive moment regions, the cracking stress is, on the average, only slightly greater than predicted by ACI 318-89, even though ρ_w was much greater than 1% for most specimens. The nominal shear strengths are greater than predicted by ACI 318-89 without regard for the extra 10% in the concrete

contribution to shear capacity allowed by section 8.11.8 of ACI 318-89. The average values of v_n(test)/v_n(ACI), 1.06 and 1.13 for negative and positive moment regions, respectively, and 1.07 and 1.10 for joists with and without stirrups, respectively, however, are not so great as to justify the 10% increase in the concrete contribution to shear strength. This point is discussed further in the next section.

3.4 Multiple web joists

In the current study, the shear cracking loads for the multiple web joists are determined based on crack pattern analysis only. Detailed explanations of the crack pattern analysis technique are found in section 3.2.1. Crack patterns for multiple web joists are shown in Figs. 2.9c and 2.9d. Plots of the total load versus average midspan deflection are found in Figs. 2.10g and 2.10h.

The current study of multiple web joist behavior is focused on the shear capacity and load sharing between joists. Section 8.11.8 of ACI 318-89 permits the concrete contribution to shear strength, V_c, specified in Eqs. 1.1 and 1.2, to be increased by 10% for joists. This increase in shear strength is justified by the commentary to ACI 318-89 on the basis of: "(1) satisfactory performance of joist construction with higher shear strengths, designed under previous ACI Building Codes, which allowed comparable shear stresses, and (2) redistribution of local overloads to adjacent joists." For Eq. 1.2, the coefficient for $\sqrt{f'_c}$ increases from 2.0 to 2.2.

As described in Section 2.8.2, the applied shear was initially carried by the joist on which the load was applied. As the load was increased, the load was transferred to and shared by the adjacent joists. Failure sequences of specimens M1 and M2 are given in Chapter 2.

For specimen M1, load was applied at the midspan of the center-east and

center-west joists. Shear cracks appeared in both positive moment regions of these joists at a total load of 42 kips (186.09 kN). With increased load, shear cracks appeared in the north-west and south-west joists' negative moment regions at 45.96 kips (204.52 kN) and 52.00 kips (231.40 kN), respectively. Upon further loading, the center-east and center-west joists failed in shear in the positive moment regions at 59.48 kips (264.68 kN). After installing external stirrups, the load was again increased until shear failure occurred in the negative moment regions of the north-west and south-west joists at 62.27 kips (277.10 kN).

The load 42 kips (186.09 kN) is the shear cracking load based on crack pattern analysis, corresponding to a shear stress of 179 psi (1.23 MPa) for the center-east joist, and 176 psi (1.21 MPa) for the center-west joist, respectively. The shear stress predicted based upon Eq. 1.2 is 140 psi (0.96 MPa) without including the additional 10% increase in shear capacity. The ratio of the measured shear stress in the center-west joist's positive moment region to the shear stress based upon Eq. 1.2 is 1.26, as shown in Table. 3.9. The ratio 1.26 indicates that the local overload carrying capacity of the center-east and center-west joist is 1.15 = (1.26/1.1) times the shear capacity predicted by ACI 318-89, suggesting a significant degree of load sharing by the adjacent joists. Load sharing is also clearly demonstrated by the appearance of shear cracks in the negative moment regions of the adjacent joists.

For specimen M2, loading was applied at midspan to the south-east and south-west joist. Shear cracks appeared in both the south-west and center-west joist's negative moment regions at 40.10 kips (178.44 kN). Shear cracks appeared in the south-east negative moment region at 44.06 kips (196.06 kN). Upon further loading, shear cracks appeared in the south-east and south-west joists' positive moment regions at 50.06 kips (222.76 kN) and 52.06 kips (231.66 kN), respectively. Failure of south-east (shear failure) and south-west (bond failure of bottom bars) joists' negative

moment regions occurred at 52.06 kips (231.66 kN). After the addition of external stirrups, failure occurred in the south-east and south-west joist's positive moment regions at 52.32 kips (232.81 kN).

The load 40.10 kips (178.44 kN) of south-west joist is the shear cracking load based on the crack pattern analysis, with a corresponding shear stress value of 183 psi (1.26 MPa). The shear stress predicted by Eq. 1.2 for the south-west joist is 136 psi (0.94 MPa) without including the additional 10% increase in load carrying capacity. The ratio of the measured shear stress in the south-west joist's negative moment region based upon Eq. 1.2 is 1.34, as shown in Table. 3.9. The ratio, 1.34, indicates that the local shear cracking load for of the south-west joist was 1.22 = (1.34/1.1) times that predicted by ACI 318-89 demonstrating, like specimen M1, that a significant degree of load is shared by the adjacent joists.

For both specimens, the observation that adjacent joists share the load is further strengthened by the significant increase in load carrying capacity between the shear cracking load and the failure load. For specimen M1, the applied load increased by 41% between initial shear cracking and failure. For specimen M2, the applied load increased by 30% between initial shear cracking and failure. The greater increase for M1 may be due to the fact that the load was shared by two adjacent joists for specimen M1 compared to a single adjacent joist for specimen M2.

For the first sections in each multiple web joist to undergo shear failure, the ratios of v_n (test) to v_n (ACI) (including the extra 10%) are 1.68 and 1.44 (Table 3.9) for specimens M1 and M2, respectively, based on a single joist carrying the load. These two multiple web joist tests leave little doubt that joists do an excellent job distributing forces in the case of local overloads, providing significant justification for the relaxed shear design provisions for joists. However, the tests, along with those for the single web joists, reveal two other important points that designers need to keep

in mind. First, although the individual joists in the multiple web specimens were able to carry a significant overload, the load transfer mechanism was not adequate to mobilize the strength of all three or even two of the joists in the specimen. Second, the shear cracking load (the current standard of design) was consistently below the predicted values from ACI 318-89 for the single web joists, with an average of 0.83 in negative moment regions and 0.92 in positive moment regions, without the extra 10% in shear capacity allowed for joists (Tables 3.4a and 3.4b). With the extra 10%, these values drop to 0.75 and 0.84, respectively. The average ratios of v_n (test) to v_n (ACI) (including the extra 10% in the concrete contribution to shear strength) for the single web joists in this study are 0.98 for negative moment region failures and 1.03 for positive moment region failures (Table 3.8), indicating that the extra 10% capacity is not consistently available for individual members, even based on strength.

The overall picture is one which shows that the extra 10% in concrete shear capacity allowed for joists is not available for joist systems as a whole. That is, a full floor system does not possess an extra 10% shear capacity just because the flexural members are joists. The relaxed shear design provisions for joists, therefore, rest solely on the ability of joists to redistribute local overloads. This ability provides significant added safety that could be used to justify what is the equivalent of a reduced load factor. However, in terms of total system capacity, an extra 10% capacity does not exist. This point should be clearly stated in the commentary to the building code.

CHAPTER 4

SUMMARY AND CONCLUSIONS

4.1 Summary

The objective of this research is to study the shear strength of continuous lightly reinforced concrete joist systems. Six two-span joists, with and without web reinforcement, and two multiple web joists without web reinforcement were tested. The main focus of this study was to determine the shear cracking capacity and to investigate load sharing between joists. Shear cracking loads are determined using crack pattern and stirrup strain analyses. Both positive and negative moment region behavior is evaluated. The primary variables in this research are the longitudinal reinforcement ratio, ρ_w (0.76% and 1.04% for negative moment regions and from 0.79% to 2.43% for positive moment regions), and nominal stirrup strength, $\rho_v f_{vy}$ (0 to 70 psi) for single web joists and placement of the load in multiple web joists. Stirrup effectiveness in joists is analyzed based upon ACI provisions and the number of stirrups intercepted by the critical shear crack. Nominal shear stresses and load sharing between the joists are compared with current ACI design provisions.

4.2 Conclusions

The following conclusions are made based on the test results and analyses described in this report:

1. The shear design provisions in ACI 318-89 were unconservative for single web joists in the current study in the negative moment regions based on shear cracking load and shear capacity.

2. The shear provisions of ACI 318-89 were unconservative for the single web joists in the current study in the positive moment regions based on shear cracking

stress, but conservative based on shear capacity.

3. The analyses confirm the findings of previous investigators that the ACI design provisions are unconservative for determining the shear cracking stress of the concrete beams, v_c, with or without stirrups, with low values of longitudinal reinforcement ratio, $\rho_w \leq 1.0\%$.

4. For the current study, the stirrup contribution to shear strength generally equals or exceeds the value predicted by ACI 318-89. The tests uniformly exhibit critical shear cracks with horizontal projections in excess of the effective depth of the joists.

5. The assumption that the concrete contribution to shear capacity is equal to the shear cracking force is not supported by the positive moment region shear failures in the current study where the concrete contribution was significantly below the shear cracking force.

6. For multiple web joists, significant load sharing occurs between adjacent joists. However, such load sharing is adequate only to distribute local overloads.

7. The relaxed shear design provisions for joists in ACI 318-89 are justified solely on the basis of the extra safety against failure under local overload. That extra safety can be viewed as justification for a reduced load factor for shear in joists, which is handled in the design provisions as an increased capacity.

8. The extra 10% concrete shear capacity allowed for joists is not available for joists system as a whole.

4.3 Future Research

The current study represents the only available data for the shear strength of lightly reinforced continuous single and multiple web joist systems. The number of variables considered were therefore limited and additional information is needed.

In reality, reinforced concrete joist systems are more likely to experience uniformly distributed loads than point loads. Hence, a better understanding could be achieved by conducting tests on multiple web joists using a uniformly distributed load.

The load sharing between the joists in multiple web joists is so great that it would be useful to consider analyzing one-way joist systems as a two-way systems. A finite element study, especially for negative moment regions, could give more information about the behavior of continuous lightly reinforced concrete joist systems in both shear and flexure.

REFERENCES

ACI-ASCE Committee 326. (1962). "Shear and Diagonal Tension," ACI Journal, *Proceedings* V. 59, No. 2, Feb, pp. 277-333.

ACI-ASCE Committee 426. (1973). "The Shear Strength of Reinforced Concrete Members," *Journal of the Structural Division*, ASCE, V. 99, No. ST6, June, pp. 1091-1187.

ACI-ASCE Committee 426. (1977). "Suggested Revisions to Shear Provisions of ACI Code 318-71," ACI Journal, *Proceedings* V. 74, No. 9, Sep, pp. 458-469.

ACI Committee 318. (1963). *Commentary of Building Code Requirements for Reinforced Concrete (ACI 318-63)*, SP-10, American Concrete Institute, Detroit, 91 pp.

ACI Committee 318. (1977). *Building Code Requirements for Reinforced Concrete (ACI 318-77)*, American Concrete Institute, Detroit, Michigan, 111 pp.

ACI Committee 318. (1983). *Building Code Requirements for Reinforced Concrete (ACI 318-83)*, American Concrete Institute, Detroit, 111 pp.

ACI Committee 318. (1989). *Building Code Requirements for Reinforced Concrete (ACI 318-89) and Commentary - ACI 318R-89*, American Concrete Institute, Detroit, pp. 140-144.

ASTM C 31-90. (1990). "Standard Practice for Making and Curing Concrete Test Specimens in the Field," *1990 Annual Book of ASTM Standards*, V 4.02, American Society for Testing and Materials, Philadelphia, PA , pp. 5-9.

Al-Nahlawi, M. K. A., and Wight, J. K. (1989). "An Experimental and Analytical Study of Shear Strength of Lightly Reinforced Concrete Beams," *Report No. UMCE 89-7*, Ann Arbor, MI, 232 pp.

Attiogbe, E. K., Palaskas, M. N., and Darwin, D. (1980). "Shear Cracking and Stirrup Effectiveness of Lightly Reinforced Concrete Beams," *SM Report* No. 1, University of Kansas Center for Research, Lawrence, 138 pp.

Batchelor. B. de V., and Kwun, M. K. (1981). "Shear in RC Beams without Web Reinforcement," *Journal of the Structural Division*, ASCE, V. 107, No. ST5, May, pp. 907-921.

Bazant, Z. P., and Kim, J. K. (1984). "Size Effect in Shear Failure of Longitudinally Reinforced Beams," ACI Journal, *Proceedings* V. 81, No. 5, Sep-Oct, pp. 456-468.

Bresler, B., and Scordelis, A. C. (1963). "Shear Strength of Reinforced Concrete Beams," ACI Journal, *Proceedings* V. 60, No. 1, Jan, pp. 51-72.

CEB-FIP. (1978). Model Code for Concrete Structures, *CEB-FIP International Recommendations*, Third Edition, Comite Euro-International du Beton, Paris, 348 pp.

Clark, A. P. (1951). "Diagonal Tension in Reinforced Concrete Beams,"ACI Journal, *Proceedings* V. 48, No. 11, Oct, pp. 145-156.

CECO. (1985). "Shear Capacity of Normal Weight Concrete Joists," *Report*, New Jersey Institute of Technology, Oak Brook, IL, 12 pp.

Elstner, R. C., Moody, K. G., Viest, I. M., and Hognestad, E. (1955). "Shear Strength of Reinforced Concrete Beams, Part 3- Tests of Restrained Beams with Web Reinforcement," ACI Journal, *Proceedings* V. 51, No. 6, Feb, pp. 525-539.

Fenwick, R. C., and Pauly, T. (1968). "Mechanism of Shear Resistance of Concrete Beams," *Journal of the Structural Division*, ASCE, V. 94, No. ST10, Oct, pp. 2325-2350.

Gergely, P. (1969). "Splitting Cracks Along the Main Reinforcement in Concrete Member," *Report to Bureau of Public Roads*, U.S. Department of Transportation, Cornell University, Ithaca, N.Y, Apr.

Haddadin, M. J., Hong, S., and Mattock, A. H. (1971). "Stirrup Effectiveness in Reinforced Concrete Beams with Axial Force," *Journal of the Structural Division*, ASCE, V. 97, No. ST9, Sep, pp. 2277-2297.

Hanson, J. W. (1969). "Square openings in Webs of Continuous Joists," Research and Development Bulletin RD 001.01D, Portland Cement Association, Skokie, IL, 14 pp.

Kani, G. N. J. (1966). "Basic Facts Concerning Shear Failure," ACI Journal, *Proceedings* V. 63, No. 6, June, pp. 675-692.

Kani, M. W., Huggins, M. W., and Wuttkop, R. R. (1979). ed *Kani on Shear in Reinforced Concrete*, University of Toronto Press, Toronto, Ontario, Canada, 225 pp.

Kani, G. N. J. (1969). "A Rational Theory for the Function of Web Reinforcement," ACI Journal, *Proceedings* V. 66, No. 3, March, pp. 185-197.

Krefeld, W. J., and Thurston, C. W. (1962) "Studies of the Shear and Diagonal Tension Strength of Simply Supported Reinforced Concrete Beams," *Report*, Columbia University, New York, N.Y, June, 96 pp.

Mathey, R. G., and Watstein, G. (1958). "Strains in Beams Having Diagonal Cracks," ACI Journal, *Proceedings* V. 55, No. 6, Dec, pp. 717-728.

Mörsch, E. (1909). "Concrete-Steel Construction-Der Eisenbetonbau," *The Engineering News Publishing Company*, London, 368 pp.

Moretto, O. (1945). "An Investigation of the Strength of Welded Stirrups in Reinforced Concrete Beams," ACI Journal, *Proceedings* V. 42, Nov, pp. 141-162.

Moody, K. G, Viest., Elstner, R. C., and Hognestad, E. (1954). "Shear Strength of Reinforcement Concrete Beams Part 1-Tests of Simple Beams," ACI Journal, *Proceedings* V. 26, No. 4, Dec, pp. 317-332.

Palaskas, M. N., and Darwin, D. (1980). "Shear Strength of Lightly Reinforced

Concrete Beams," *SM Report* No. 3, University of Kansas for Research, Lawrence, Sep, 198 pp.

Palaskas, M. N., Attiogbe, E. K., and Darwin, D. (1981). "Shear Strength of Lightly Reinforced T-Beams," ACI Journal, *Proceedings* V. 78, No. 6, Nov-Dec, pp. 447-455.

Pasley, P. G., Gogoi. S., Darwin, D., and McCabe, L. S. (1990). "Shear Strength of Continuous Lightly Reinforced T-Beams," *SM Report* No. 26, University of Kansas Center for Research, Lawrence, Dec, 61 pp.

Placas, P., and Regan, P. E. (1971). "Shear Failures of Reinforced Concrete Beams," ACI Journal, *Proceedings* V. 68, Oct, pp. 763-773.

Phillips, C. and Schultz. (1988). "Shear strength of Lightly Reinforced Concrete joists: Effect of Rib Vertical Taper," *Interim Master's degree report*, NCSU.

Rangan, B. V. (1974). "A Comparison of Code Requirements for Shear Strength of Reinforced Concrete Beams," *Shear in Reinforced Concrete, SP-42* V. 1, ACI, Detroit, MI, pp. 285-293.

Rajagopalan, K. S. and Ferguson, P. M. (1968). "Exploratory Shear Tests Emphasizing Percentage of Longitudinal Steel," ACI Journal, *Proceedings* V. 65, No. 8, Aug, pp. 634-638.

Rodrigues, C. P. and Darwin, D. (1984). "Negative Moment Region Shear Strength of Lightly Reinforced T-Beams," *SM Report* No. 13, University of Kansas for Research, Lawrence, June, 111 pp.

Rodrigues, C. P. and Darwin, D. (1987). "Shear Strength of Lightly Reinforced T-Beams in Negative Bending," ACI Journal, *Proceedings* V. 84, No. 1, Jan-Feb, pp. 77-85.

Rodrigues, C. P. and Darwin, D. (1987). Closure to discussion, "Shear Strength of Lightly Reinforced T-Beams in Negative Bending," *A CI Structural Journal*, V. 84, No. 6, Nov-Dec, pp. 548-550.

Rodriguez, J. J., Bianchini, A. C.,Viest, I. M., Kesler, C. E. (1959). "Shear Strength of Two Span Continuous Reinforced Concrete Beams," ACI Journal, *Proceedings* V. 55, No. 10, Apr, pp. 1089-1130.

Ritter, W. (1899). "Die Bauweise Hennebique" (The Hennebique System), *Schweizerische Bauzeitung*, Bd. XXXIII, No. 7, Jan.

Somes, N. F. and Corley, W. G., (1974). "Circular Openings in Webs of Continuous Beams," *Shear and Reinforced Concrete*, SP 42, V. 1, American Concrete Institute, Detroit, pp. 359-398.

Taylor, H. P. J. (1970). "Investigation of the Forces Carried Across Cracks in Reinforced Concrete Beams in Shear by Interlock of Aggregate," *Cement and Concrete Association*, Technical Report 42.477, London, England.

Zsutty, T. C. (1968). "Beam Shear Strength Prediction by Analysis of Existing Data,"

ACI Journal, *Proceedings* V. 65, No. 71, Nov, pp. 943-951.

Table 2.1 Joist properties: Negative moment regions

Joist	d	A_s	$\rho_w = A_s/b_w d$	$\rho_v = A_v/b_w s$	$\rho_v f_{vy}$
	in.	$in.^2$			psi
			east span		
K1	13.18	0.61	0.77	0.0	0.0
K2	13.43	0.61	0.76	0.0007	25.0
K3	13.18	0.61	0.77	0.0	0.0
L1	12.50	0.78	1.04	0.0	0.0
L2	12.50	0.78	1.04	0.0012	44.6
L3	13.25	0.78	1.00	0.0	0.0
M1	13.12	0.78	1.00	0.0	0.0
M2	13.12	0.78	1.00	0.0	0.0
			west span		
K1	13.18	0.61	0.77	0.0007	24.8
K2	13.43	0.61	0.76	0.0012	45.2
K3	13.18	0.61	0.77	0.0007	23.8
L1	12.50	0.78	1.04	0.0007	25.1
L2	12.50	0.78	1.04	0.0019	69.7
L3	13.25	0.78	1.00	0.0007	23.8
M1	13.12	0.78	1.00	0.0	0.0
M2	13.12	0.78	1.00	0.0	0.0

1 in. = 25.4 mm
1 psi = 6.895×10^{-3} MPa

Table 2.2 Joist properties: Positive moment regions

Joist	d	A_s	$\rho_w = A_s/b_w d$	$\rho_v = A_v/b_w s$	$\rho_v f_{vy}$
	in.	$in.^2$			psi
			east span		
K1	12.81	0.61	0.79	0.0	0.0
K2	12.25	1.49	2.01	0.0007	25.0
K3	12.56	1.23	1.63	0.0	0.0
L1	13.00	0.88	1.13	0.0	0.0
L2	12.12	1.77	2.43	0.0012	44.6
L3	13.12	0.88	1.12	0.0	0.0
M1	13.56	0.88	1.12	0.0	0.0
M2	13.06	0.88	1.12	0.0	0.0
			west span		
K1	12.81	0.61	0.79	0.0007	24.8
K2	12.25	1.49	2.01	0.0012	45.2
K3	12.56	1.23	1.63	0.0007	23.8
L1	13.00	0.88	1.13	0.0007	25.1
L2	12.12	1.77	2.43	0.0019	69.7
L3	13.12	0.88	1.12	0.0007	23.8
M1	13.56	0.88	1.12	0.0	0.0
M2	13.06	0.88	1.12	0.0	0.0

1 in. = 25.4 mm
1 psi = 6.895×10^{-3} MPa

Table 2.3 Concrete properties

Joist	Mix proportion lbs. per cu. yard*	Slump in.	Air %	Temp F	f'_c psi**	Age at test days
		Single web joists				
K1	517:267:1490:1490	3	4.3	60	4200	7
K2	517:267:1490:1490	5 1/4	3.1	77	4150	9
K3	517:225:1603:1616	5	3.1	75	4130	15
L1	517:267:1490:1490	4 1/4	3.5	76	3980	13
L2	517:225:1603:1616	3	3.4	79	4130	13
L3	538:225:1590:1590	3 1/4	5.8	55	4417	11
		Multiple web joist				
M1	538:225:1590:1590	2	4	83	4910	16
M2	538:225:1590:1590	3	4	61	4638	15

* Cement : water : fine aggregate : coarse aggregate
** Compresive strength of 6 x 12 in. test cylinders

1 in. = 25.4 mm
1 lb = 4.45 N
1 cu. yard = 0.7646 m^3
1 psi = 6.895 x 10^{-3} MPa

Table 2.4 Steel properties

Bar size	Dia. (in.)	Area ($in.^2$)	Yield force (kips)	Yield stress (ksi)	Tensile force (kips)	Tensile stress (ksi)
No. 4	0.500	0.20	13.3	66.5	20.5	102.5
No. 5	0.625	0.31	20.2	65.2	31.7	102.3
No. 6	0.750	0.44	32.8	74.5	48.6	110.4
Wire 1	0.125	0.012	0.45	36.4		
Wire 2	0.167	0.022	0.81	37.1		
Wire 3	0.210	0.035	1.25	36.2		

1 in. = 25.4 mm
1 in^2 = 645.16 mm^2
1 kip = 4.45 kN
1 ksi = 6.895 MPa

Table 2.5 Single web joists: Peak loads and middle support reactions at failure

Joist	Failure Region	Load, kips		Middle support reaction	Total load
		west span	east span	kips	kips
K1	East Negative	12.74	11.74	16.51	24.48
K2	East Positive	22.64	21.44	24.73	44.08
K2	East Negative	24.68	23.69	25.15	48.37
K2	West Negative	25.64	24.61	26.65	50.25
K2	West Positive	29.13	28.05	29.93	57.18
K3	East Negative	17.19	16.81	20.04	34.00
K3	West Negative	19.39	18.90	21.86	38.33
K3	East Positive	19.39	18.90	21.86	38.33
L1	East Negative	14.55	13.84	16.06	28.39
L1	West Negative	14.57	14.26	16.28	28.83
L1	East Positive	18.64	18.95	21.57	37.59
L2	East Negative	26.50	25.48	27.52	51.98
L2	West Positive	31.69	31.12	31.76	62.81
L3	East Negative	17.71	17.69	20.60	35.40
L3	West Positive	18.24	18.76	21.76	37.00

1 kip = 4.45 kN

Table 2.6 Single web joists: Measured shear strength at failure

Joist	V_n(test) kips	v_n(test)* psi	Failure Region
K1	9.71	122.83	East Negative
K2	12.54	170.62	East Positive
K2	14.04	174.18	East Negative
K2	15.28	189.54	West Negative
K2	15.69	213.54	West Positive
K3	11.63	147.01	East Negative
K3	12.76	161.35	West Negative
K3	11.27	149.64	East Positive
L1	9.56	127.49	East Negative
L1	9.92	132.29	West Negative
L1	11.32	145.19	East Positive
L2	15.21	202.92	East Negative
L2	16.48	226.56	West Positive
L3	12.00	150.94	East Negative
L3	11.22	142.51	West Positive

* Based on average web width
1 kip = 4.45 kN
1 psi = 6.895 x 10^{-3} MPa

Table 2.7 Multiple web joists: Peak loads and middle support reactions at failure

Joist	Failure Region	Load, kips		Middle support reaction	Total load
		west span	east span	kips	kips
M1	center-east positive	29.14	29.65	37.44	58.79
M1	center-west positive	29.14	29.65	37.44	58.79
M1	center-east negative	30.78	31.49	39.15	62.27
M1	center-west negative	30.78	31.49	39.15	62.27
M2	south-east negative	25.93	26.13	31.83	52.06
M2	south-east negative	25.93	26.13	31.83	52.06
M2	south-east positive	26.12	26.20	31.69	52.32
M2	south-west positive	26.12	26.20	31.69	52.32

1 kip = 4.45 kN

Table 3.1a Single web joists: Negative moment region shear cracking forces and stresses

	Force, V_c (kips)		Stress, v_c (psi)*	
		east span		
Joist	Crack pattern	Stirrup strain	Crack pattern	Stirrup strain
K1	7.66	--	97	--
K2	7.20	5.51	89	68
K3	9.37	--	119	--
L1	7.89	--	105	--
L2	8.41	7.32	112	98
L3	9.07	--	114	--
		west span		
K1	6.83	5.99	86	75
K2	9.01	7.40	112	92
K3	8.88	7.15	112	90
L1	7.12	8.32	95	111
L2	9.26	10.97	123	146
L3	10.17	6.04	128	76

* based on average web width
-- no stirrups used
1 kip = 4.45 kN
1 psi = 6.895 x 10^{-3} MPa

Table 3.1b Single web joists: Positive moment regions shear cracking forces and stresses

	Force, V_c (kips)		Stress, v_c (psi)*	
		east span		
Joist	Crack pattern	Stirrup strain	Crack pattern	Stirrup strain
K1	**	--	**	--
K2	11.23	7.58	152	103
K3	9.31	--	118	--
L1	8.27	--	106	--
L2	12.60	10.54	173	145
L3	10.01	--	127	--
		west span		
K1	**	8.23	**	107
K2	11.21	5.51	152	75
K3	8.85	5.91	117	78
L1	7.40	8.72	95	112
L2	12.03	12.03	165	165
L3	9.95	6.50	126	82

* based on average web width
** method produced no results
-- no stirrups used
1 kip = 4.45 kN
1 psi = 6.895 x 10^{-3} MPa

Table 3.2a Calculated negative moment region shear cracking stresses, v_c(psi)

Joist	ACI 318-89 (Eq. 1.2)	Zsutty (Eq. 1.7)	Rajagopalan & Ferguson (Eq. 1.8)	ACI-ASCE Committee 426 (Eq. 1.10)	Batchelor & Kwun (Eq. 1.11)	Bazant & Kim (Eq. 1.12)
			east span			
K1	130	119	102	112	94	100
K2	129	129	100	110	92	98
K3	128	135	101	111	93	99
L1	126	**	116	129	110	**
L2	128	**	118	132	112	**
L3	133	145	120	133	113	111
			west span			
K1	130	118	102	112	94	100
K2	129	134	100	110	92	98
K3	128	136	101	111	93	99
L1	126	**	116	129	110	**
L2	128	**	118	132	112	**
L3	133	149	120	133	113	111

** M/Vd < 2.5

1 psi = 6.895 x 10^{-3} MPa

Table 3.2b Calculated positive moment region shear cracking stresses, v_c(psi)

Joist	ACI 318-89 (Eq. 1.2)	Zsutty (Eq. 1.7)	Rajagopalan & Ferguson (Eq. 1.8)	ACI-ASCE Committee 426 (Eq. 1.10)	Batchelor & Kwun (Eq. 1.11)	Bazant & Kim (Eq. 1.12)
			east span			
K1	130	**	103	113	95	**
K2	129	140	181	207	181	138
K3	128	134	156	177	154	129
L1	126	115	122	136	116	110
L2	128	144	208	239	210	147
L3	133	125	133	149	128	118
			west span			
K1	130	**	103	113	95	**
K2	129	139	181	207	181	138
K3	128	133	156	177	154	128
L1	126	123	122	136	116	110
L2	128	146	207	239	210	147
L3	133	125	133	149	128	118

** method produced no results
1 psi = 6.895 x 10^{-3} MPa

Table 3.3a Shear span and shear span-to-depth ratios at shear cracking load for negative moment regions

	M/V(inches)		M/(Vd)	
Joist	Crack pattern	Stirrup strain	Crack pattern	Stirrup strain
		east negative moment regions		
K1	50.84	--	3.85	--
K2	39.46	45.19	2.93	3.36
K3	34.11	--	2.58	--
L1	31.22	--	2.49	--
L2	28.55	29.93	2.28	2.39
L3	38.33	--	2.89	--
		west negative moment regions		
K1	51.22	52.01	3.88	3.94
K2	34.90	38.27	2.59	2.84
K3	33.26	35.46	2.52	2.68
L1	28.24	29.28	2.25	2.34
L2	26.69	26.34	2.13	2.10
L3	35.41	37.06	2.67	2.79

-- no stirrups used
1 in. = 25.4 mm

Table 3.3b Shear span and shear span-to-depth ratios at shear cracking load for positive moment regions

	M/V(inches)		M/(Vd)	
Joist	Crack pattern	Stirrup strain	Crack pattern	Stirrup strain
	east positive moment regions			
K1	**	--	**	--
K2	74.50	69.66	6.08	5.68
K3	70.38	--	5.33	--
L1	76.20	--	5.86	--
L2	80.03	77.60	6.60	6.40
L3	71.21	--	5.42	--
	west positive moment regions			
K1	**	52.67	**	4.11
K2	75.14	66.73	6.13	5.44
K3	72.18	71.01	5.74	5.65
L1	62.75	77.87	4.82	5.99
L2	78.57	78.57	6.48	6.48
L3	71.01	67.51	5.41	5.14

** method produced no results
-- no stirrups used
1 in. = 25.4 mm

Table 3.4a Comparison of test and calculated shear cracking stresses in negative moment regions based on crack pattern analysis

v_c(test)/v_c(equations)

Joist	ACI 318-89 (Eq. 1.2)	Zsutty (Eq. 1.7)	Rajagopalan & Ferguson (Eq. 1.8)	ACI-ASCE Committee 426 (Eq. 1.10)	Batchelor & Kwun (Eq. 1.11)	Bazant & Kim (Eq. 1.12)
			east span			
K1	0.74	0.81	0.95	0.86	1.03	0.97
K2	0.69	0.68	0.88	0.81	0.96	0.90
K3	0.92	0.88	1.17	1.06	1.27	1.19
L1	0.83	0.76	0.90	0.81	0.95	0.97
L2	0.87	**	0.95	0.85	1.00	**
L3	0.85	0.76	0.95	0.85	1.01	1.02
			west span			
K1	0.66	0.72	0.84	0.77	0.92	0.86
K2	0.86	0.85	1.11	1.01	1.20	1.13
K3	0.87	0.82	1.11	1.01	1.20	1.13
L1	0.75	**	0.81	0.73	0.86	**
L2	0.96	**	1.04	0.93	1.10	**
L3	0.96	0.86	1.06	0.96	1.13	1.14
Mean	0.83	0.79	1.06	0.89	1.05	1.04
Std. dev	0.099	0.065	0.114	0.105	0.128	0.119
COV, %	11.83	8.24	11.58	11.82	12.11	11.39

** M/(Vd) < 2.5

Table 3.4b Comparison of test and calculated shear cracking stresses in positive moment regions based on crack pattern analysis

v_c(test)/v_c(equations)

Joist	ACI 318-89 (Eq. 1.2)	Zsutty (Eq. 1.7)	Rajagopalan & Ferguson (Eq. 1.8)	ACI-ASCE Committee 426 (Eq. 1.10)	Batchelor & Kwun (Eq. 1.11)	Bazant & Kim (Eq. 1.12)
			east span			
K1	**	**	**	**	**	**
K2	1.18	1.10	0.84	0.73	0.84	1.10
K3	0.91	0.88	0.75	0.66	0.76	0.92
L1	0.84	0.93	0.87	0.77	0.91	0.96
L2	1.34	1.18	0.83	0.72	0.82	1.17
L3	0.95	1.04	0.95	0.85	0.99	1.05
			west span			
K1	**	**	**	**	**	**
K2	1.18	1.09	0.84	0.73	0.84	1.10
K3	0.91	0.88	0.75	0.66	0.76	0.91
L1	0.75	0.83	0.78	0.69	0.81	0.86
L2	1.28	1.13	0.79	0.69	0.78	1.12
L3	0.95	1.03	0.95	0.84	0.99	1.05
Mean	1.03	1.01	0.83	0.74	0.85	1.02
Std. dev	0.201	0.120	0.072	0.068	0.085	0.107
COV, %	19.52	11.90	8.66	9.25	9.98	10.38
			both negative and positive moment regions			
Mean	0.92	0.91	0.91	0.82	0.96	1.03
Std. dev	0.181	0.145	0.121	0.117	0.149	0.109
COV, %	19.58	15.98	13.23	14.30	15.49	10.58

** method produced no results

Table 3.5a Comparison of test and calculated shear cracking stresses in negative moment regions based on stirrup strain analysis

v_c(test)/v_c(equations)

Joist	ACI 318-89 (Eq. 1.2)	Zsutty (Eq. 1.7)	Rajagopalan & Ferguson (Eq. 1.8)	ACI-ASCE Committee 426 (Eq. 1.10)	Batchelor & Kwun (Eq. 1.11)	Bazant & Kim (Eq. 1.12)
			east span			
K1	--	--	--	--	--	--
K2	0.53	0.52	0.68	0.62	0.73	0.69
K3	--	--	--	--	--	--
L1	--	--	--	--	--	--
L2	0.75	**	0.82	0.74	0.87	**
L3	--	--	--	--	--	--
			west span			
K1	0.58	0.63	0.74	0.67	0.80	0.75
K2	0.71	0.70	0.91	0.83	0.99	0.93
K3	0.70	0.66	0.89	0.81	0.97	0.91
L1	0.88	**	0.95	0.85	1.00	**
L2	1.13	**	1.23	1.11	1.30	**
L3	0.57	0.51	0.63	0.57	0.67	0.68
Mean	0.73	0.60	0.86	0.77	0.92	0.79
Std. dev	0.198	0.083	0.190	0.169	0.197	0.119
COV, %	27.03	13.65	22.06	21.74	21.43	14.99

-- no stirrups used
** M/(Vd) <2.5

Table 3.5b Comparison of test and calculated shear cracking stresses in positive moment regions based on stirrup strain analysis

v_c(test)/v_c(equations)

Joist	ACI 318-89 (Eq. 1.2)	Zsutty (Eq. 1.7)	Rajagopalan & Ferguson (Eq. 1.8)	ACI-ASCE Committee 426 (Eq. 1.10)	Batchelor & Kwun (Eq. 1.11)	Bazant & Kim (Eq. 1.12)
			east span			
K1	--	--	--	--	--	--
K2	0.80	0.74	0.57	0.49	0.57	0.74
K3	--	--	--	--	--	--
L1	--	--	--	--	--	--
L2	1.12	0.99	0.69	0.60	0.68	0.98
L3	--	--	--	--	--	--
			west span			
K1	0.82	**	1.04	0.94	1.12	**
K2	0.58	0.54	0.41	0.36	0.41	0.54
K3	0.61	0.59	0.50	0.44	0.51	0.61
L1	0.88	0.98	0.91	0.82	0.96	1.01
L2	1.28	1.13	0.79	0.69	0.78	1.12
L3	0.62	0.67	0.62	0.55	0.64	0.68
Mean	0.84	0.80	0.69	0.61	0.71	0.81
Std. dev	0.254	0.226	0.212	0.196	0.235	0.223
COV, %	30.23	28.03	30.57	31.83	33.08	27.41
			both negative and positive moment regions			
Mean	0.78	0.72	0.77	0.69	0.81	0.80
Std. dev	0.227	0.202	0.212	0.196	0.236	0.180
COV, %	28.84	27.90	27.34	28.10	28.90	22.34

-- no stirrups used
** method produced no results

Table 3.6 Single web joists: Stirrup effectiveness, $v_n - v_c$ (psi)

Joist	$v_n - v_c$ (psi)	$\rho_v f_{vy}$ (psi)	ρ_w	span
		negative moment region		
K2	84.76	25.50	0.76	east negative
K2	103.17	45.20	0.76	west negative
K3	48.91	23.80	0.77	west negative
L1	37.29	25.10	1.04	west negative
L2	90.31	44.60	1.04	east negative
		positive moment region		
K2	17.72	25.50	2.01	east positive
K2	60.96	45.20	2.01	west positive
L2	61.08	69.70	2.43	west positive
L3	16.07	23.80	1.12	west positive

1 psi = 6.895×10^{-3} MPa

Table 3.7 Stirrups intercepted and stirrup contribution to shear strength at failure

Josit	span	# of stirrups intercepted	$v_{si}=nA_vf_{vy}/b_wd$ (psi)	$\rho_v f_{vy}$ (psi)
		negative moment region		
K2	east	5	54.37	25.50
K2	west	4	81.90	45.20
K3	west	3	31.65	23.80
L1	west	4	46.93	25.10
L2	east	4	86.82	44.60
		positive moment region		
K2	east	4	47.69	25.50
K2	west	3	67.34	45.20
L2	west	4	139.73	69.70
L3	west	3	31.79	23.80

1 psi = 6.895×10^{-3} MPa

Table 3.8 Single web joists: Comparison of test and calculated nominal shear stresses, v_n, psi

Joist	span	v_n(test) psi	v_n(ACI)* psi	$\frac{v_n \text{ (test)}}{v_n \text{ (ACI)}^*}$	v_n(ACI)**	$\frac{v_n\text{(test)}}{v_n\text{(ACI)}^{**}}$
			negative moment region failures			
K1	east	123	130	0.95	142	0.86
K2***	east	174	154	1.13	170	1.02
K2***	west	189	174	1.09	191	0.99
K3	east	147	128	1.14	141	1.04
K3***	west	161	152	1.06	167	0.96
L1	east	127	126	1.01	139	0.91
L1***	west	132	151	0.87	166	0.79
L2	east	203	173	1.17	190	1.07
L3	east	151	133	1.14	146	1.03
Mean of negative joist failures				1.06		0.96
			COV, %	9.48		9.48
			positive moment region failures			
K2***	east	170	154	1.19	167	1.02
K2***	west	213	174	1.22	187	1.14
K3	east	149	128	1.16	141	1.06
L1	east	145	126	1.15	139	1.05
L2***	west	226	198	1.14	211	1.07
L3***	west	142	156	0.90	170	0.83
Mean of positive joist failures				1.13		1.03
			COV, %	10.19		10.19
Mean of all joists with stirrups				1.07		
			COV, %	11.94		
Mean of all joist without stirrups				1.10		
			COV, %	8.06		

* Eq. 1.2, does not include the additional 10% allowed by section 8.11.8 of ACI

** Eq. 1.2, including the additional 10% allowed in the concrete contribution to shear capacity by section 8.11.8 of ACI

*** span contains stirrups

1 psi = 6.985×10^{-3} MPa

Table. 3.9 Multiple web joists: Shear cracking stress, v_c, based on crack pattern analysis and shear failure stresses, v_n.

Joist	v_c(test) psi	v_c(ACI)* psi	$\frac{v_c(test)}{v_c(ACI)^*}$	v_n(test) psi	v_n(ACI)** psi	$\frac{v_n(test)}{v_n(ACI)^{**}}$
negative moment region (M1)						
north-west	202	140	1.44	260	154	1.69
center-east	***	140	***	261	154	1.69
center-west	***	140	***	260	154	1.69
south-west	228	140	1.63	260	154	1.69
		average ratio	1.53			1.69
positive moment region (M1)						
center-east	179	140	1.28	256	154	1.66
center-west	176	140	1.26	252	154	1.64
		average ratio	1.27			1.65
combined average ratio			1.40			1.68
negative moment region (M2)						
south-east	197	136	1.45	227	150	1.51
south-west	183	136	1.34	224	150	1.51
center-east	183	136	1.34	--	--	--
		average ratio	1.38			1.51
positive moment region (M2)						
south-east	204	136	1.50	207	150	1.38
south-west	207	136	1.52	207	150	1.38
		average ratio	1.51			1.38
combined average ratio			1.43			1.44

* shear stress calculated without including the additional 10%
** shear stress calculated including the additional 10%
*** no shear cracking
-- no failure occurred
1 psi = 6.895 x 10^{-3} MPa

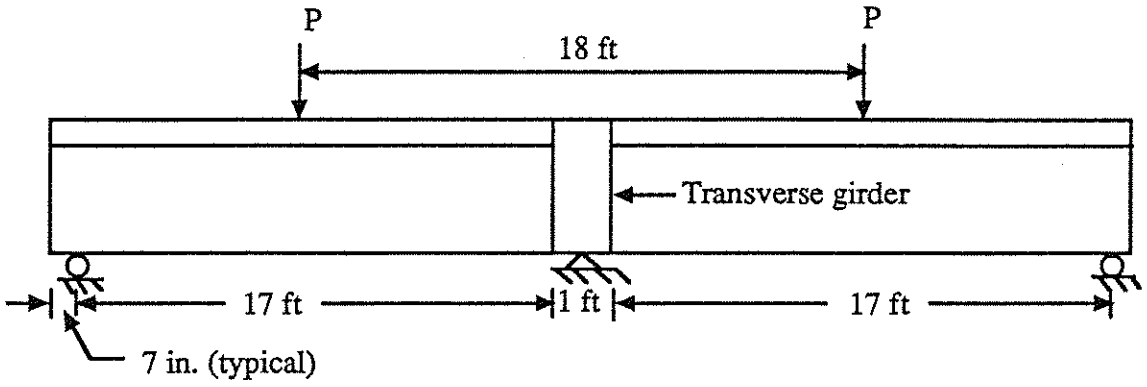

Joist elevation

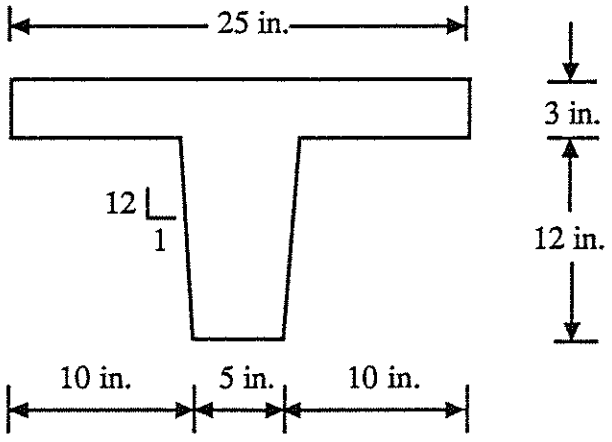

Joist cross section

Fig. 2.1 Single web joist dimensions

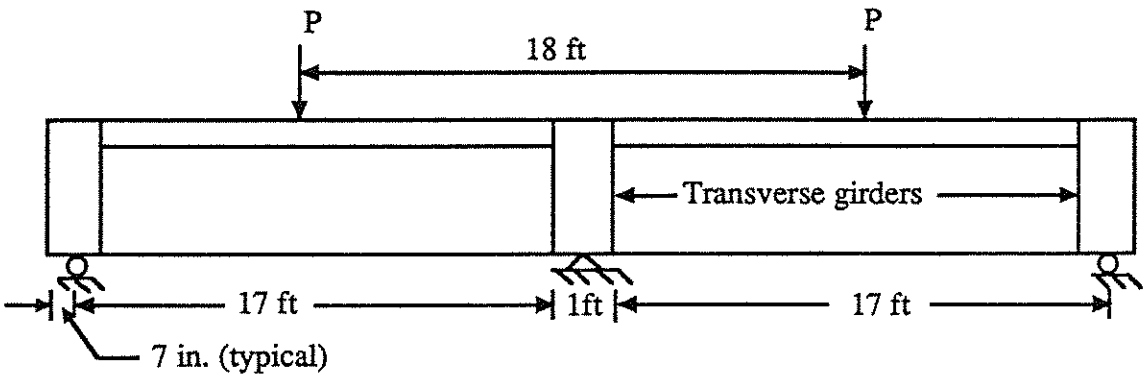

Joist elevation

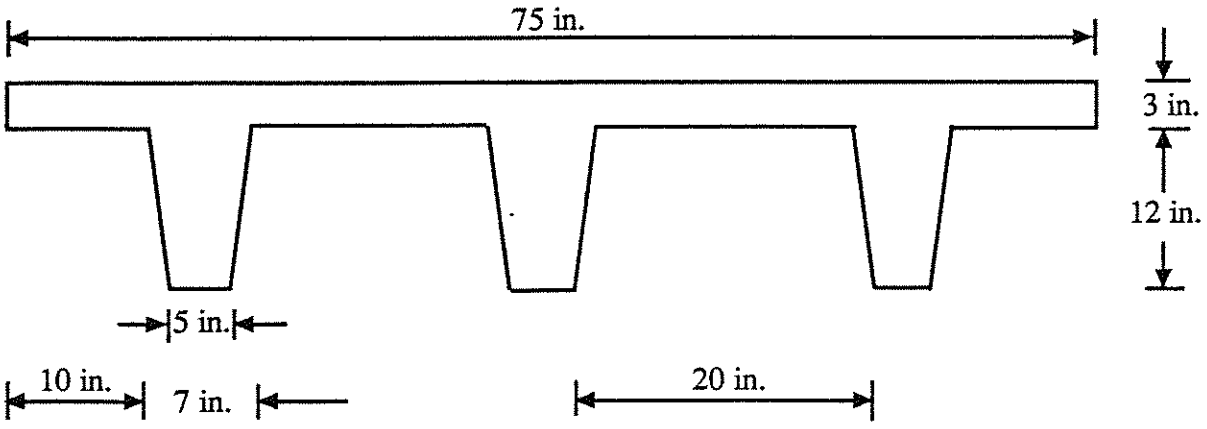

Joist cross section

Fig. 2.2 Multiple web joist dimensions

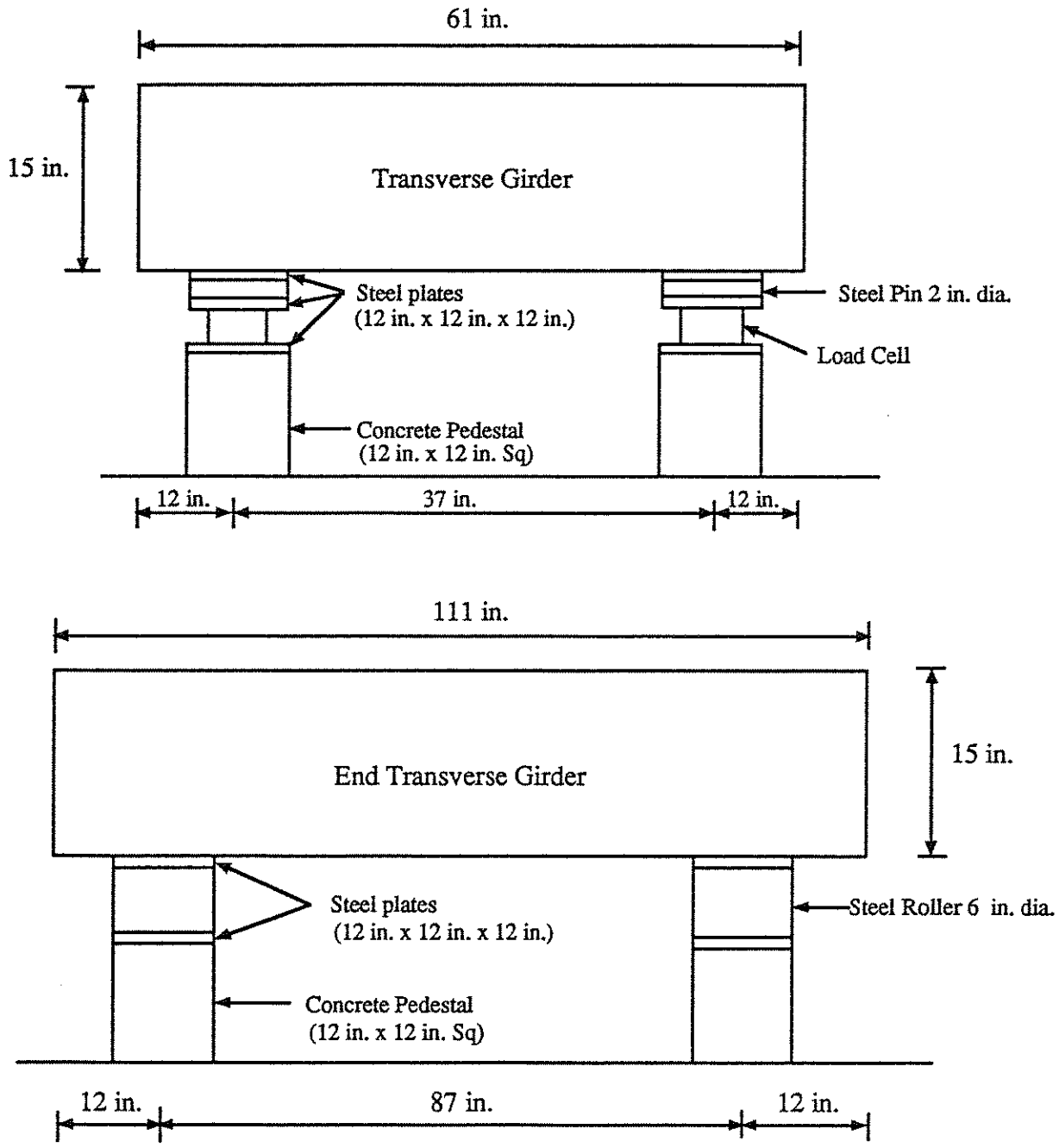

Fig. 2.3 Typical pin and roller supports for the joist

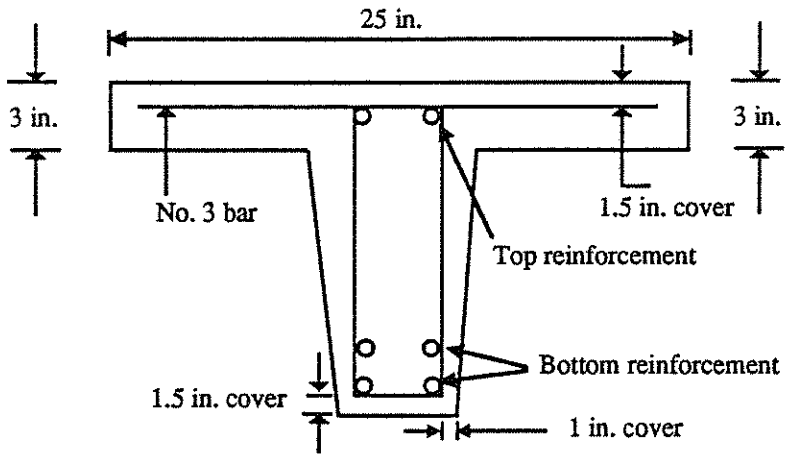

Single web joist reinforcement

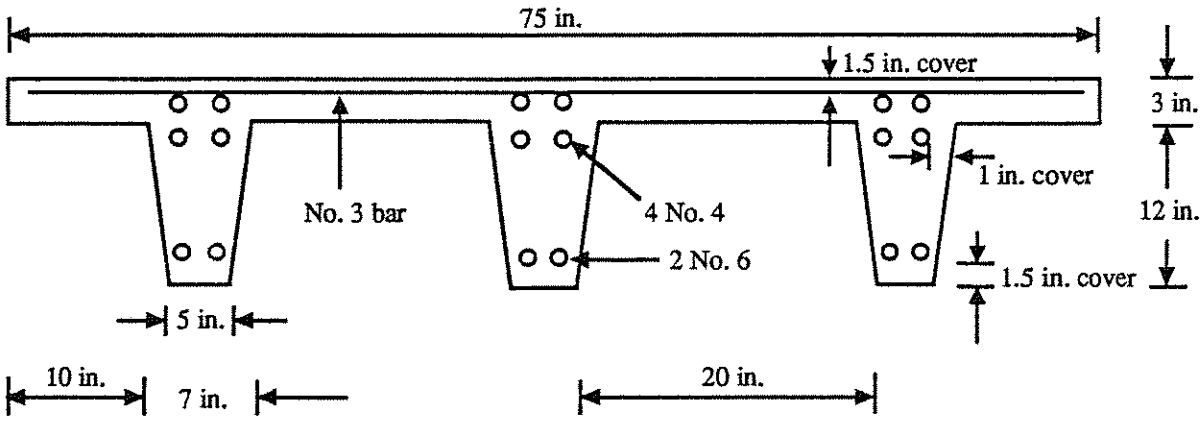

Multiple web joist reinforcement

Fig. 2.4 Joist reinforcement details

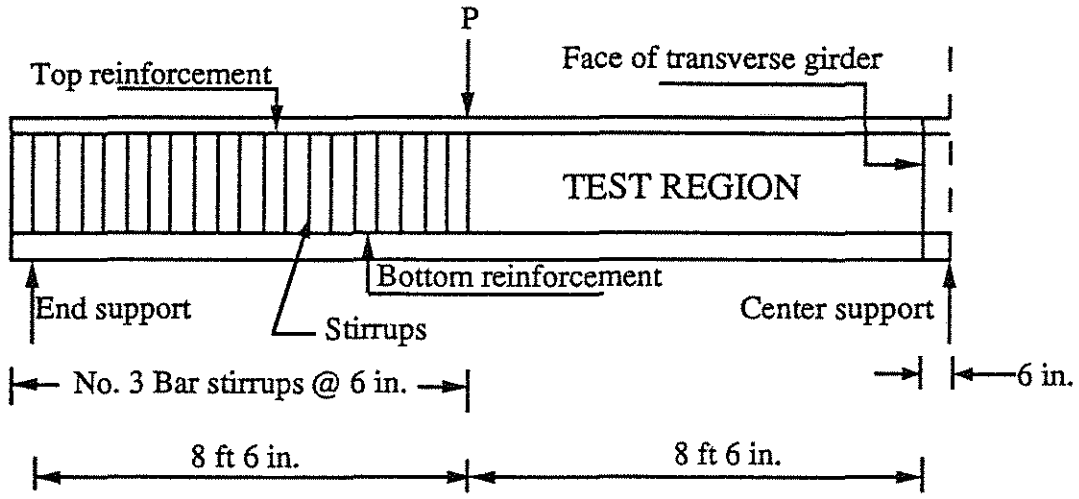

Stirrup arrangement for joist without test stirrups

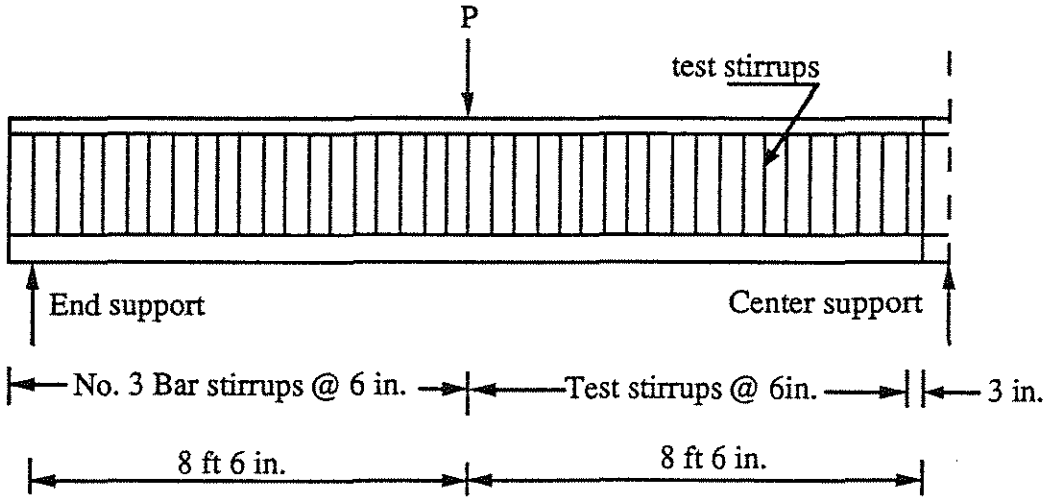

Stirrup arrangement for joist with test stirrups

Fig. 2.5 Typical stirrup location for single web joists

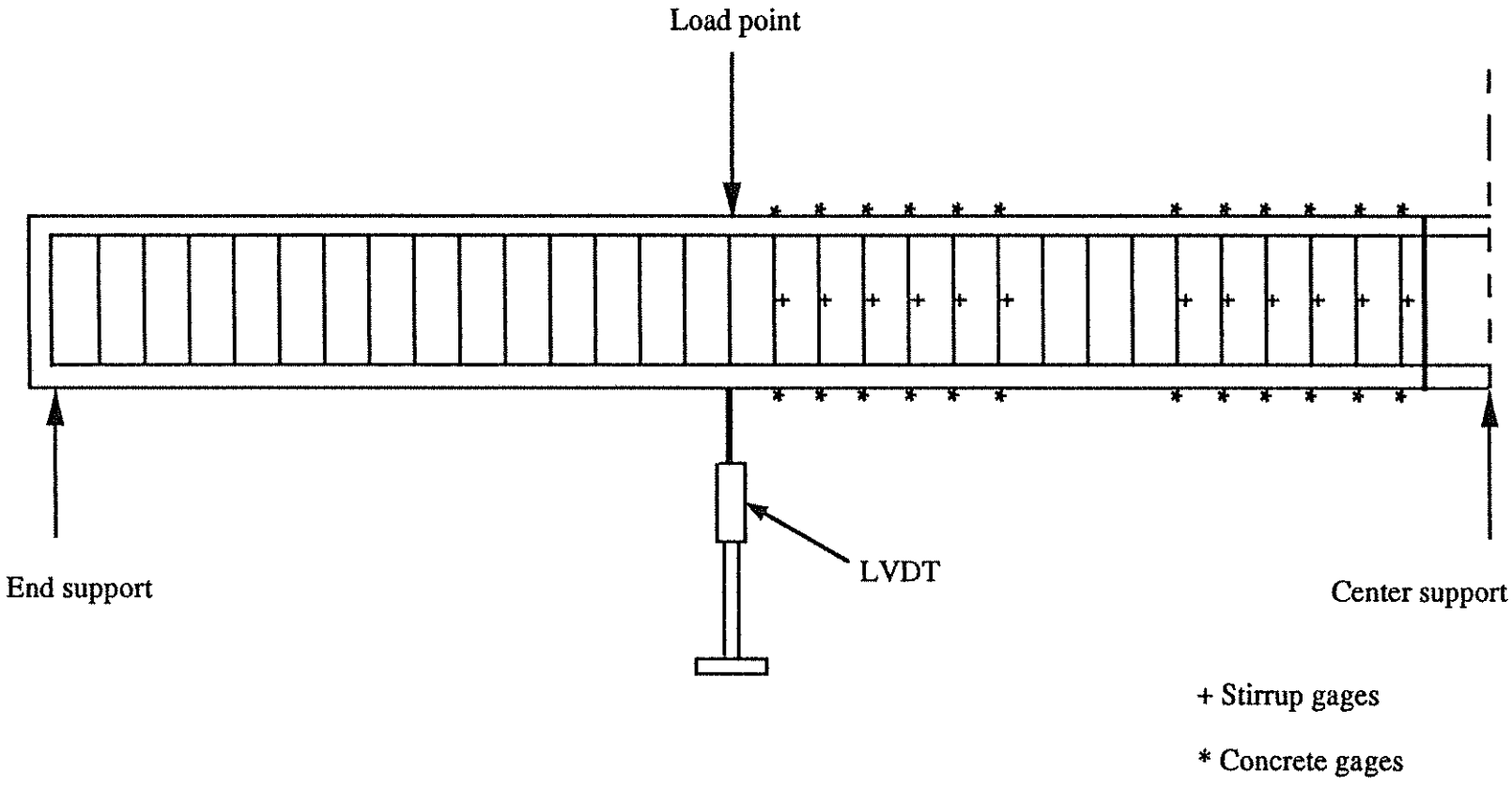

Fig. 2.6 Typical strain gage locations

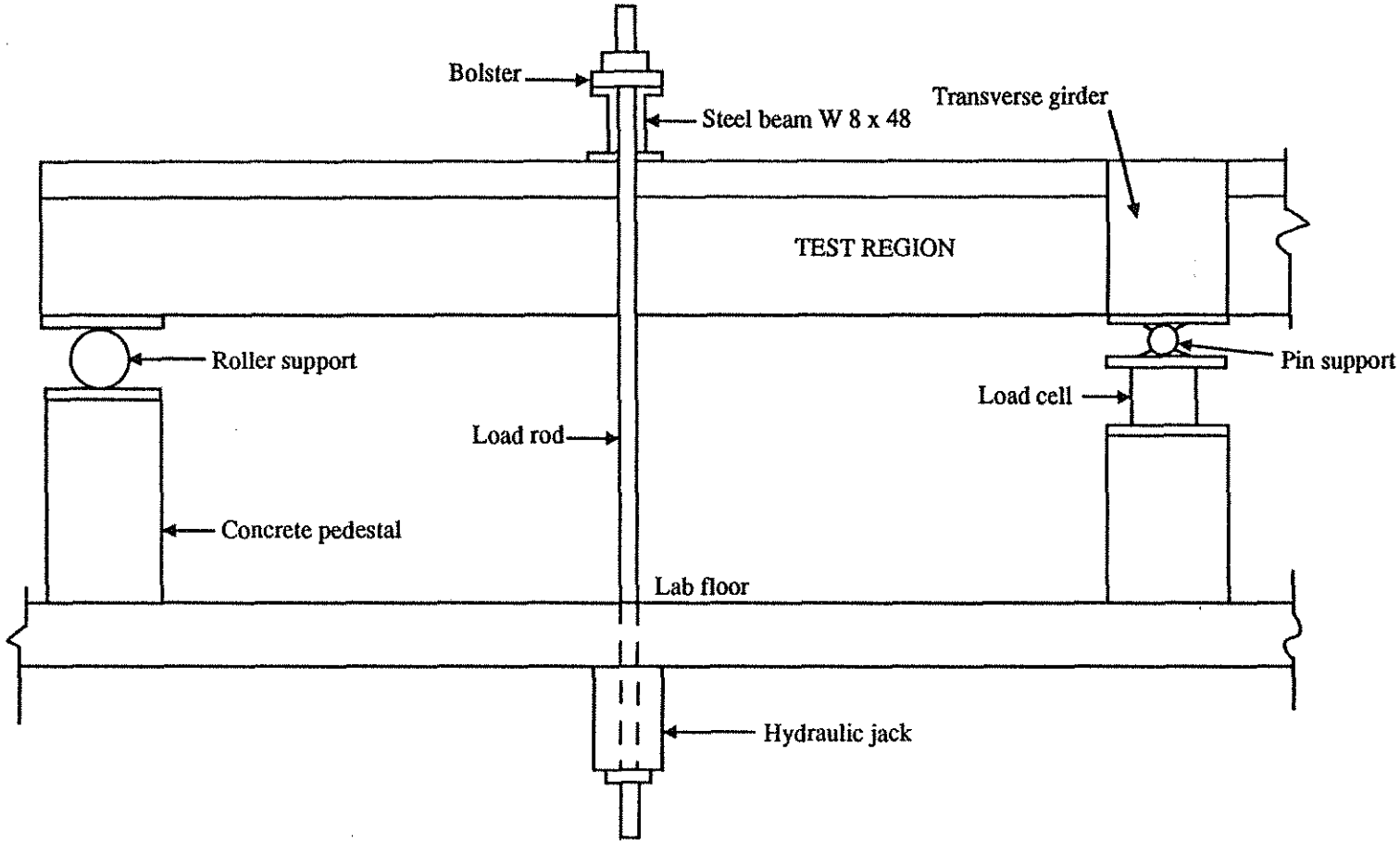

Fig. 2.7 Loading arrangement

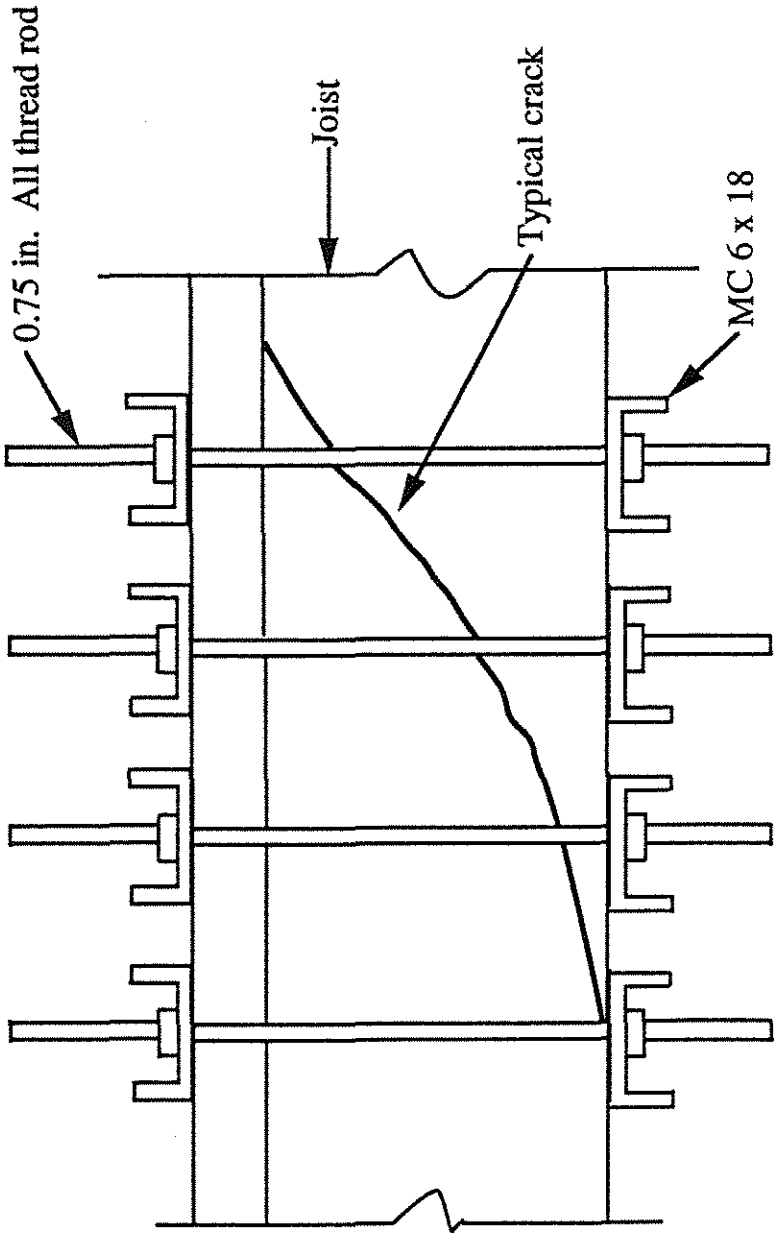

Fig. 2.8 External stirrups

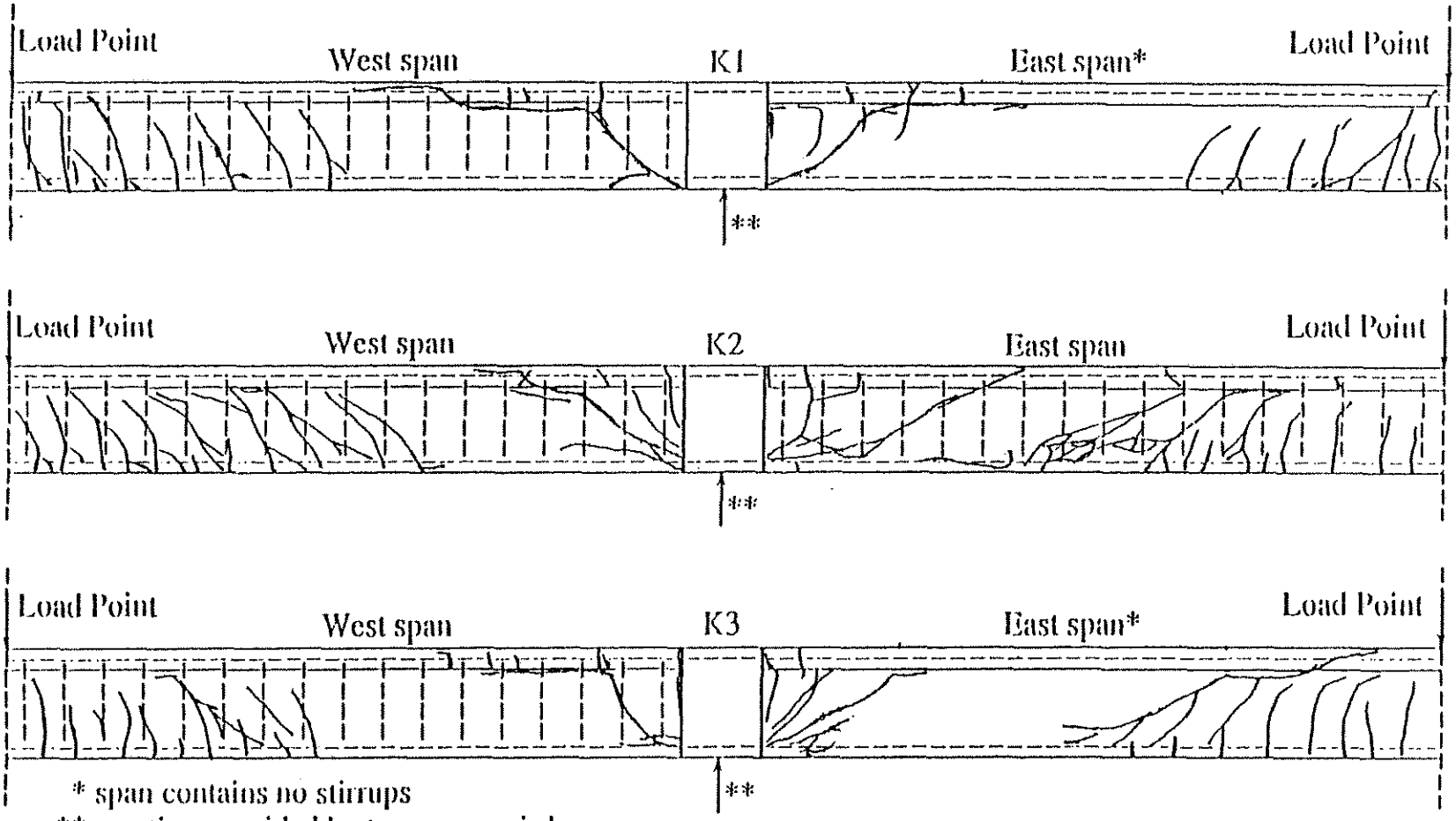

Fig. 2.9a Crack patterns for joist K1, K2 and K3

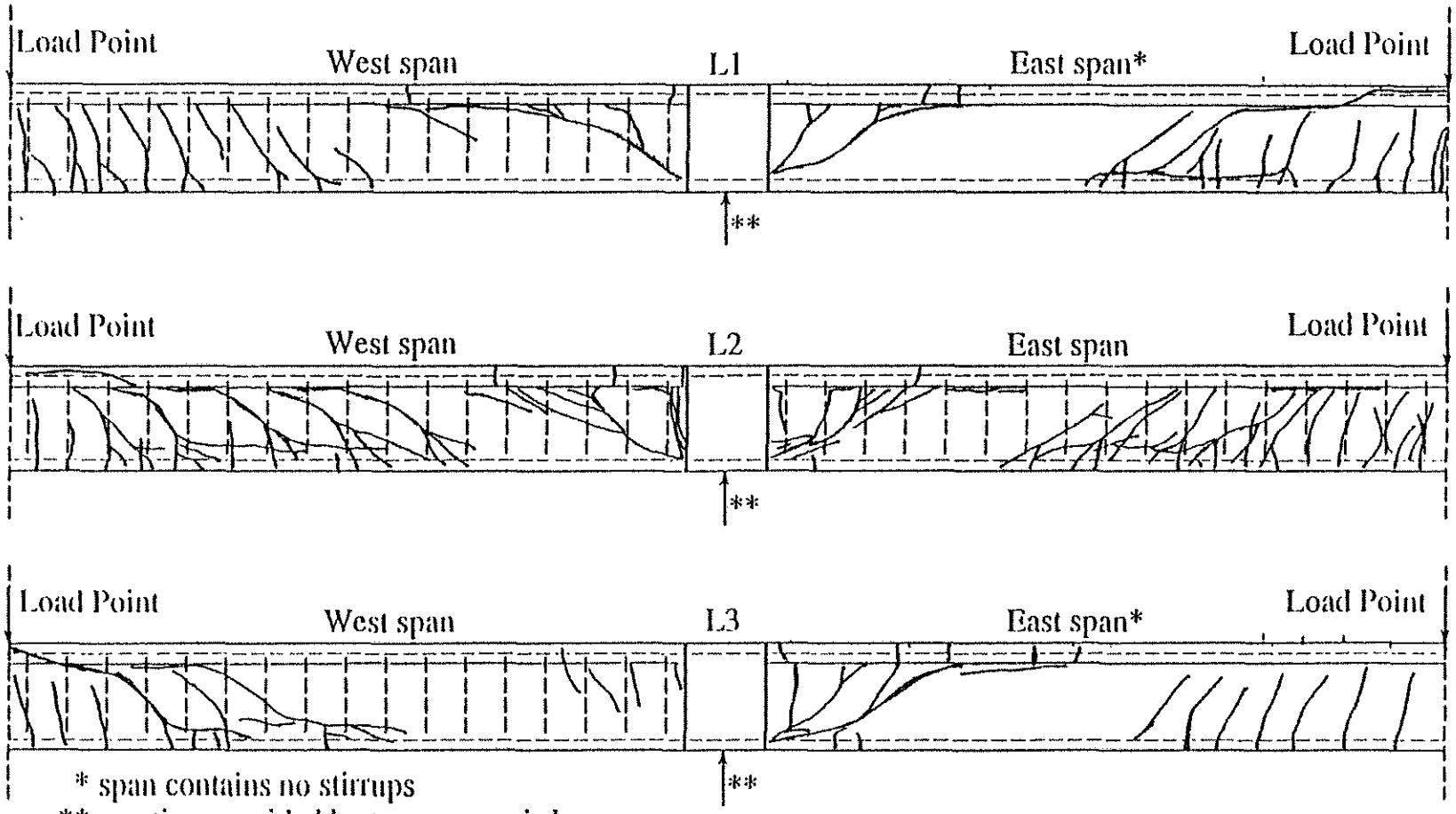

Fig. 2.9b Crack patterns for joists L1, L2 and L3

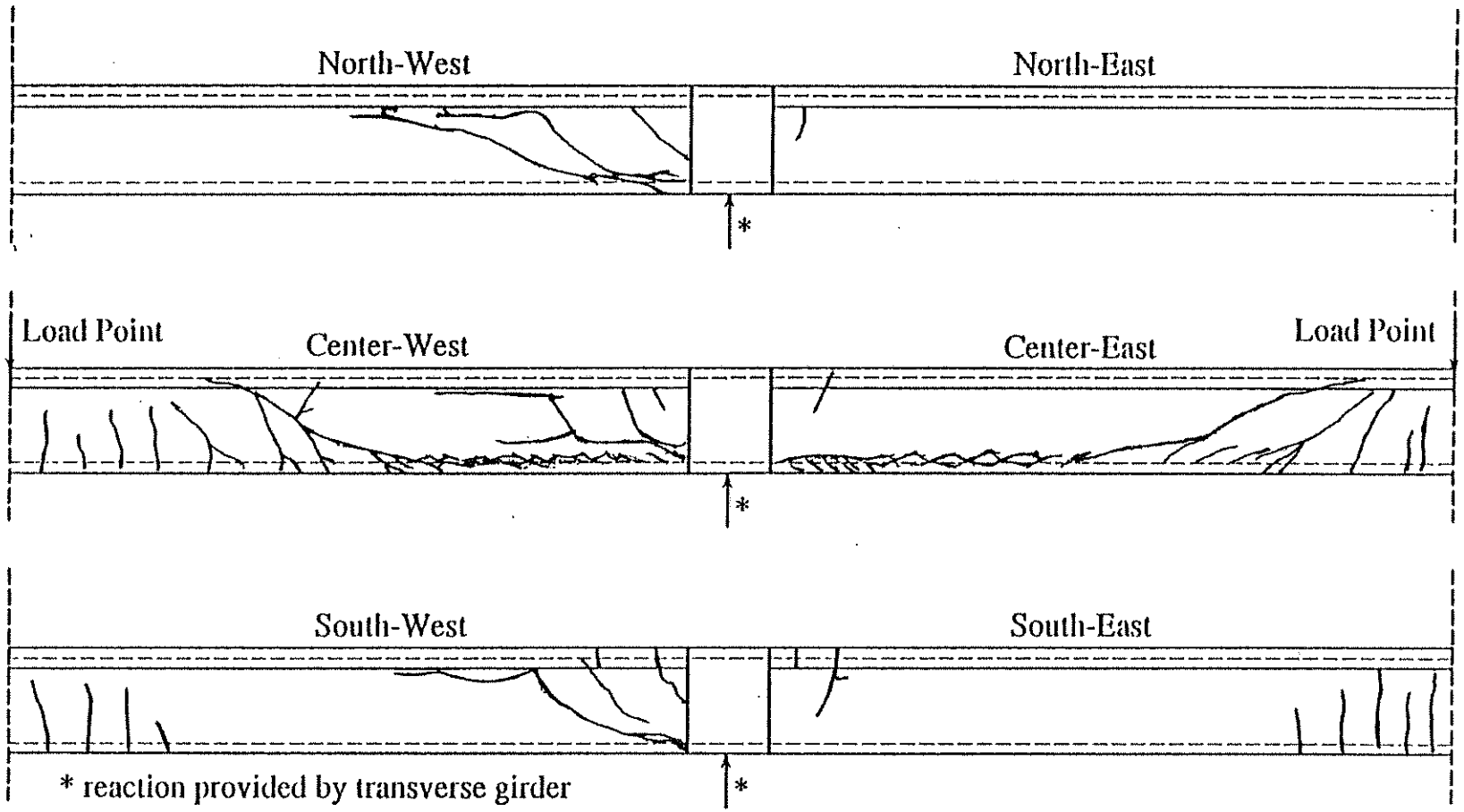

Fig. 2.9c Crack patterns for specimen M1

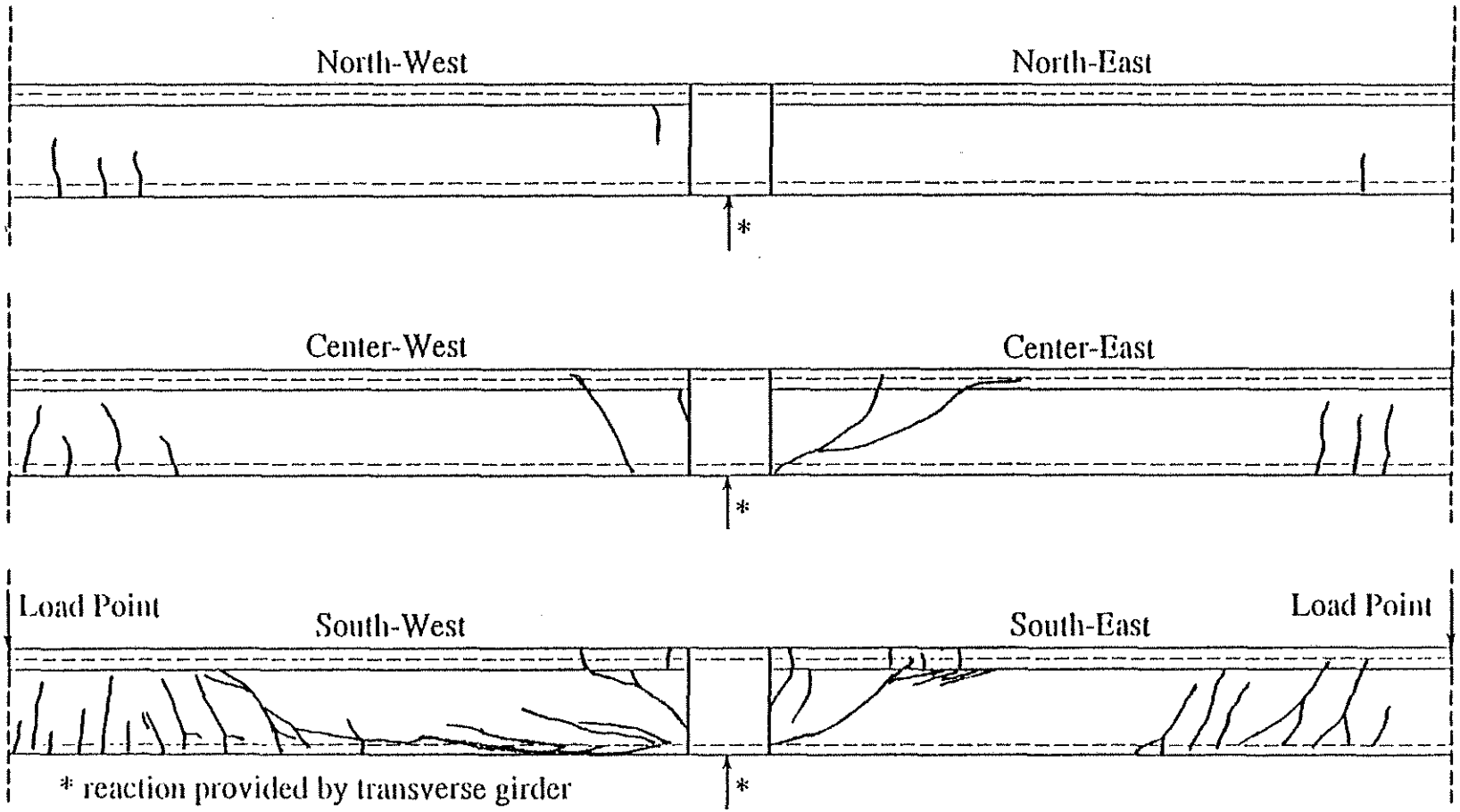

Fig. 2.9d Crack patterns for specimen M2

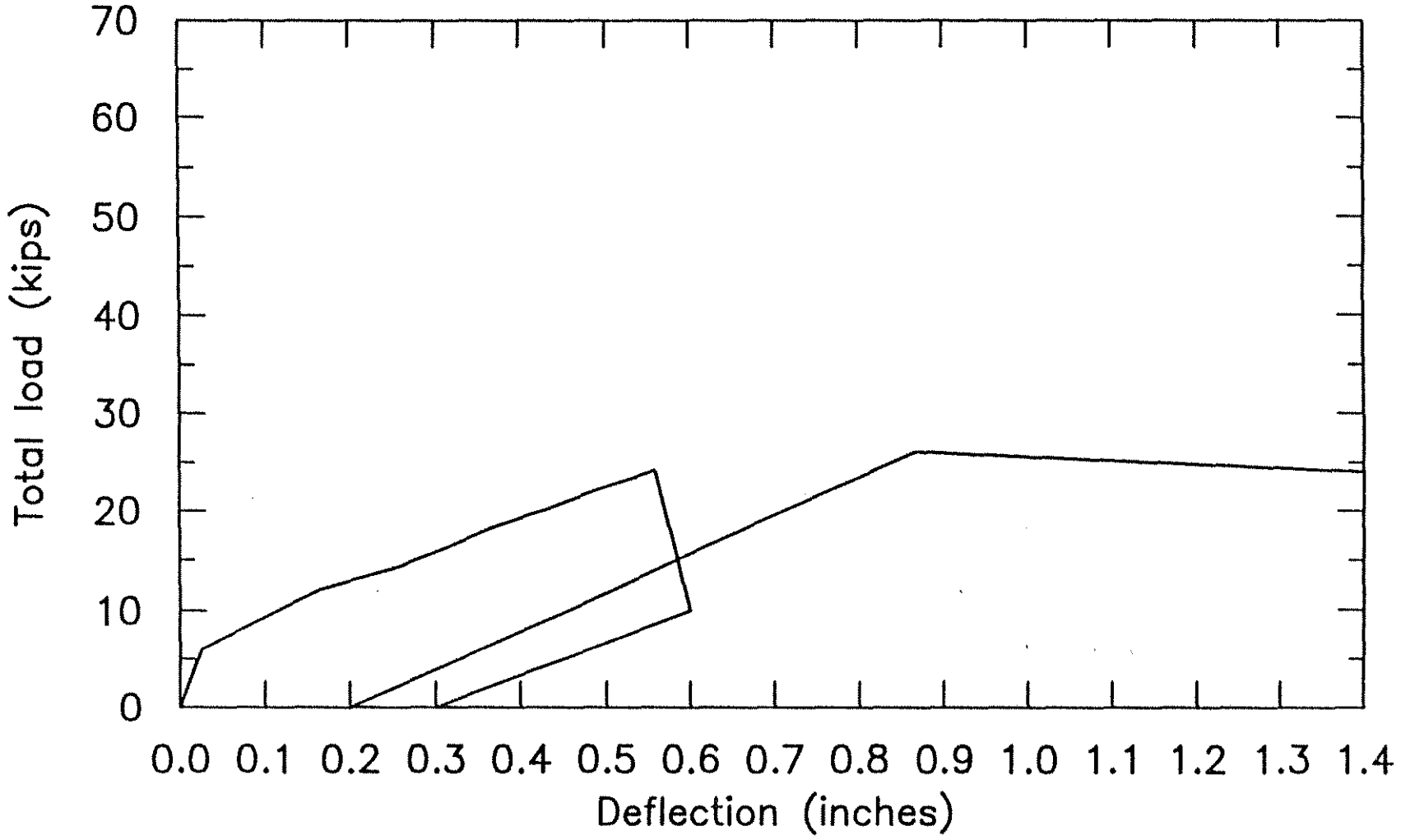

Fig. 2.10a Total load versus average midspan deflection for joist K1

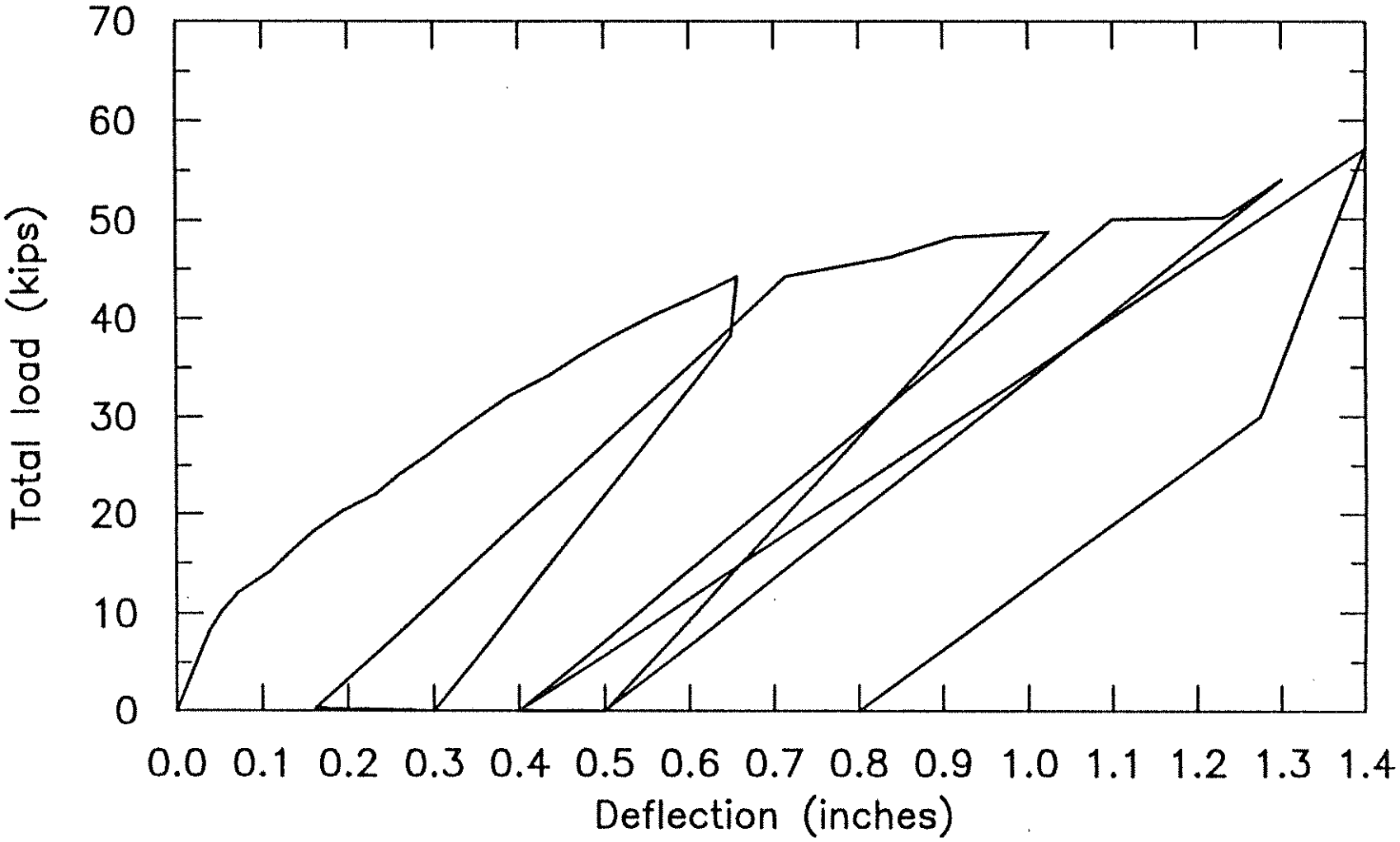

Fig. 2.10b Total load versus average midspan deflection for joist K2

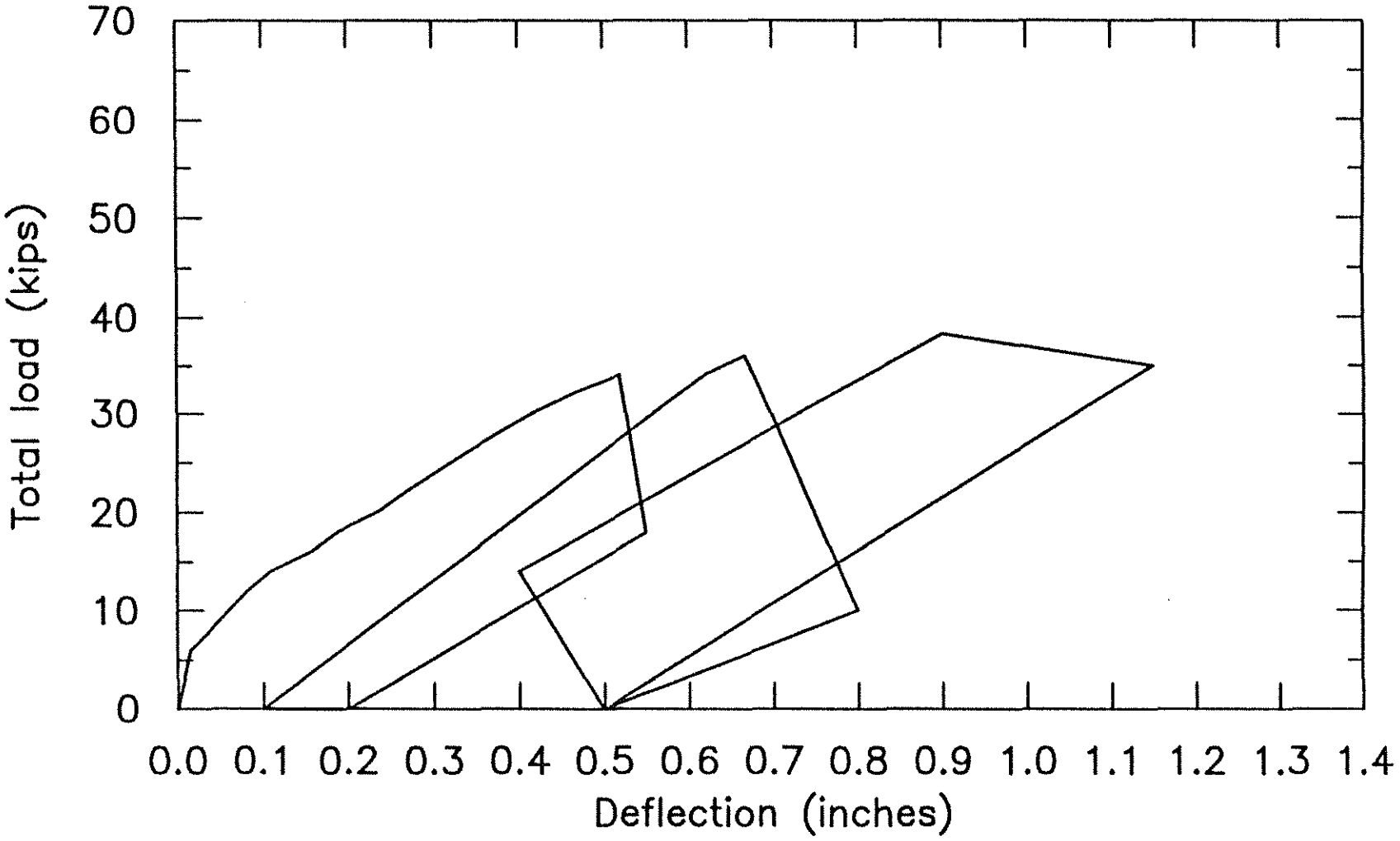

Fig. 2.10c Total load versus average midspan deflection for joist K3

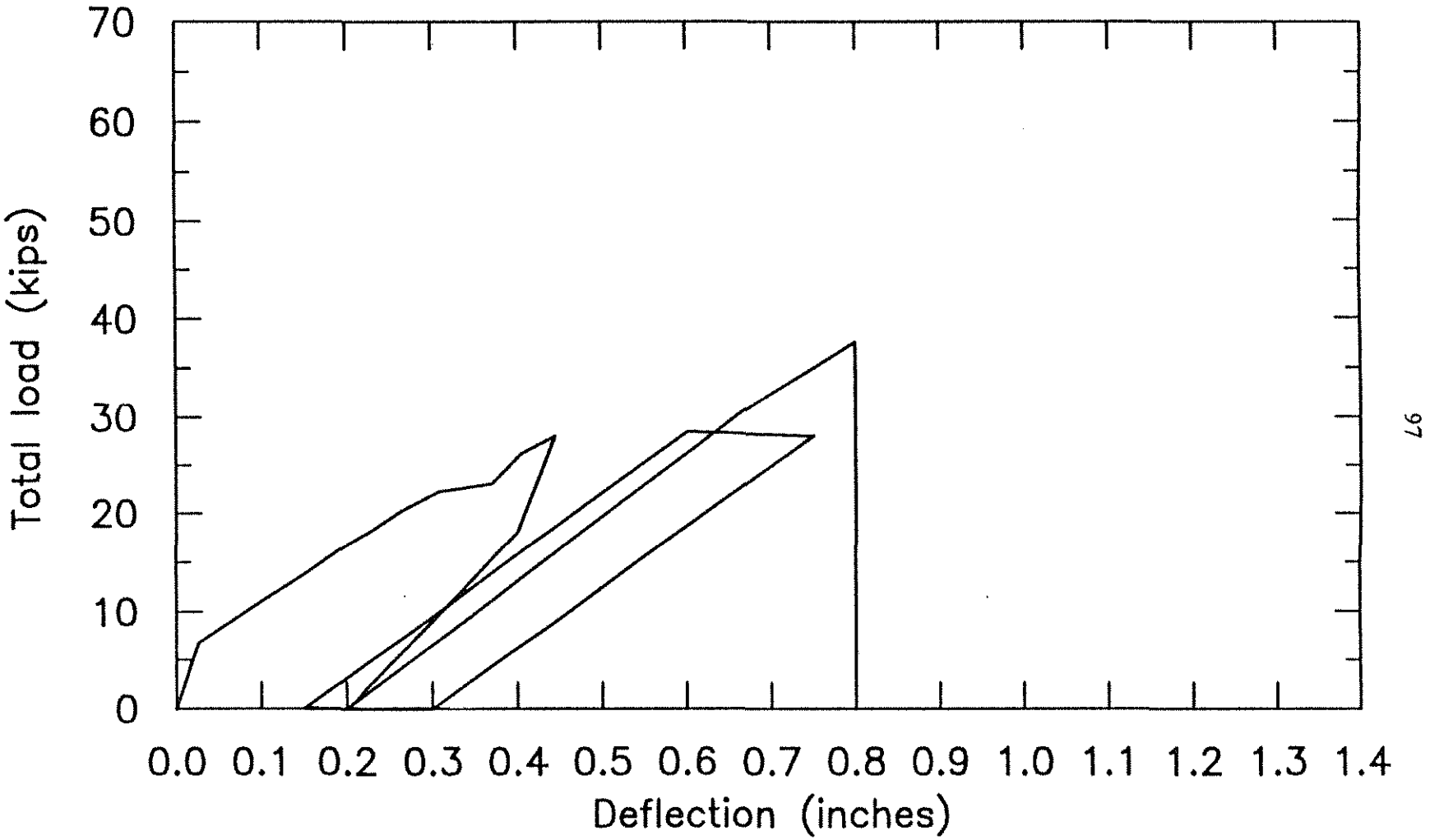

Fig. 2.10d Total load versus average midspan deflection for joist L1

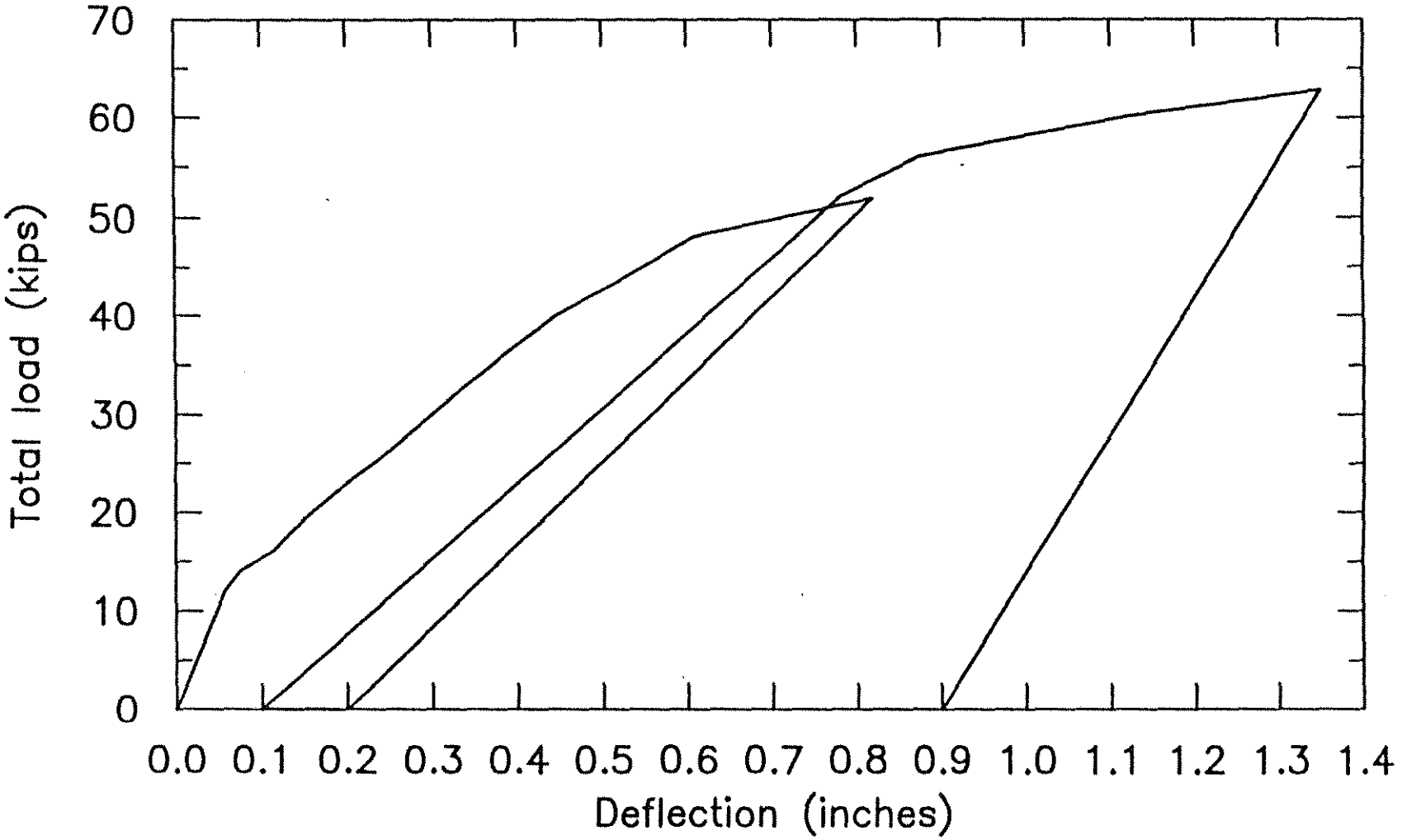

Fig. 2.10e Total load versus average midspan deflection for joist L2

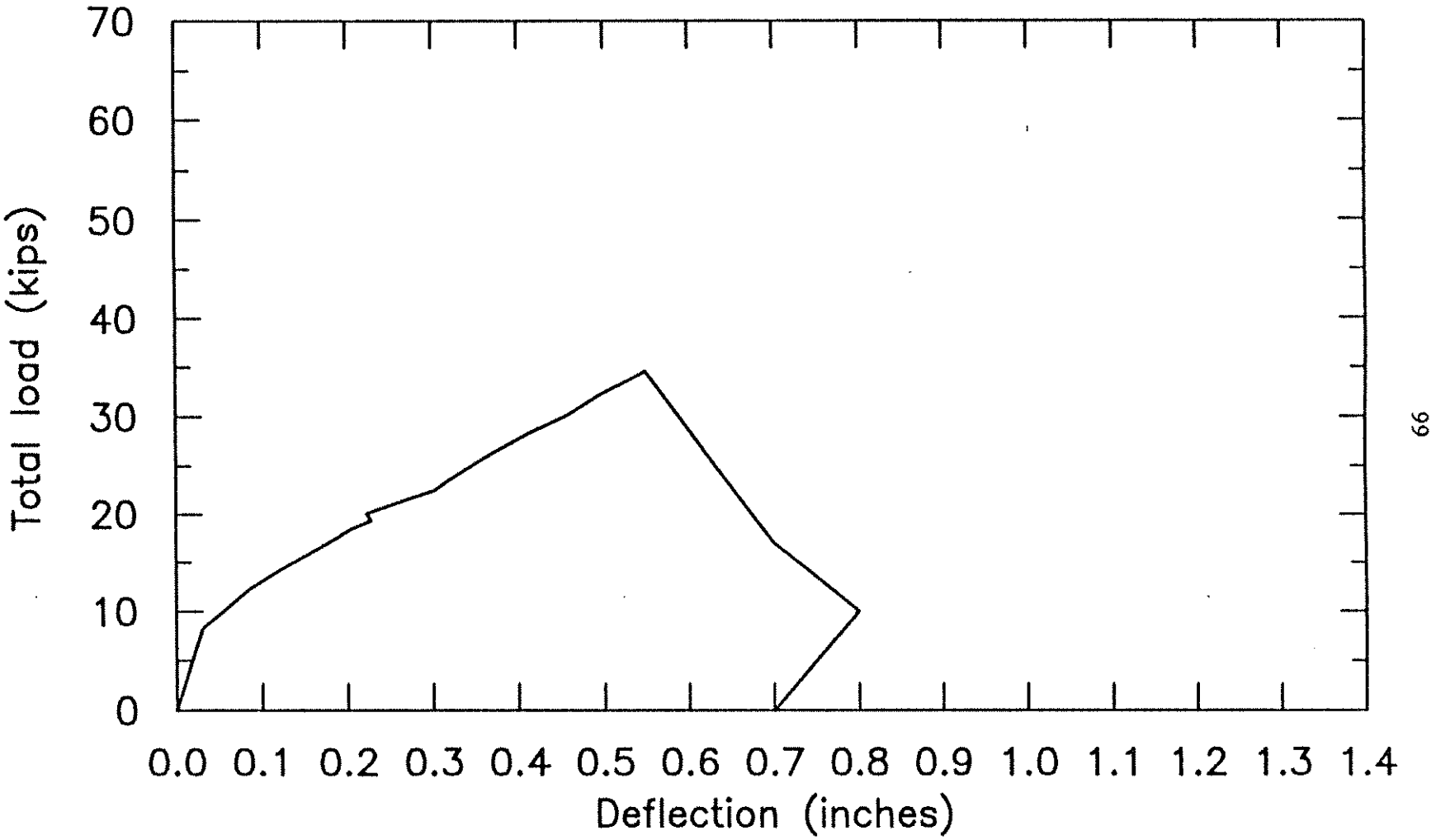

Fig. 2.10f Total load versus average midspan deflection for joist L3

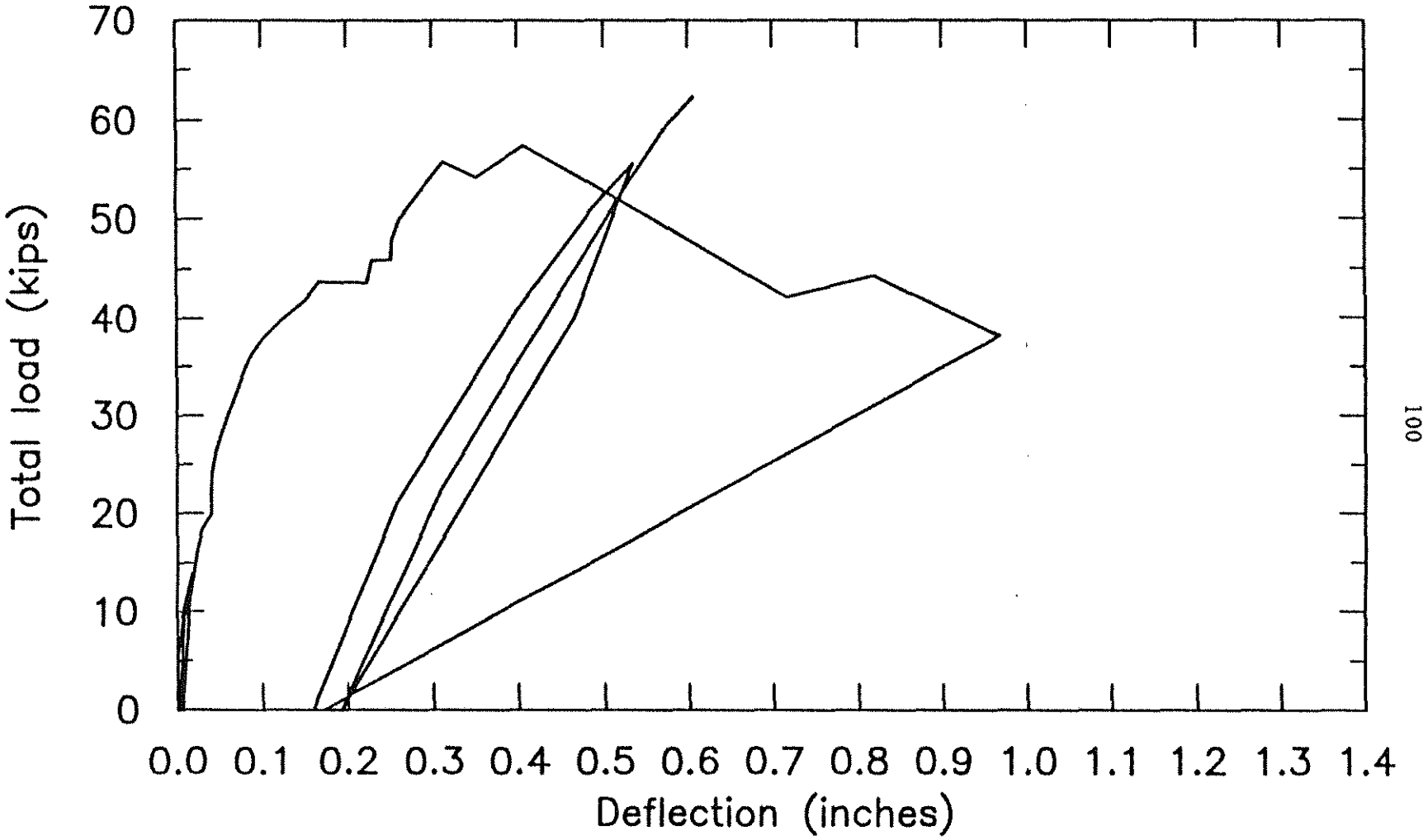

Fig. 2.10g Total load versus average midspan deflection for joist M1

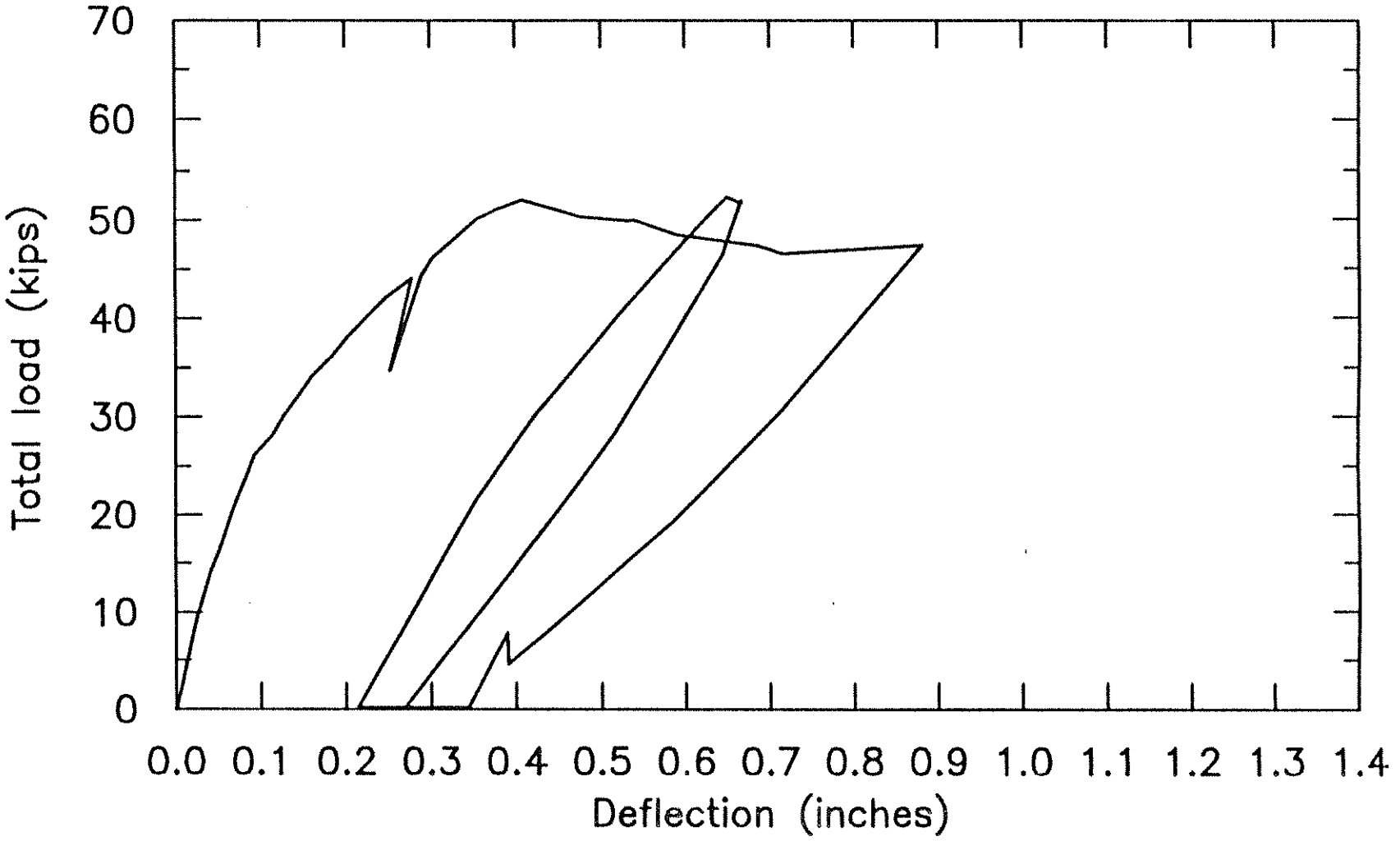

Fig. 2.10h Total load versus average midspan deflection for joist M2

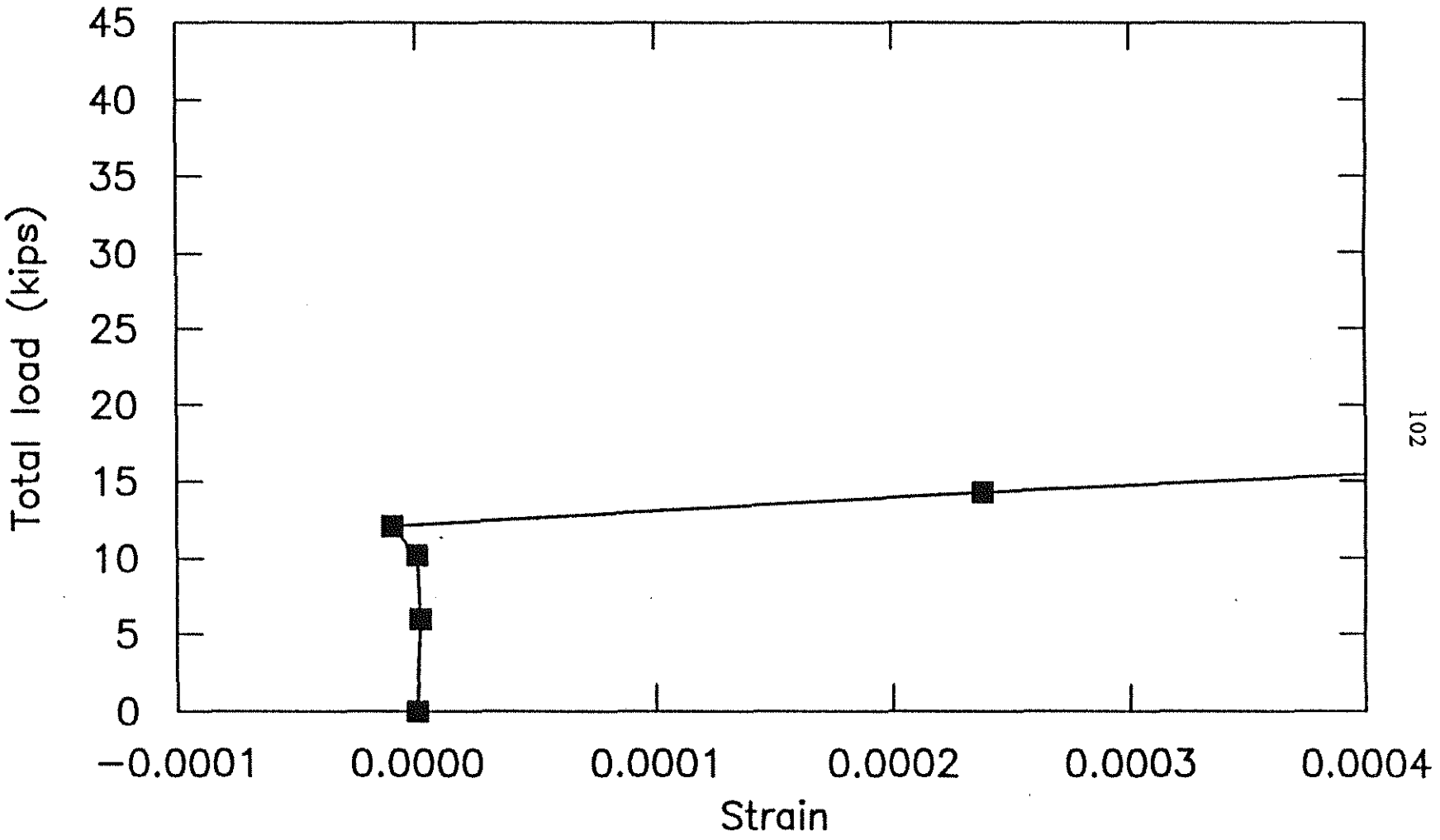

Fig. 3.1a Total load versus strain for stirrup 2 in west negative moment region stirrup strain of joist K1

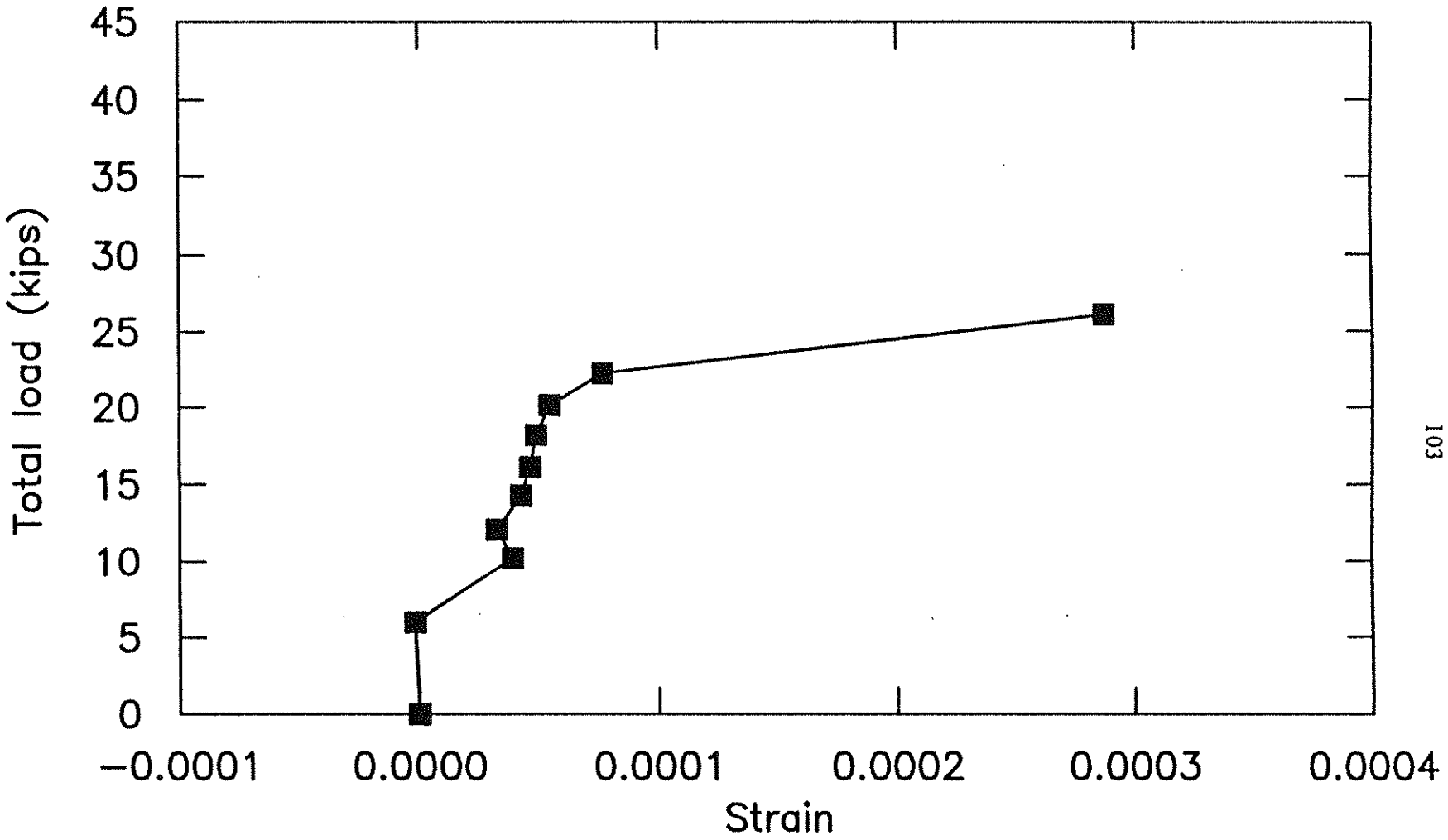

Fig. 3.1b Total load versus strain for stirrup 16 in west positive moment region stirrup strain of joist K1

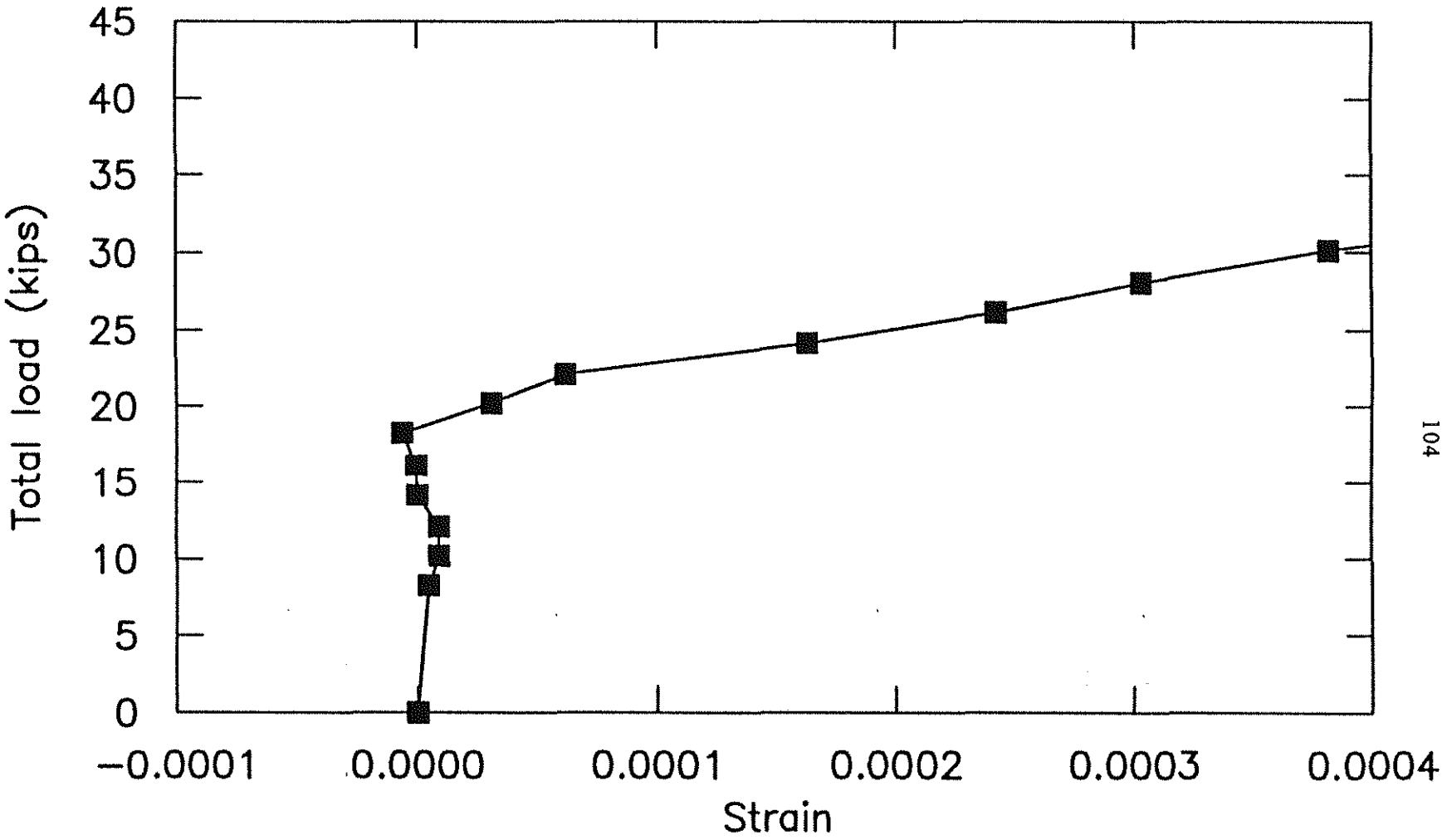

Fig. 3.1c Total load versus strain for stirrup 1 in west negative moment region stirrup strain of joist K2

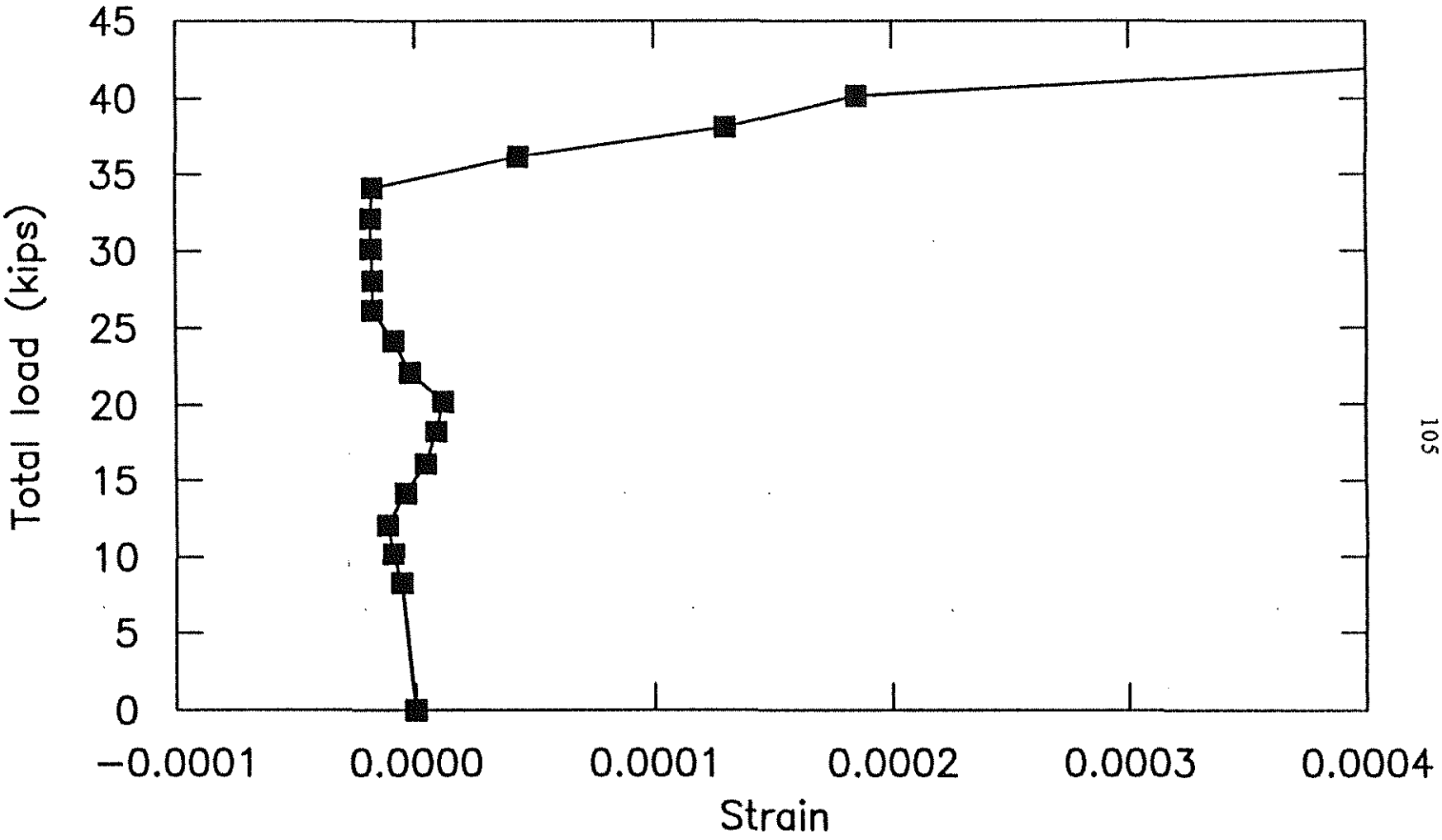

Fig. 3.1d Total load versus strain for stirrup 2 in east negative moment region stirrup strain of joist K2

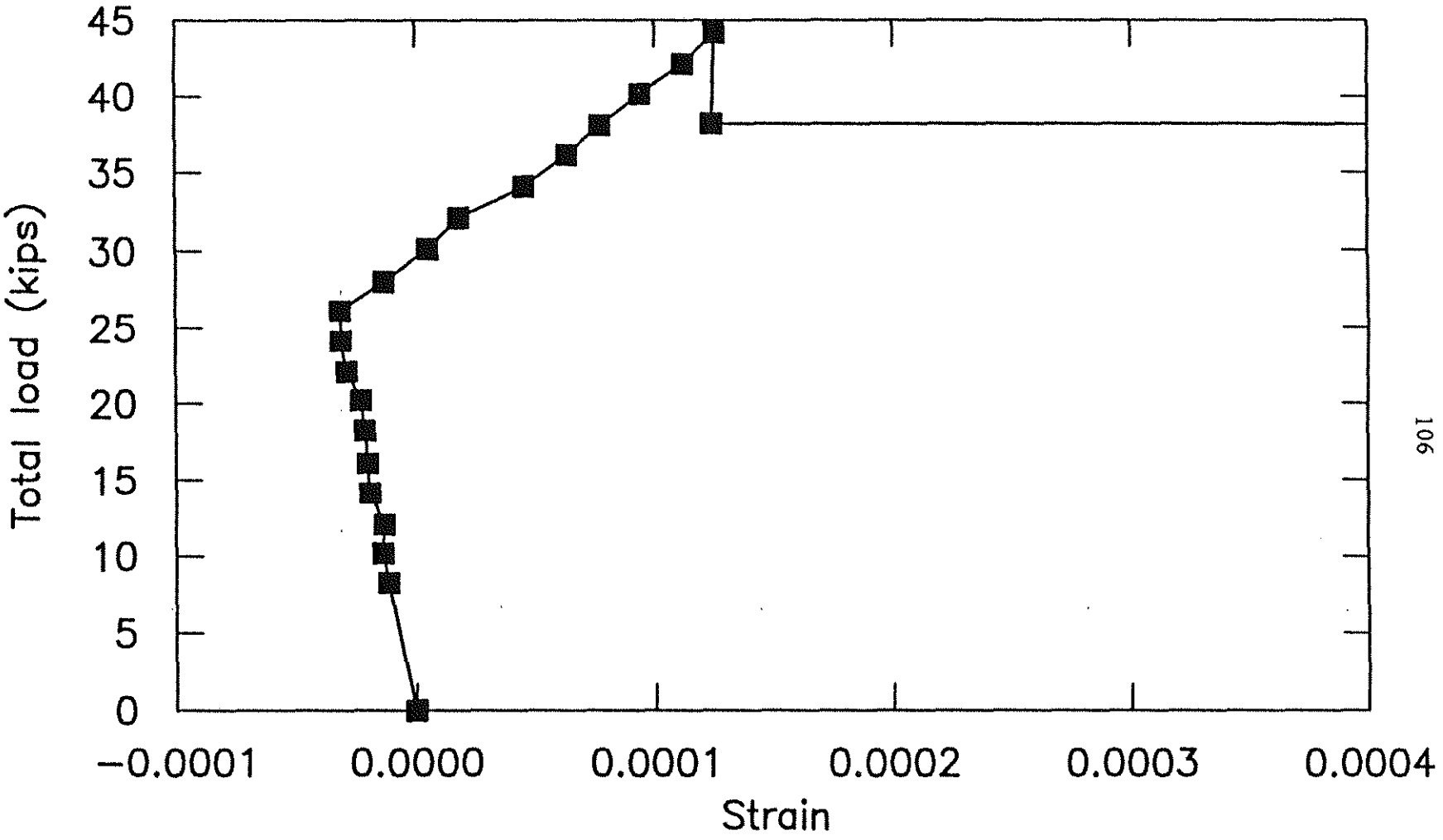

Fig. 3.1e Total load versus strain for stirrup 14 in west positive moment region stirrup strain of joist K2

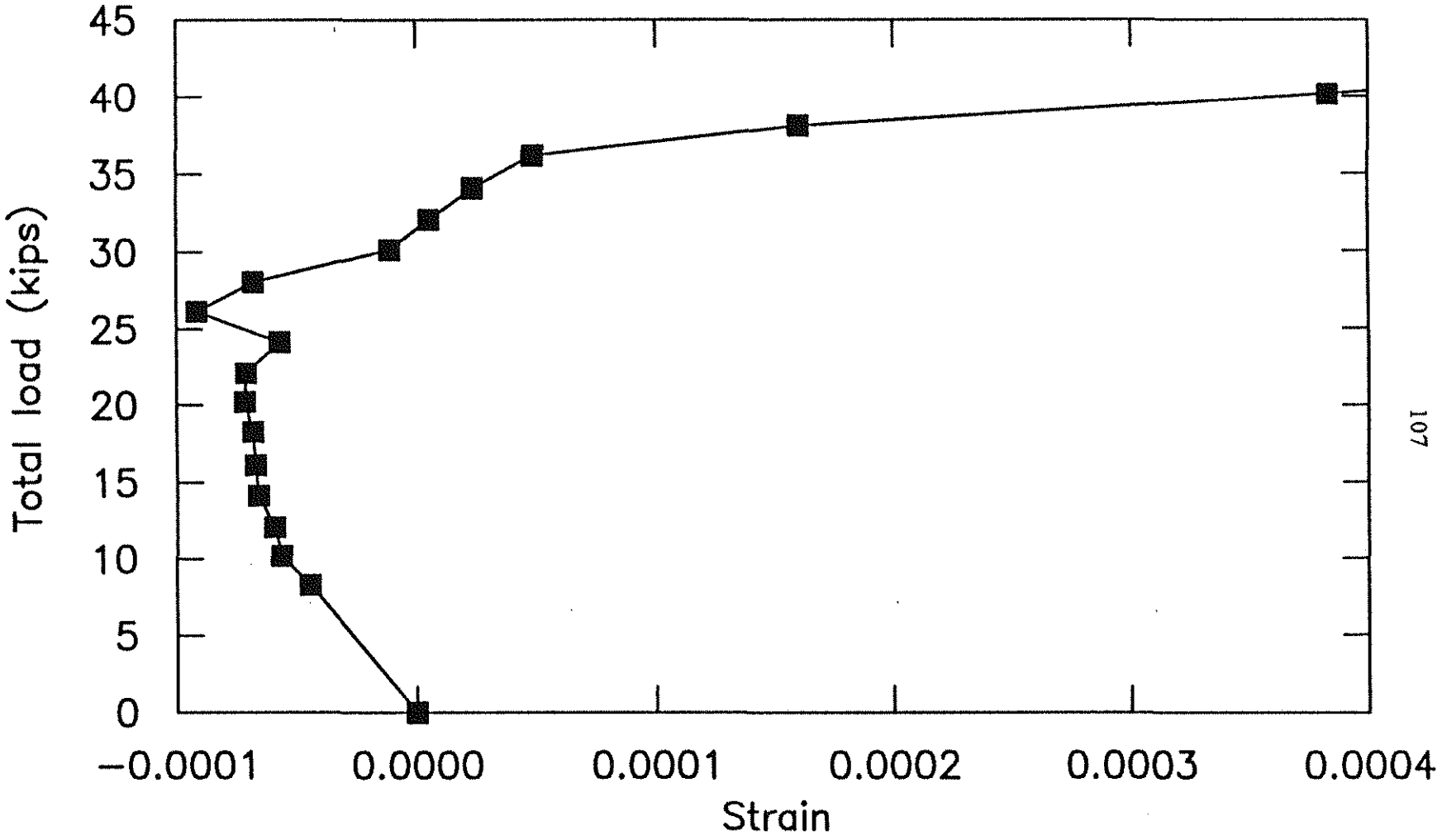

Fig. 3.1f Total load versus strain for stirrup 13 in east positive moment region stirrup strain of joist K2

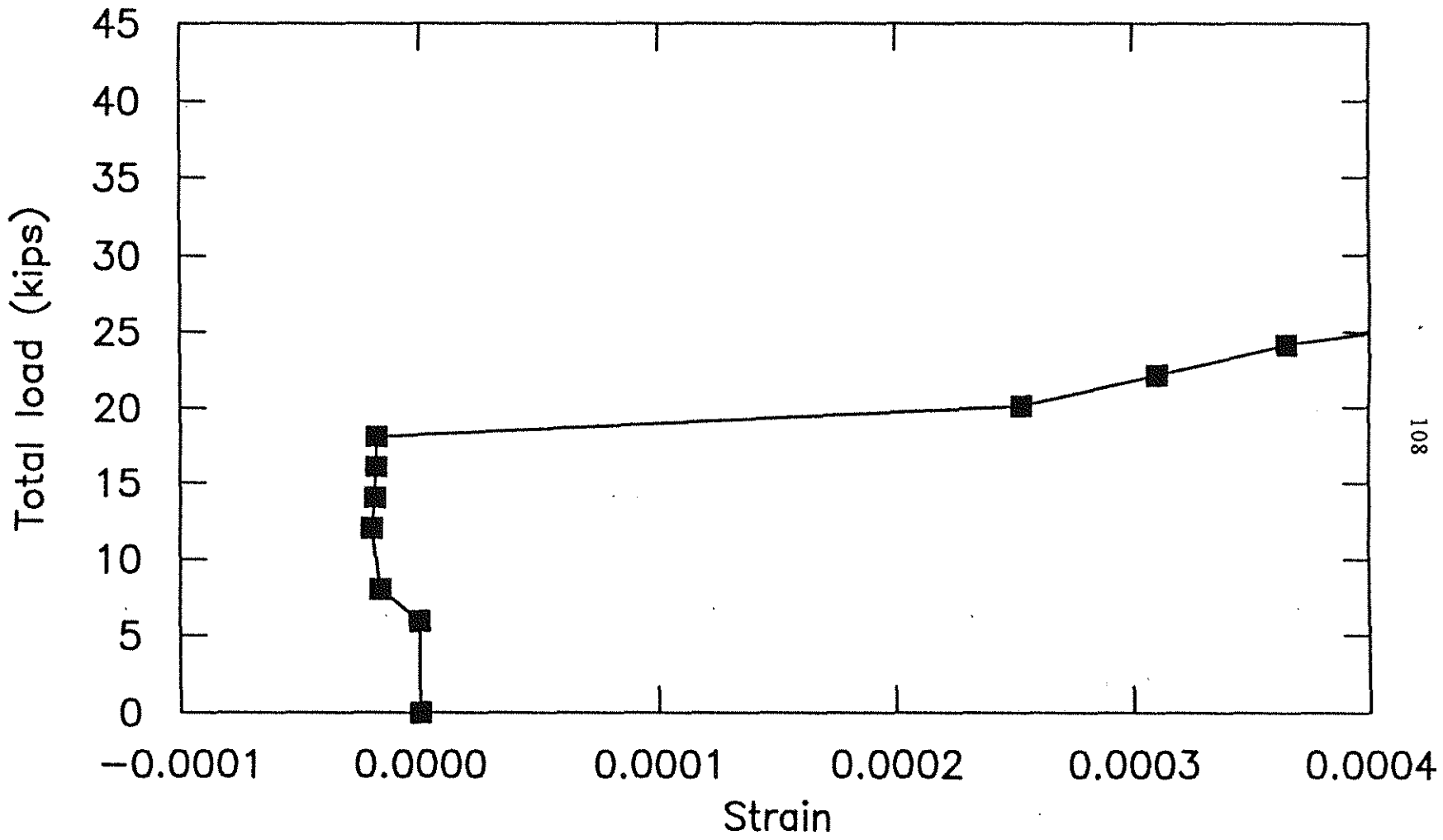

Fig. 3.1g Total load versus strain for stirrup 2 in west negative moment region stirrup strain of joist K3

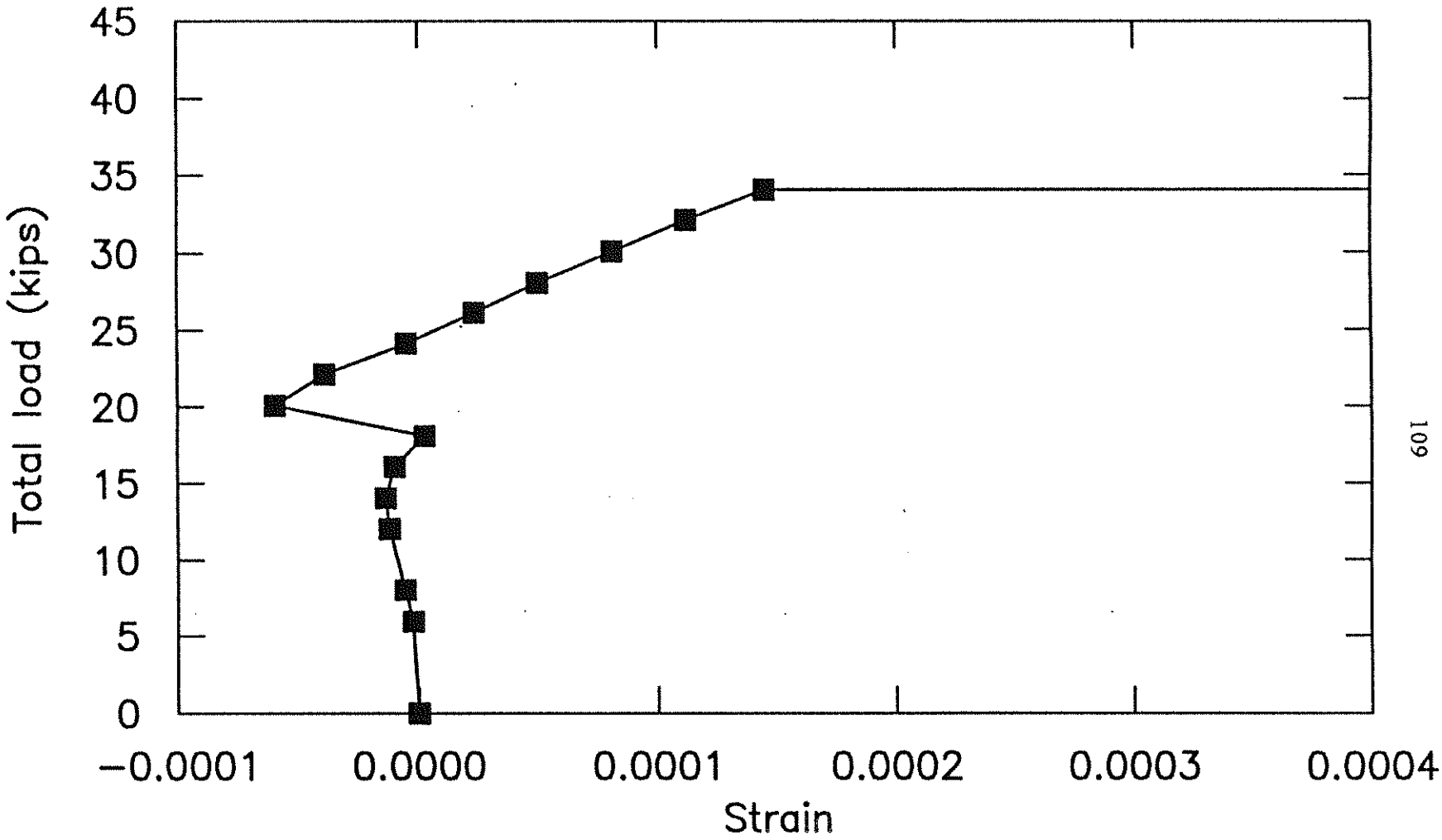

Fig. 3.1h Total load versus strain for stirrup 13 in west positive moment region stirrup strain of joist K3

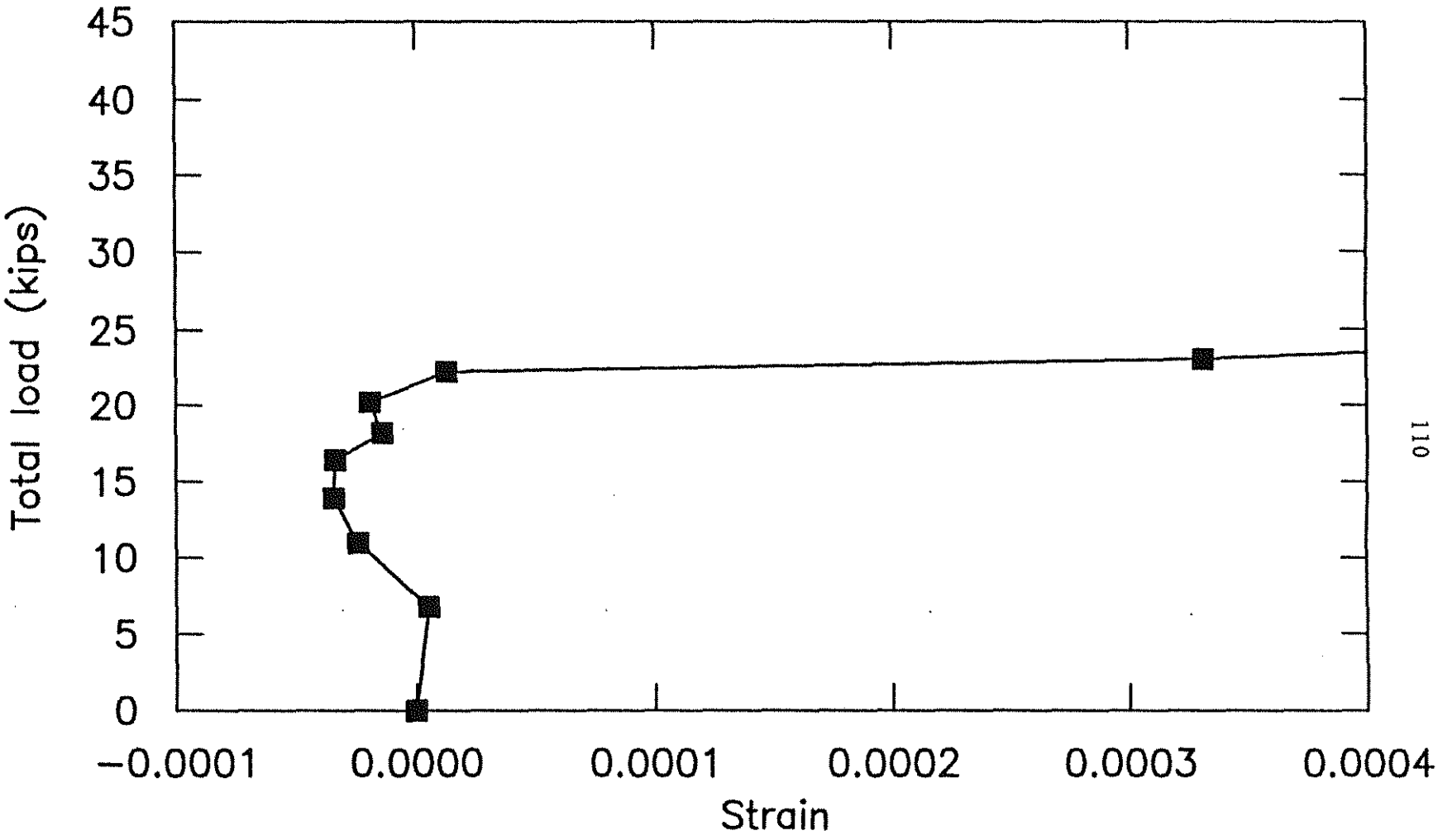

Fig. 3.1i Total load versus strain for stirrup 1 in west negative moment region stirrup strain of joist L1

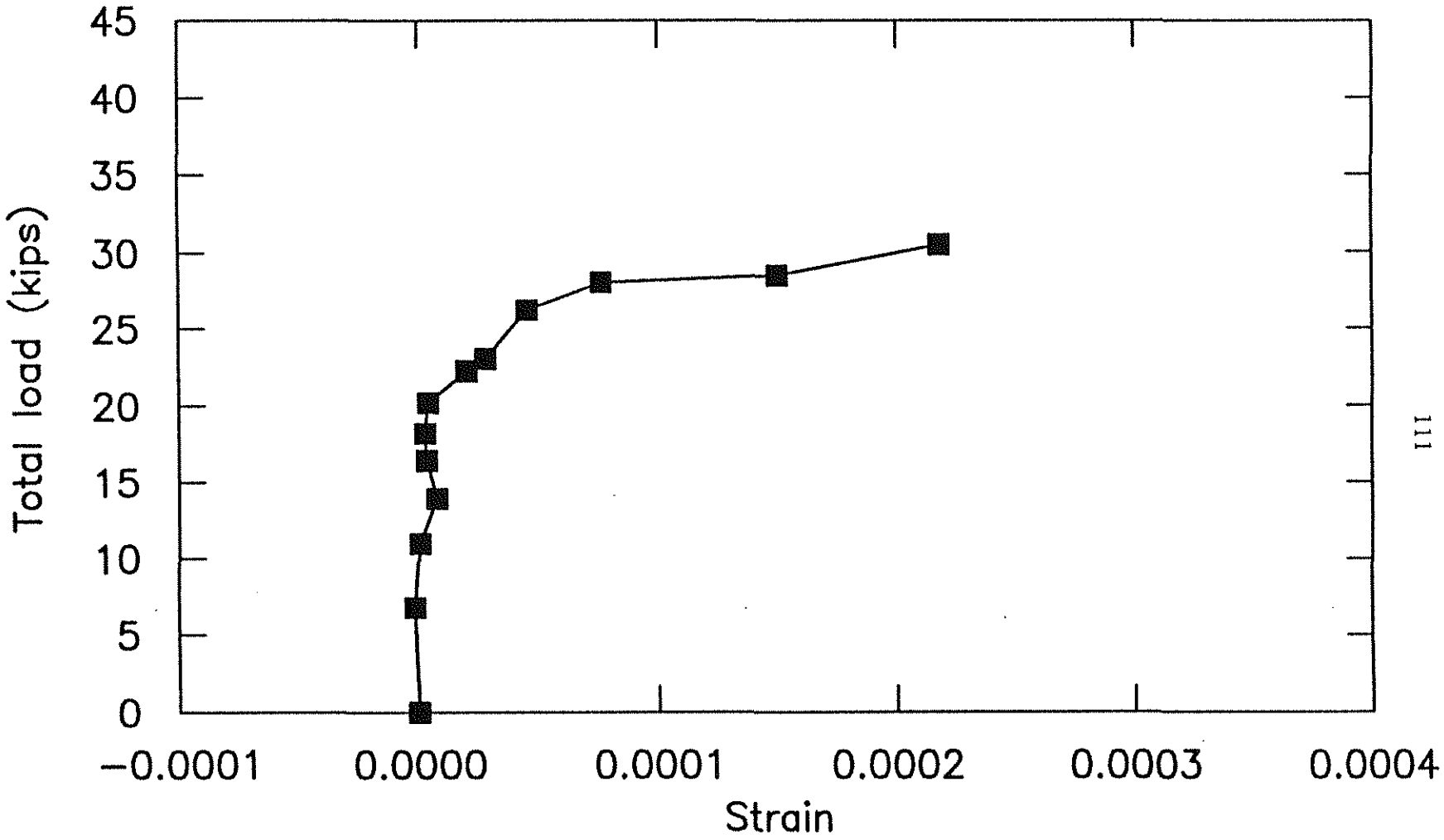

Fig. 3.1j Total load versus strain for stirrup 14 in west positive moment region stirrup strain of joist L1

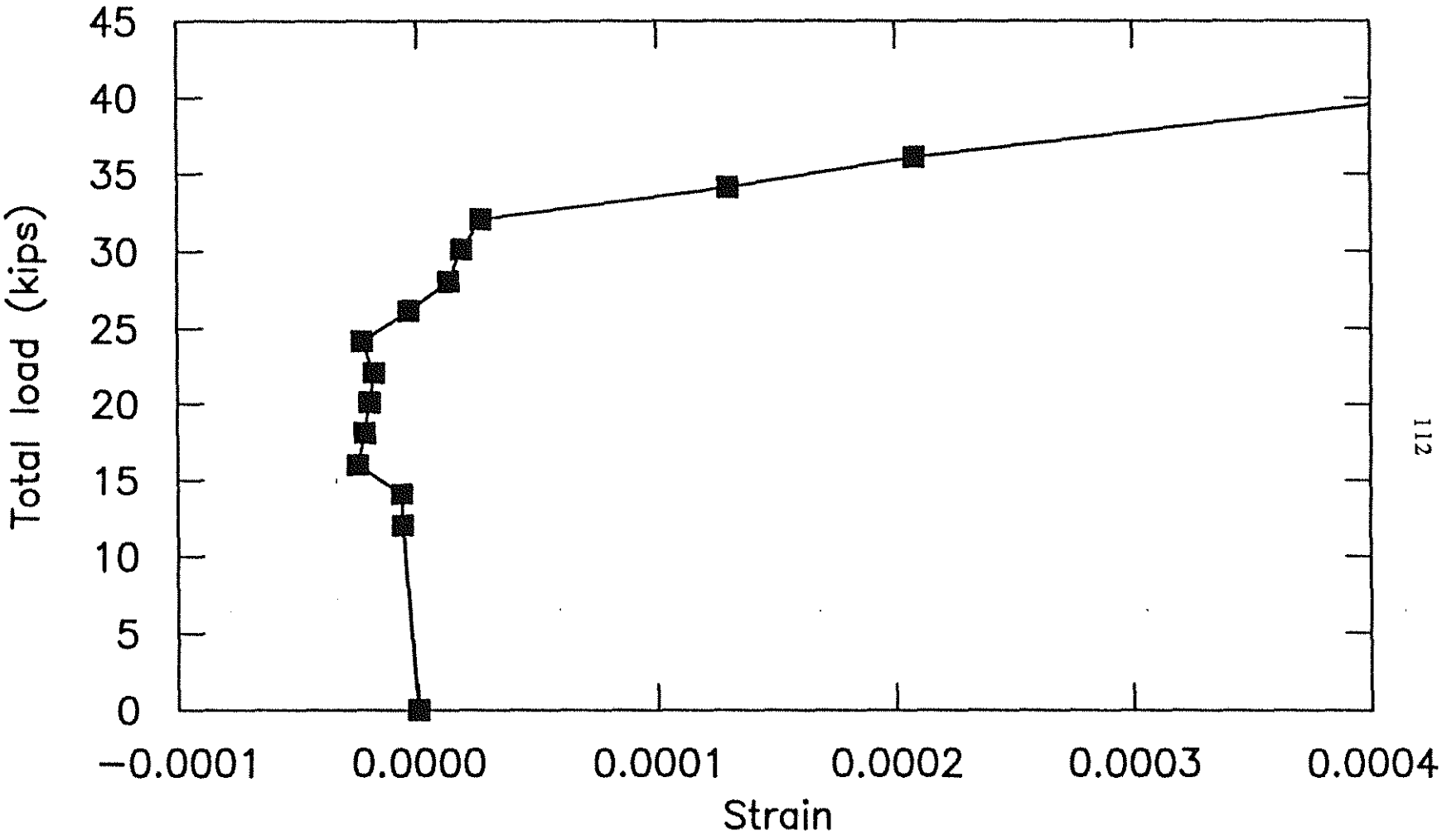

Fig. 3.1k Total load versus strain for stirrup 2 in west negative moment region stirrup strain of joist L2

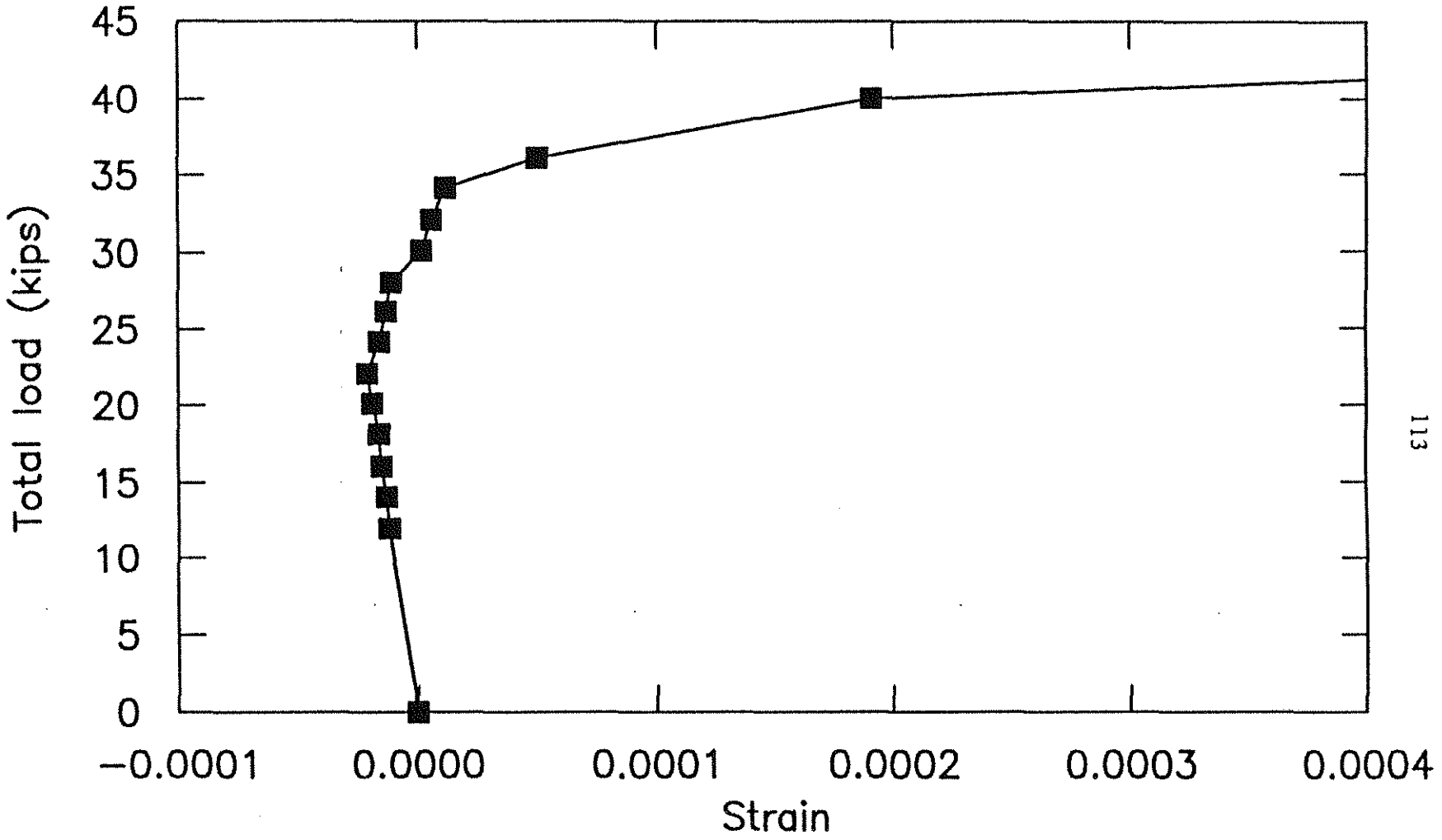

Fig. 3.11 Total load versus strain for stirrup 2 in east negative moment region stirrup strain of joist L2

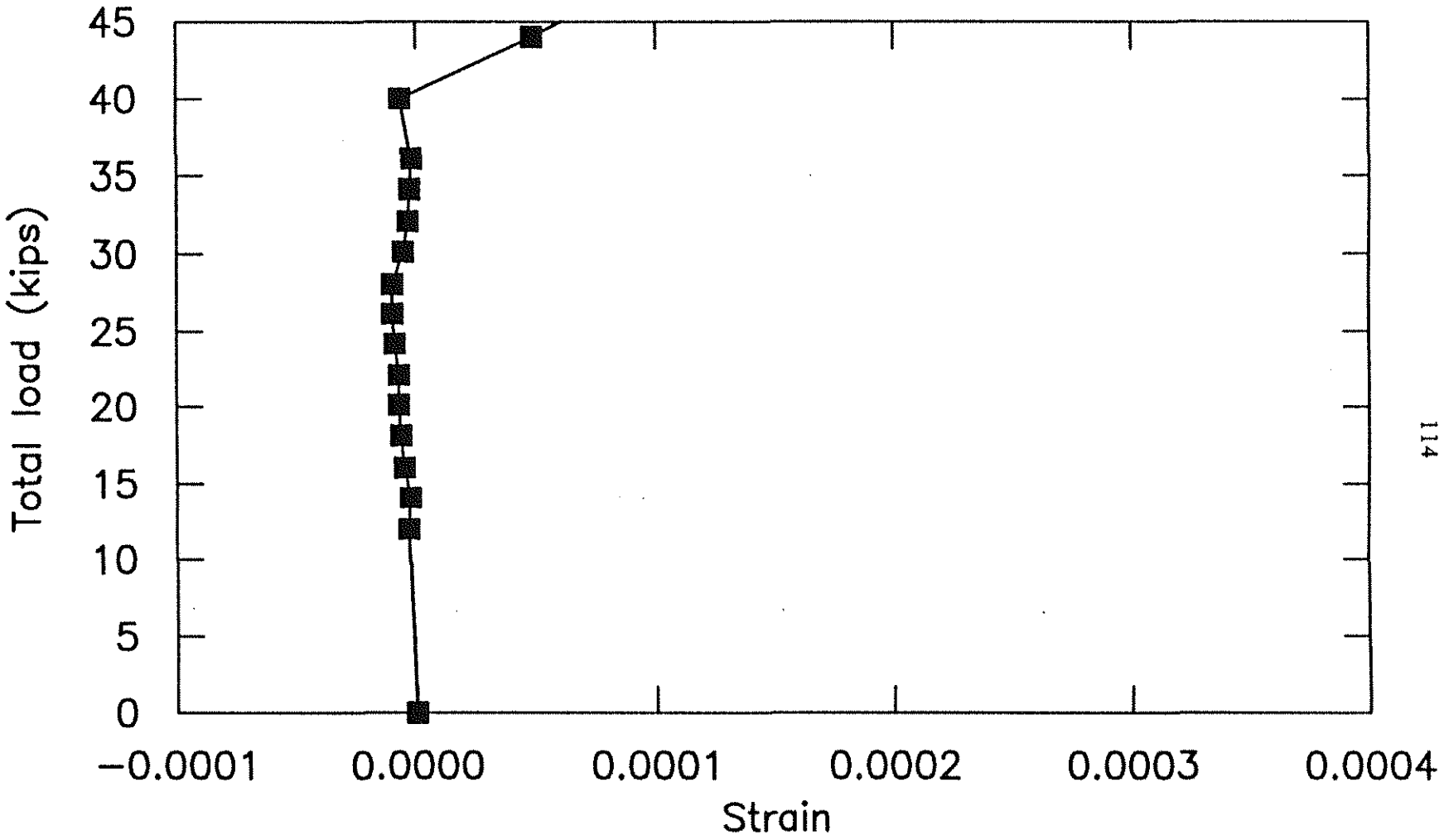

Fig. 3.1m Total load versus strain for stirrup 10 in west positive moment region stirrup strain of joist L2

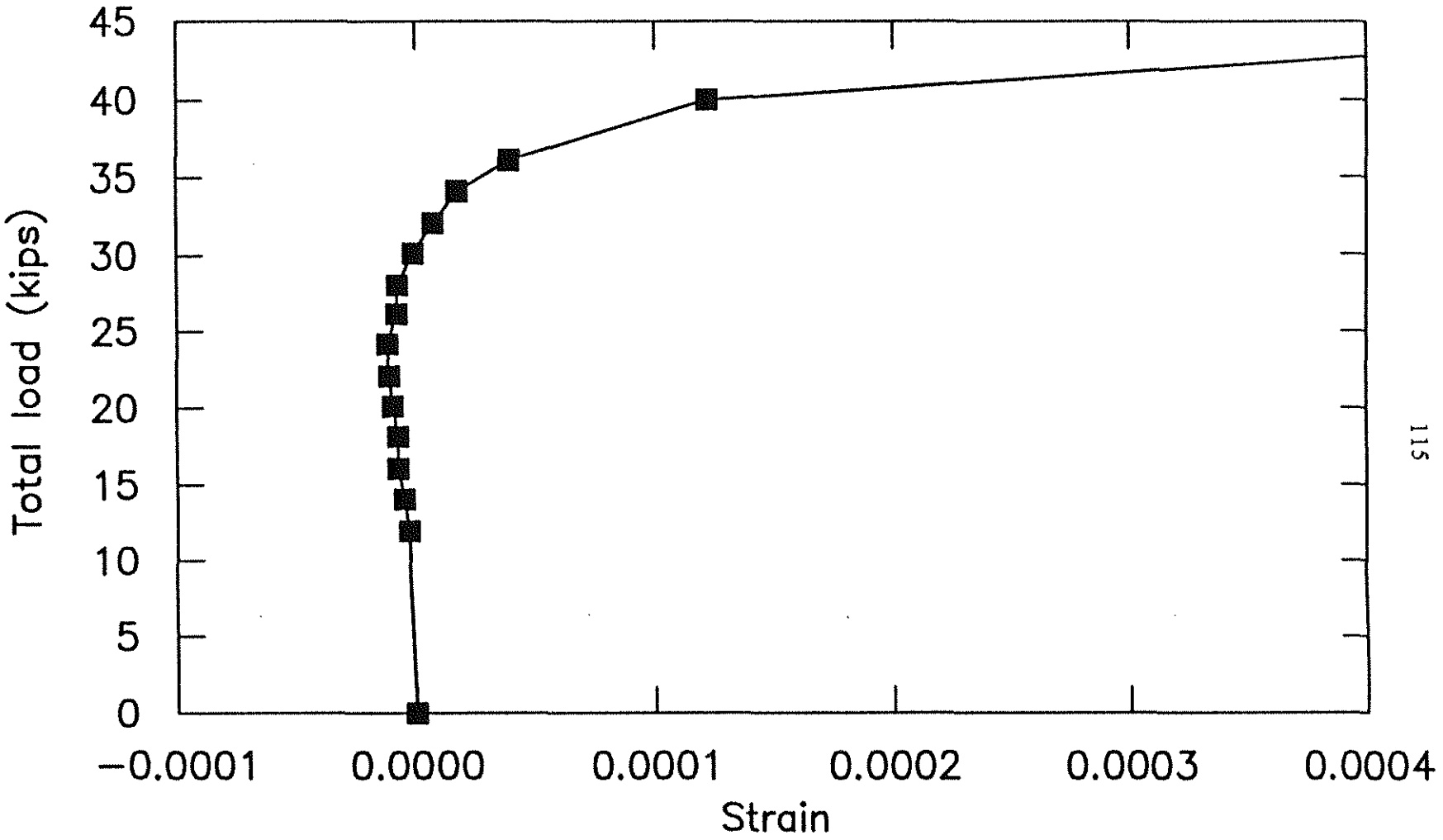

Fig. 3.1n Total load versus strain for stirrup 11 in east positive moment region stirrup strain of joist L2

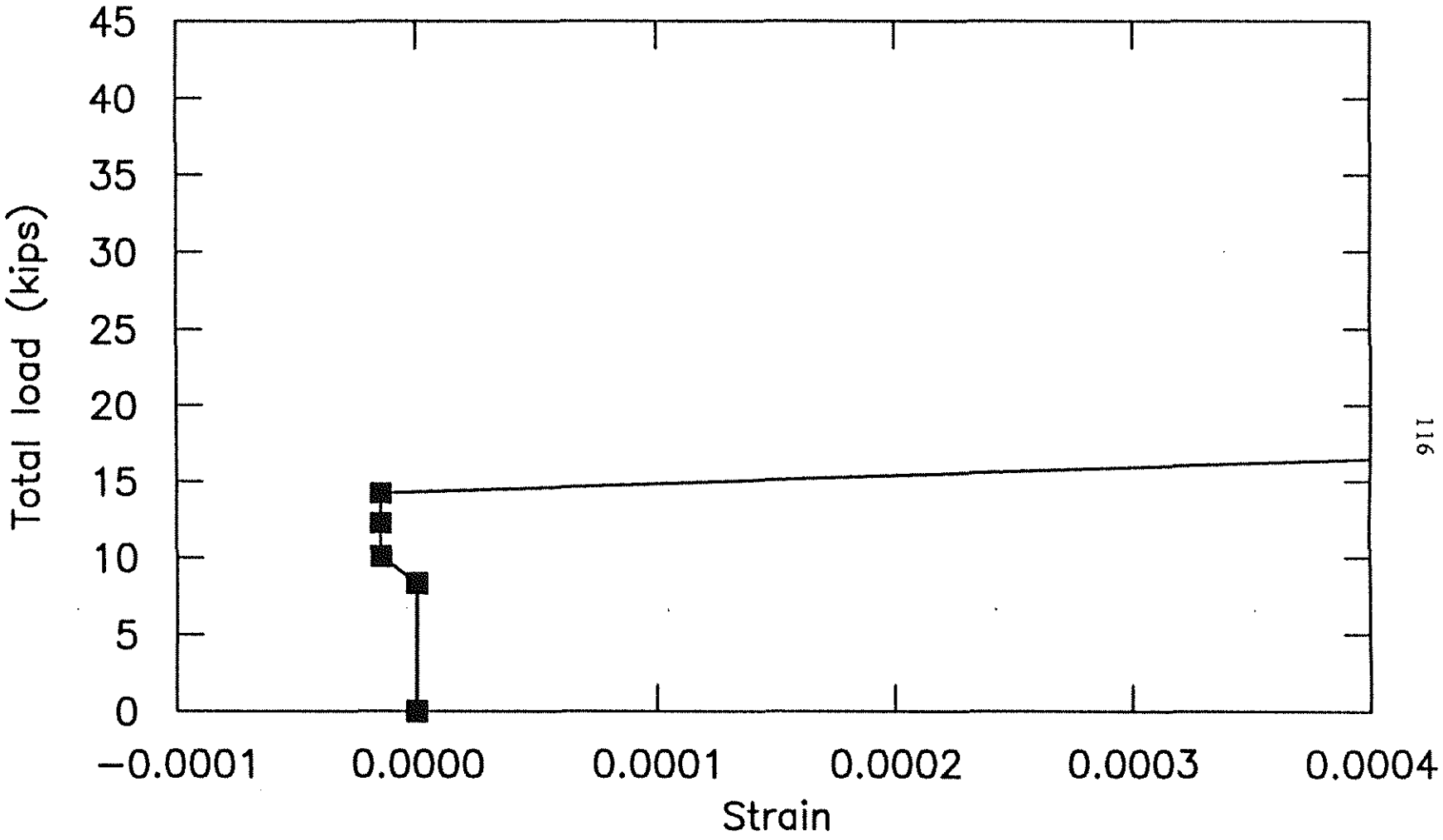

Fig. 3.1o Total load versus strain for stirrup 2 in west negative moment region stirrup strain of joist L3

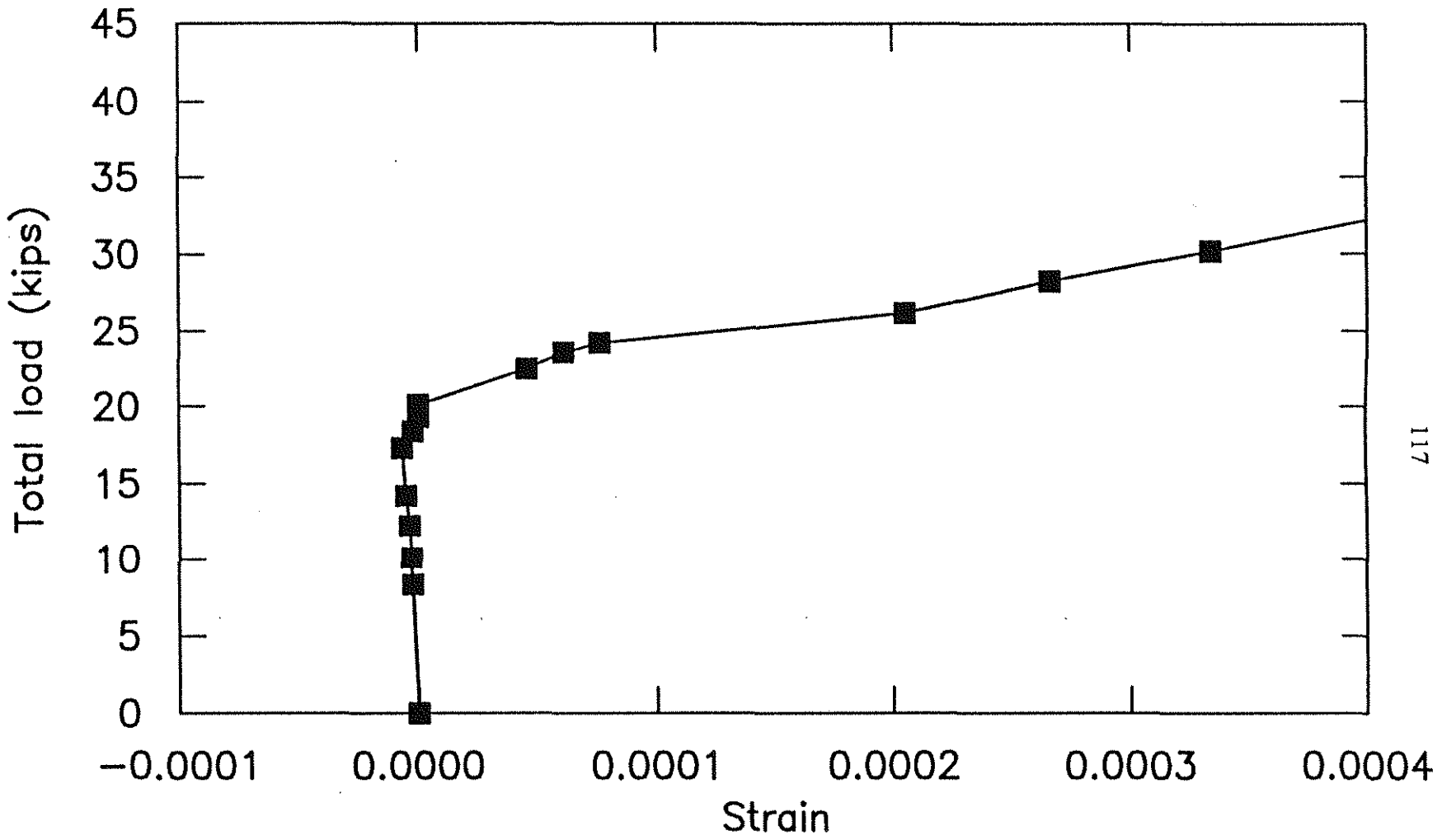

Fig. 3.1p Total load versus strain for stirrup 13 in west positive moment region stirrup strain of joist L3

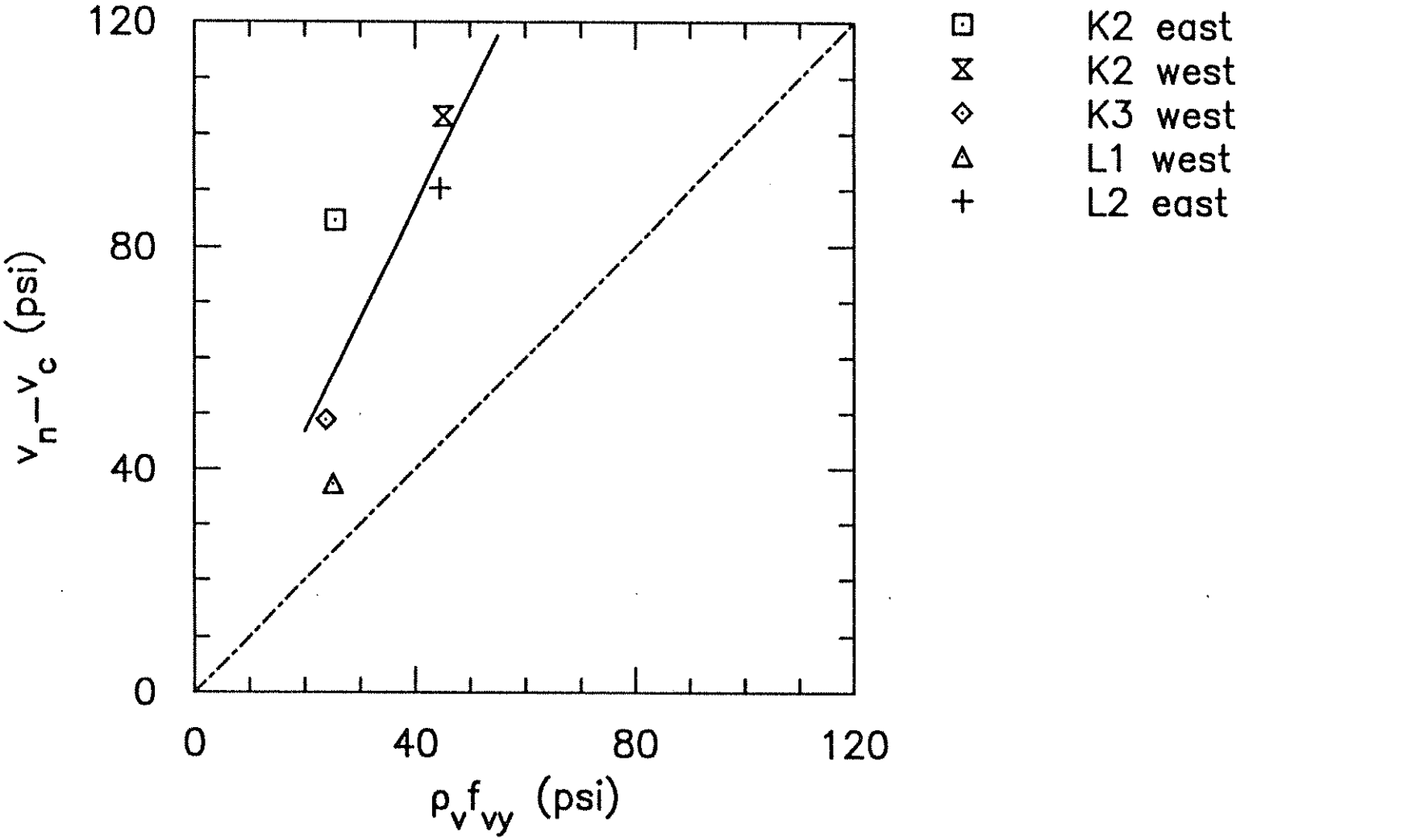

Fig. 3.2a Increase in shear stress above cracking stress, v_n - v_c, versus nominal stirrup capacity, $\rho_v f_{vy}$, in the negative moment region

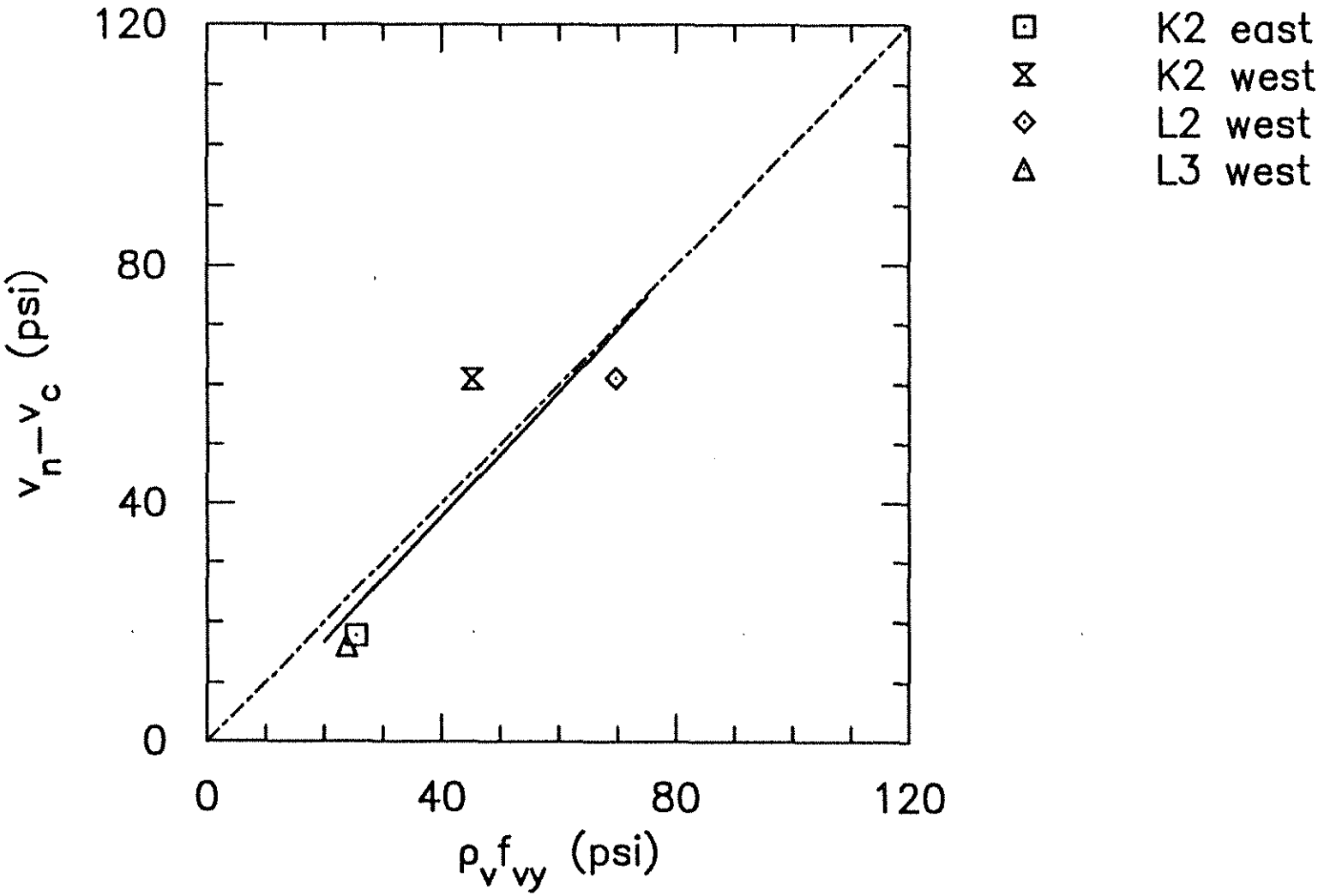

Fig. 3.2b Increase in shear stress above cracking stress, v_n - v_c, versus nominal stirrup capacity, $\rho_v f_{vy}$, in the positive moment region

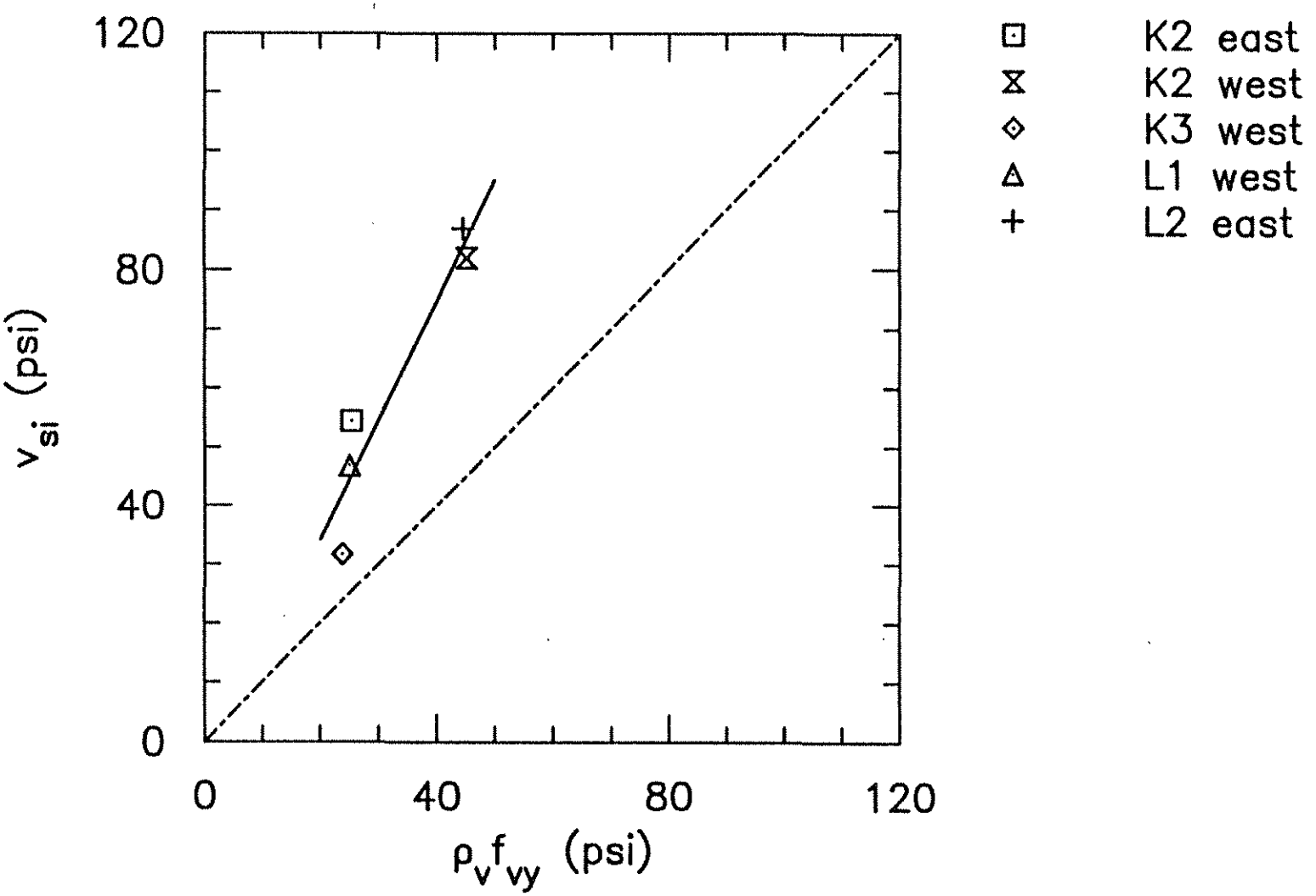

Fig. 3.3a Shear carried by stirrups alone in the negative moment region

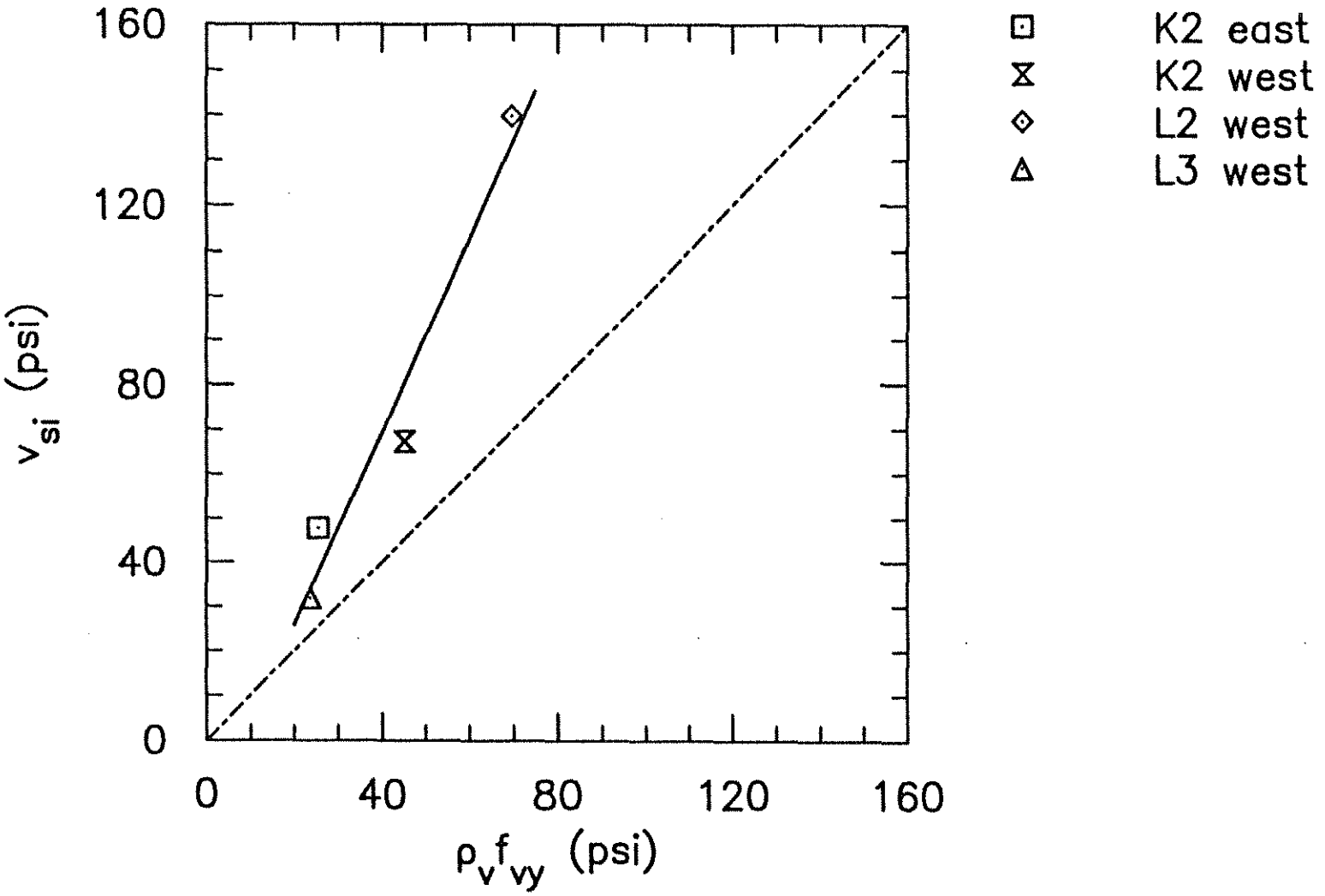

Fig. 3.3b Shear carried by stirrups alone in the positive moment region

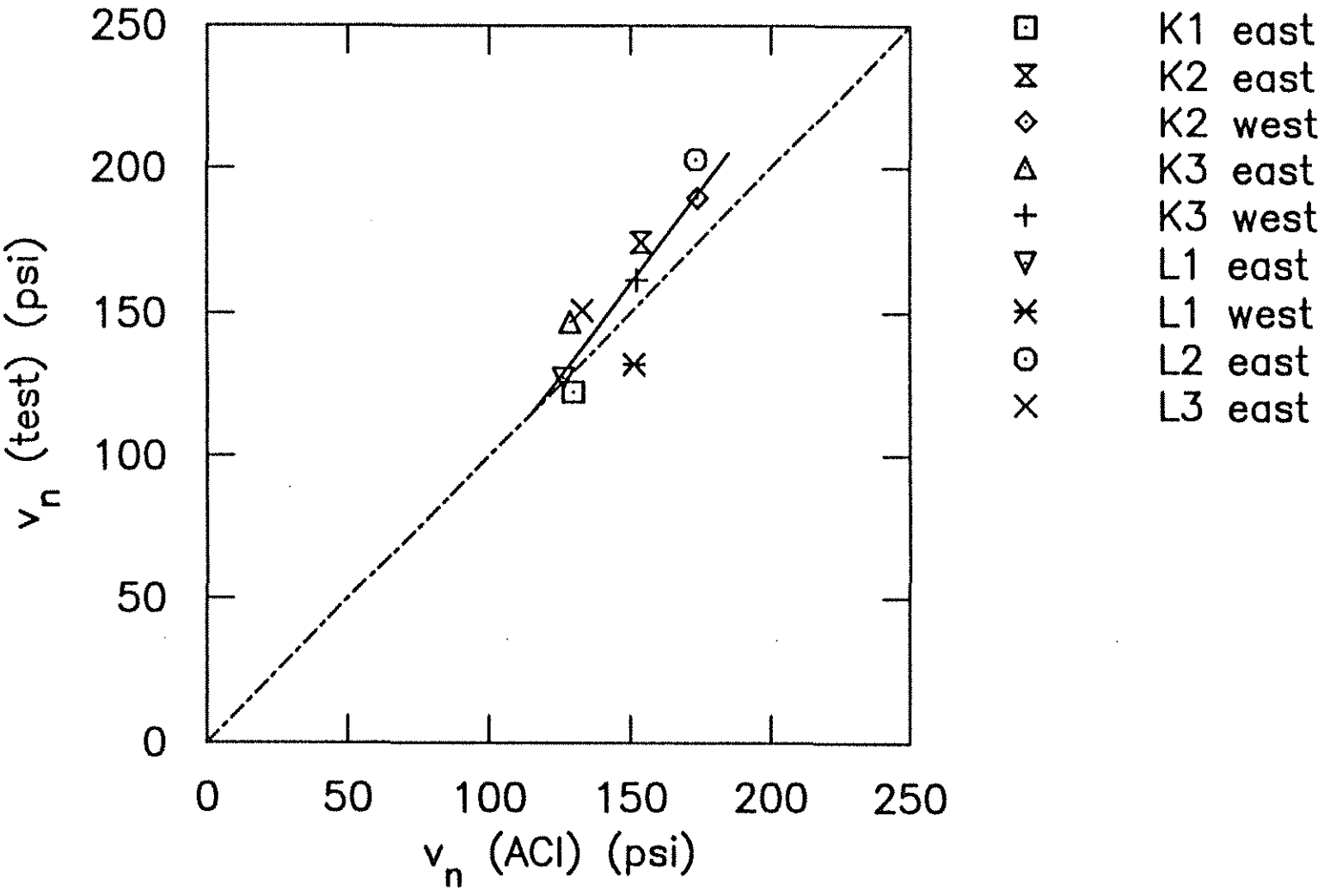

Fig. 3.4a Negative moment region nominal shear stress

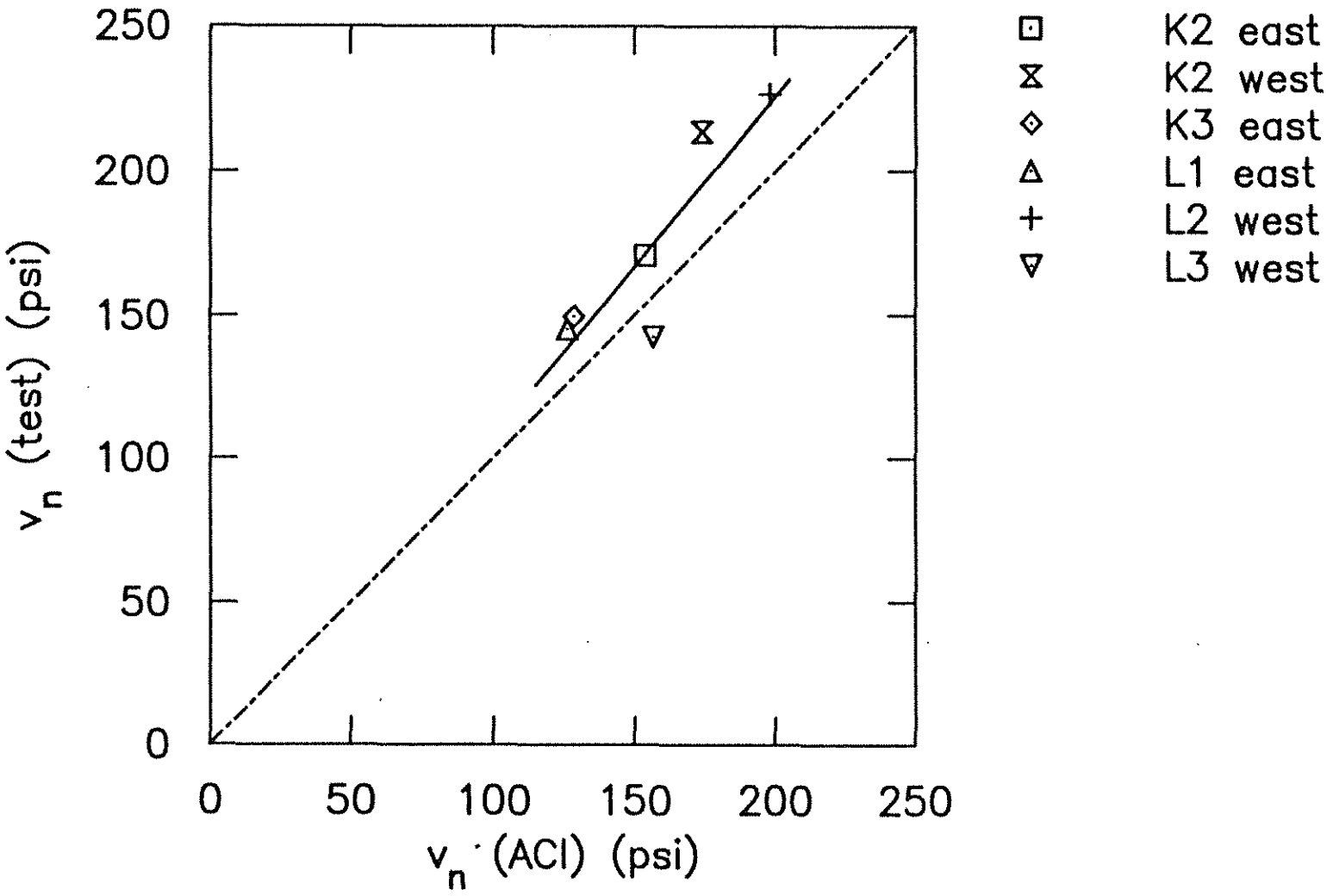

Fig. 3.4b Positive moment region nominal shear stress

APPENDIX A

NOTATION

A_s = area of flexural reinforcement, sq. in.

A_v = area of shear reinforcement, sq. in.

a = shear-span, set equal to the ratio of the moment to the shear

b_w = average web width of joist, in.

d = distance from extreme compression fiber to centroid of flexural reinforcement (effective depth of joist), in.

d_a = diameter of maximum size aggregate, in.

f'_c = compressive strength of concrete measured on 6 x 12 in. cylinders, psi

f_{vy} = yield stress of web reinforcement, psi

M = bending moment, lb-in.

M_u = factored bending moment at section, lb-in.

r = coefficient of variation

s = spacing of shear reinforcement, in.

V = shear force, lbs

V_c = nominal shear strength provided by concrete, lbs

V_s = nominal shear strength provided by shear reinforcement, lbs

V_u = factored shear force, lbs

V_n = nominal shear strength, lbs

v_c = average shear stress carried by concrete at failure or average stress in concrete corresponding to formation of initial shear crack, psi

v_n = nominal shear stress, psi

v_{si} = equivalent concrete shear stress carried by stirrups alone, psi

ρ_v = ratio of shear reinforcement area to the average width of the joist, b_w (within the spacing of the shear reinforcement, s)

ρ_w = ratio of longitudinal flexural reinforcement area to the gross vertical concrete

cross section area

ϕ = strength reduction factor